Differential DNA hypermethylation and hypomethylation signatures in colorectal cancer

Jordi Frigola, Xavier Solé, Maria F. Paz, Victor Moreno, Manel Esteller, Gabriel Capellà and Miguel A. Peinado

Human Molecular Genetics, 2005, Vol. 14, No. 2 319–326

CAPÍTOL 2

A la bibliografia existent, s'han descrit dos tipus de canvis de metilació de l'ADN associats al procés tumoral: (1) pèrdues de metilació generals (o hipometilació), sovint associades a seqüències transposables i repetitives; i, paral·lelament, (2) guanys localitzats de metilació (o hipermetilació), associats en aquest cas als gens que presenten en la seva regió promotora una illa CpG. La relació entre els dos tipus de canvis de metilació ha estat objecte de molt pocs estudis i, sovint, es mostren els dos canvis com conseqüències d'un mateix procés general, contribuint de manera conjunta al procés tumoral.

L'elaboració d'un estudi global dels canvis de metilació genòmica, juntament amb altres dades genètiques i clinicopatològiques de les mostres, ens va permetre analitzar: (1) el grau d'interrelació entre els dos canvis, (2) la contribució específica de cadascun d'ells al llarg del procés tumoral, i (3) el seu valor pronòstic. Concretament, es descriuen els resultats obtinguts en l'aplicació de la tècnica AIMS a una sèrie llarga de tumors colorectals (n=98). De manera molt resumida, la utilització de l'AIMS ens va permetre obtenir informació dels canvis de metilació associats al procés tumoral en més de 200 fragments genòmics i, a partir d'aquests canvis, vam poder fer una estimació del grau d'hipo- i hipermetilació de cada tumor.

Human Molecular Genetics, 2005, Vol. 14, No. 2 ***319–326***
doi:10.1093/hmg/ddi028
Advance Access published on December 1, 2004

Differential DNA hypermethylation and hypomethylation signatures in colorectal cancer

Jordi Frigola[1], Xavier Solé[2], Maria F. Paz[3], Victor Moreno[2], Manel Esteller[3], Gabriel Capellà[2] and Miguel A. Peinado[1,*]

[1]IDIBELL-Institut de Recerca Oncològica and [2]IDIBELL-Institut Català d'Oncologia, L'Hospitalet, Barcelona, Spain and [3]Cancer Epigenetics Laboratory, Spanish National Cancer Center (CNIO), Madrid, Spain

Received August 27, 2004; Revised October 28, 2004; Accepted November 23, 2004

Cancer cells are characterized by a generalized disruption of the DNA methylation pattern involving an overall decrease in the level of 5-methylcytosine together with regional hypermethylation of particular CpG islands. The extent of both DNA hypomethylation and hypermethylation in the tumor cell is likely to reflect distinctive biological and clinical features, although no studies have addressed its concurrent analysis until now. DNA methylation profiles in sporadic colorectal carcinomas, synchronous adenoma–carcinoma pairs and their matching normal mucosa were analyzed by using the amplification of inter-methylated sites (AIMS) method. A total of 208 AIMS generated sequences were tagged and evaluated for differential methylation. Global indices of hypermethylation and hypomethylation were calculated. All tumors displayed altered patterns of DNA methylation in reference to normal tissue. On average, 24% of the tagged sequences were differentially methylated in the tumor in regard to the normal pair with an overall prevalence of hypomethylations to hypermethylations. Carcinomas exhibited higher levels of hypermethylation than did adenomas but similar levels of hypomethylation. Indices of hypomethylation and hypermethylation showed independent correlations with patient's sex, tumor staging and specific gene hypermethylation. Hierarchical cluster analysis revealed two main patterns of DNA methylation that were associated to particular mutational spectra in the *K-ras* and the *p53* genes and alternative correlates of hypomethylation and hypermethylation with survival. We conclude that DNA hypermethylation and hypomethylation are independent processes and appear to play different roles in colorectal tumor progression. Subgroups of colorectal tumors show specific genetic and epigenetic signatures and display distinctive correlates with overall survival.

INTRODUCTION

Colorectal cancer is one of the best-studied systems of multistage human carcinogenesis. Epigenetic modification of DNA in the form of hypomethylation was included in early Vogelstein's tumor progression model together with a series of genetic alterations (1). DNA methylation is a post-replication modification predominantly found in cytosines of the dinucleotide CpG that is infrarepresented throughout the genome except at small regions named CpG islands (2). The pattern of DNA methylation in a given cell appears to be associated with the stability of gene expression states (3).

The biological significance of DNA hypomethylation, an early and common feature in colorectal cancer (4), is poorly understood (5). A relationship between global hypomethylation and genetic instability has been postulated (5,6). More recently, the attention of investigators has shifted to the study of cancer-associated regional hypermethylation at specific CpG islands and its association to transcriptional silencing (7,8) and loss of imprinting (9). Inspite of the large number of studies that have investigated cancer-associated hypermethylation in selected CpG islands, the obtention of global estimates of genome hypermethylation has been seldomly addressed (3,10,11).

Therefore, the roles of cumulated hypermethylation and hypomethylation in colorectal cancer progression and outcome are still unknown. By application of a methylome fingerprinting technique (amplification of inter-methylated sites, AIMS) (12), we have obtained information on the methylation status of more than 200 selected sequences in a

*To whom correspondence should be addressed at: IDIBELL-Institut de Recerca Oncològica, Hospital Duran i Reynals, Granvia km 2.7, 08907 L'Hospitalet, Barcelona, Spain. Tel: +34 932607464; Fax: +34 932607466; Email: mpeinado@iro.es

series of colorectal carcinomas collected in a prospective design. We have also analyzed 11 adenomas synchronous to carcinomas of the former series. AIMS bands represent unique short DNA sequences (up to ~1 kb long) flanked by two methylated *Sma*I sites (CCCGGG). Lack of methylation at either site will prevent amplification of the band. The AIMS generated sequences that can be tagged, isolated and individually characterized (12–14). Global estimates of hypermethylation and hypomethylation in the tumor in regard to the paired normal tissue have been used to investigate the possible association of DNA methylation profiles with genetic and clinicopathological parameters. Our results unveil different roles for hypermethylation and hypomethylation in colorectal cancer progression and clinical behavior.

RESULTS

Selection of samples and AIMS bands

A total of 93 carcinomas and 11 adenomas with their paired normal tissues produced reproducible and consistent AIMS fingerprints and were included in the analysis of DNA methylation indices. Five additional cases showed inconsistent results in one or more AIMS experiments and were not considered for analysis. Most failures could be attributed to genomic DNA degradation.

DNA methylation profiles were obtained in three AIMS experiments performed with different sets of primers. On the basis of band display consistency (see Materials and Methods), 208 sequences were tagged and considered for analysis (set A: 77 bands, set B: 62 bands and set C: 69 bands). An illustrative example is shown in Figure 1. Differential display of certain bands was observed among normal tissues, indicating the polymorphic nature of their representation. Eighty-four tagged bands (40%) were present in all normal tissues and therefore considered as non-polymorphic. Sixty-four bands were low polymorphic (31%) and 60 (29%) were high polymorphic (see Materials and Methods). Because it has been noted that DNA methylation in normal tissues may be related to aging (15), we investigated the possible association of apparent polymorphisms with age. Fifteen of the high polymorphic sequences exhibited age-related display (14 were lost and one gained associated to aging) and were excluded from the analysis. At the end, 193 tagged bands were scored for differential display between normal and tumor tissues, allowing the calculation of indices of hypermethylation (increase in the intensity of the band) and hypomethylation (decrease in the intensity of the band) in each tumor in relation to its paired normal tissue.

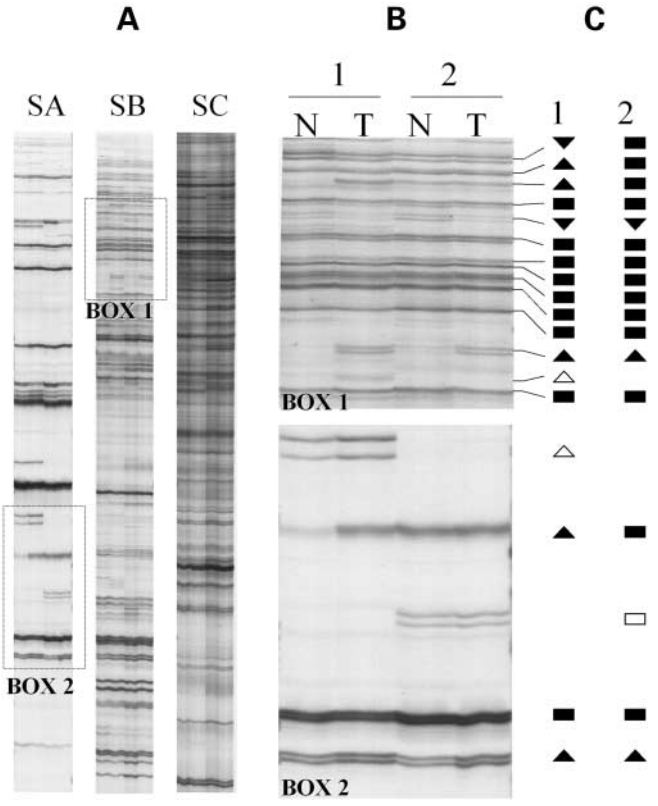

Figure 1. AIMS analysis of two normal (N)–tumor (T) pairs. (**A**) A general image of the fingerprints generated with each of the three primer sets (SA, SB and SC). Boxed areas in (A) are shown enlarged in (**B**). (**C**) Band intensity changes in the tumor in regard to the paired normal tissue. Hypermethylations (gain of intensity) and hypomethylations are indicated by up and down arrowheads, respectively. No changes are represented by rectangles. Polymorphic bands are shown as empty geometric figures.

Tagged bands behavior

On average, a given tagged band was informative in 88 ± 5 (range 72–93) normal–tumor pairs. All tagged bands showed differential DNA methylation in at least one tumor when compared with normal tissue and showed a wide distribution of the hypermethylation/hypomethylation ratios (Fig. 2A). Almost half of the tagged bands (46%) underwent more hypomethylations than hypermethylations (>2-fold), whereas only 16% of the tagged bands showed the opposite behavior. Hypermethylation and hypomethylation showed a negative correlation ($r = -0.196$ and $P = 0.006$), indicating that most bands tended to be either hypermethylated or hypomethylated (Fig. 2A). Recurrent changes affecting >25% of the tumors appeared as hypomethylated in 13 bands and hypermethylated in four bands. Polymorphic and non-polymorphic sequences showed similar behavior in regard to the likelihood of change between normal and tumor, although the most recurrent hypermethylations and hypomethylations occurred in polymorphic and non-polymorphic bands, respectively (Supplementary Material, Figs S1 and S2). Isolation and sequence characterization have been performed in a subset of the tagged bands. These data are supplied in Supplementary Material (Appendix A).

DNA methylation indices in colorectal carcinomas

The DNA methylation indices were obtained from the analysis of 185 ± 20 tagged bands per case (range 123–193). Hypomethylation was more prominent than hypermethylation ($P < 0.001$) (Table 1), although a wide distribution of the hypermethylation/hypomethylation ratios was observed (Fig. 2B). The main associations between the indices of DNA hypomethylation and hypermethylation and different

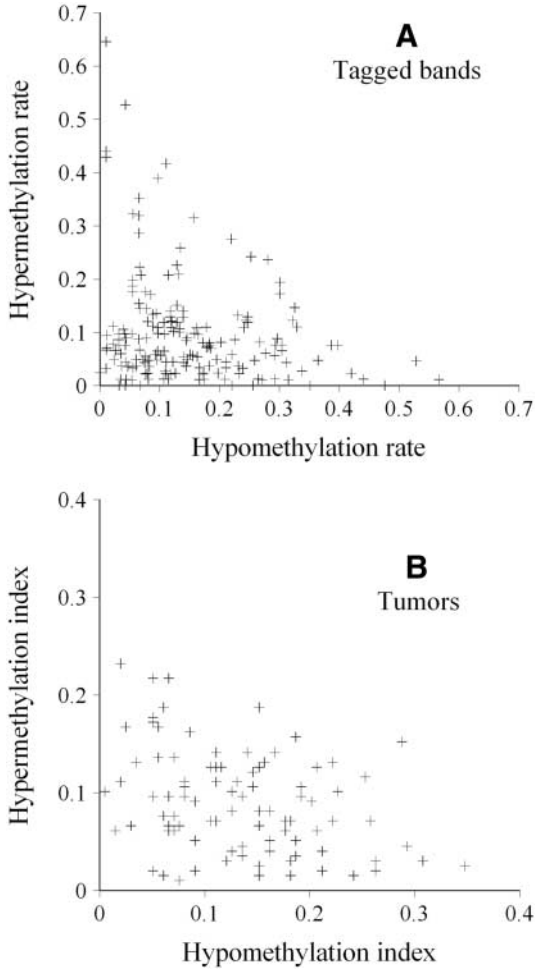

Figure 2. (**A**) Distribution of the hypomethylation and hypermethylation rates in the 193 AIMS bands considered. (**B**) Distribution of the hypomethylation and hypermethylation indices in the 93 colorectal carcinomas analyzed.

genetic and clinicopathological parameters are summarized in Table 1. No significant differences in the DNA methylation indices were observed regarding age (data not shown), tumor localization, *p53* and *K-ras* mutations and MSI. However, a remarkable sexual dimorphism was observed regarding both the hypermethylation and the hypomethylation indices. The hypermethylation index was higher in tumors with distant invasion, although it did not reach statistical significance ($P = 0.062$). Note that a strong correlation was found between the hypermethylation index and the number of hypermethylated specific gene promoters, suggesting that generalized hypermethylation equally affects sequences generated by AIMS and the promoter regions of selected genes with a putative role in carcinogenesis. Individual case results are available in Supplementary Material (Appendix B).

DNA methylation indices along the adenoma–carcinoma transition

Indices of DNA hypermethylation and hypomethylation (in reference to normal tissue) were obtained in 11 cases with paired adenoma and carcinoma. The number of tagged bands per case was 174 ± 17 (range 124–180). Carcinomas showed enhanced indices of hypermethylation when compared with adenomas ($P = 0.030$), whereas hypomethylation was similar in both adenomas and carcinomas (Fig. 3A). These results indicate that hypomethylation is an early event in tumor progression, whereas hypermethylation accumulates in more advanced stages. This trend is clearly illustrated in the representation of the hypermethylation/hypomethylation ratios of the adenoma–carcinoma pairs (Fig. 3B). In regard to the methylation status of the panel of six CpG islands specifically investigated (*hMLH1*, *APC*, *p16*, *p14*, *MGMT* and *LKB1*) and previously reported to be hypermethylated in cancer (16), a similar number of methylated genes was observed in carcinomas (1.5 ± 0.8) and adenomas (1.3 ± 0.8). The methylation profile was not always coincident in the adenoma–carcinoma pairs (data not shown), suggesting the basic role of stochastic components behind the occurrence and clonal expansion of these alterations.

Profiles of DNA methylation in colorectal carcinomas

Next, we studied whether common patterns of DNA methylation could be used to classify tumors. Two-way hierarchical cluster analysis of AIMS data outlined two main groups of tumors and four main groups of tags (Fig. 4A). As expected, the two clusters of tumors were characterized by the prevalence of either hypermethylations (cluster 1) or hypomethylations (cluster 2) (Table 2). Thirty tagged bands exhibited differential behavior between the two groups of tumors: 12 tagged bands grouped as class 1 (Fig. 4A) showed hypermethylation in group 1 and hypomethylation or unchanged in group 2; 18 tagged bands grouped as class 2 showed hypomethylation in cluster 2 tumors and mostly unchanged in cluster 1. Bands with similar behavior in both clusters of tumors were classified as class 3 (hypermethylation) and 4 (hypomethylation). Interestingly, the two clusters of tumors displayed multiple distinctive molecular and phenotypic traits including tumor staging and specific spectra of mutations in the *K-ras* and *p53* genes (Table 2). No statistically significant differences were observed for the rest of the parameters considered (data not shown).

DNA methylation indices as a prognostic factor

The indices of hypermethylation and hypomethylation were not indicators of prognosis in univariate and multivariate analyses. Cox regression analysis showed a trend for hypomethylation with poor prognosis and hypermethylation with good prognosis (data not shown), although the association was not significant. When the analysis was performed separately for the two clusters of tumors, a higher hypermethylation index was associated to good prognosis in tumors belonging to cluster 1, whereas in cluster 2, a higher hypomethylation index was associated to poor survival (Fig. 4B). Moreover, in cluster 1, the hypermethylation index (lower 50th percentile) was an independent predictor of survival (HR = 3.2, CI 95% 1.2–8.3 and $P = 0.015$) when compared with the Dukes' stage (C–D versus A–B, HR = 2.5, CI 95% 0.9–6.8 and $P = 0.064$).

Table 1. Indices of DNA hypermethylation and hypomethylation in colorectal carcinomas

	Categories[a]	Hypermethylation index	*P*-value[b]	Hypomethylation index	*P*-value[b]
All carcinomas		0.096 ± 0.060		0.146 ± 0.081	
Sex	Female (40)	0.113 ± 0.072	0.021	0.123 ± 0.082	0.015
	Male (53)	0.084 ± 0.047		0.164 ± 0.077	
Localization	Left (66)	0.101 ± 0.064	0.258	0.147 ± 0.089	0.813
	Right (27)	0.082 ± 0.050		0.143 ± 0.059	
Duke stage	A–B (49)	0.085 ± 0.053	0.062	0.157 ± 0.079	0.192
	C–D (44)	0.109 ± 0.066		0.135 ± 0.083	
p53 gene	Wild-type (58)	0.096 ± 0.060	0.916	0.140 ± 0.077	0.210
	Mutated (35)	0.095 ± 0.062		0.162 ± 0.089	
K-ras gene	Wild-type (55)	0.097 ± 0.054	0.728	0.154 ± 0.081	0.231
	Mutated (37)	0.093 ± 0.070		0.133 ± 0.081	
MSI status	Stable (83)	0.096 ± 0.062	0.464	0.149 ± 0.082	0.660
	Instable (5)	0.075 ± 0.044		0.165 ± 0.083	
Methylated genes[c]	<3 (65)	0.084 ± 0.056	<0.001	0.156 ± 0.081	0.091
	≥3 (10)	0.159 ± 0.059		0.106 ± 0.091	

[a]Numbers in parentheses indicate number of cases in each group.
[b]Two tailed *t*-test.
[c]Six genes were included in the analysis: *hMLH1*, *APC*, *p16*, *p14*, *MGMT* and *LKB1*.

DISCUSSION

Several conclusions may be drawn from the direct analysis of the raw data. Firstly, the DNA methylation pattern of the normal colonic mucosa is variable among individuals. The polymorphic nature of the band did not appear to affect its behavior in the tumor (hypomethylation or hypermethylation) and therefore we have made no distinction in the calculation of the indices, except for the age-related polymorphisms (8% of the screened CpG sites), which were excluded from further analysis. Secondly, the cancer-related changes tend to be unidirectional for each sequence: some bands preferentially show hypomethylations, whereas others display hypermethylations (Figs 2A and 4A). For most bands, a predominance of hypomethylation over hypermethylation was observed, which is in agreement with other studies (5,17). Note that many bands showed an erratic behavior, with hypermethylations in some tumors and hypomethylations in others. These results may be explained by the heterogeneous nature of the methylation in the sample due to allele-specific methylation (imprinting) or tissue heterogeneity (i.e. endothelial tissue may show different patterns than epithelial tissue). Therefore, the increase (or decrease) in the intensity of a band in the tumor when compared with the same preexisting band in the normal tissue sample should be interpreted as the homogenization of the methylated (or unmethylated) status rather than as a *de novo* methylation change.

DNA methylation indices in colorectal carcinomas

Our estimations of the overall abnormal DNA methylation in the tumor are a novel figure, and reveal the ubiquity of epigenetic alterations in colorectal neoplasia together with its wide range from tumor to tumor (7–44% of the tagged bands). The fraction of hypermethylated CpG sites in colorectal adenomas and carcinomas when compared with normal tissue (~10% of the screened sequences) is in the same range as data reported by using CpG island array approaches in different types of human tumors (10,11). The hypermethylation index was associated with the number of methylated gene promoters analyzed by MSP (Table 1). Therefore, we can postulate that both the sequences represented in AIMS fingerprints and the genes selected because of their putative role in tumorigenesis display a common signature of the same process. In this sense, the AIMS approach has been recently used successfully to identify new hypermethylated genes in colon cancer (13). Regarding overall hypomethylation, most of the data in the literature have been generated by determination of the 5dC content in the genome. Note that the reported demethylation levels in colorectal neoplasia (4,18–21) are in similar ranges as our estimations, suggesting that the AIMS fingerprints are also representative of the genomic global methylation status.

The sexual dimorphism in the DNA methylation profile has been noted previously in the analysis of specific CpG islands, with higher frequencies of hypermethylation at specific loci in women (22,23). Conversely, we also report that hypomethylation is higher in men (Table 1). We have no clues on the causes and possible implications of the gender-specific differences, but they deserve further investigation.

As a whole, the indices of hypermethylation and hypomethylation displayed a continuous distribution and did not appear to differentiate subgroups of tumors with distinctive features. The CpG island methylator phenotype described by Toyota *et al.* (24) was not foreseen from our data. We also did not find the reported correlations between hypermethylation and right localization, MSI and *K-ras* mutations (22,24,25). The significance of this classification should be revised under the light of recent studies (26,27), whose conclusions are supported by our results.

DNA methylation changes along tumor progression

The comparison of the methylation profiles between adenomas and carcinomas has confirmed that hypomethylation is an early event in colorectal cancer (4,18,21,28), whereas cumulated hypermethylation is more prominent in carcinomas.

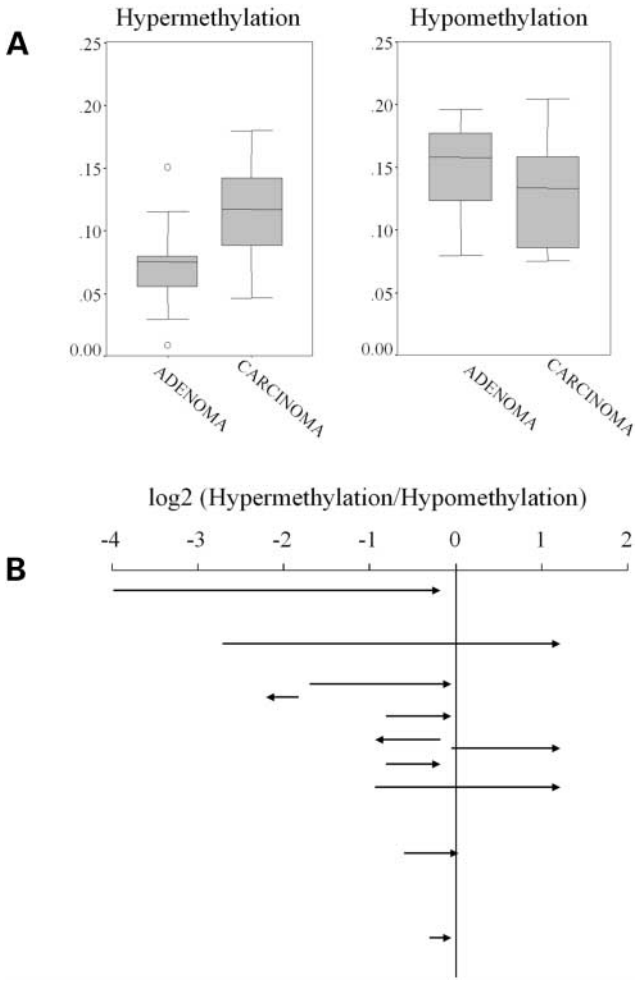

Figure 3. (**A**) Box plot of hypermethylation and hypomethylation indices in paired adenomas and carcinomas. (**B**) Shift in the hypermethylation/hypomethylation ratio between synchronous adenomas (arrow origin) and carcinomas (arrow head). The log 2 transformation of the ratio is represented in the *x*-axis. Samples have been sorted (*y*-axis) according to the hypermethylation index of the adenoma (at the top, the lowest hypermethylation index).

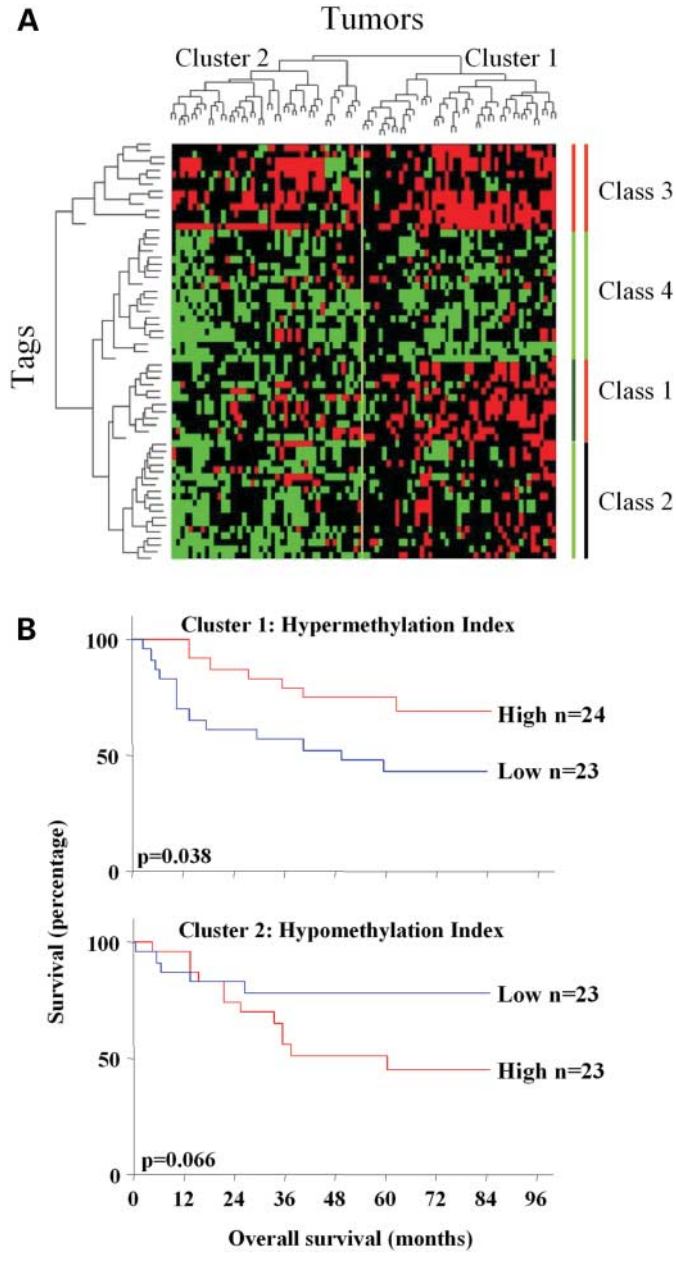

Figure 4. (**A**) Tree-type classification and heat map representation of the tumors (columns) and bands (rows) in two-way hierarchical clustering. Hypomethylation is green-coded, hypermethylation is red-coded and no change is shown black. The two bars at right represent the average status of the four classes of tags in the two clusters of tumors following the same color-code. (**B**) Kaplan–Meier overall survival curves in the two clusters of tumors classified by their DNA methylation signatures. A high hypermethylation index (50th percentile) was an indicator of better outcome in cluster 1 tumors (upper panel). A high hypomethylation index (50th percentile) was an indicator of poor outcome in cluster 2 tumors (lower panel). Survival rates have been corrected by the number of survivors after each time-point. Curves have been traced to the last recorded event.

The trend to accumulate methylations is also exhibited in carcinoma progression, where advanced Dukes' stages showed higher levels than early stages (Table 1). These trends are not clearly reflected in the methylation of specific CpG islands, although in most cases the number of hypermethylated CpG islands tends to be higher in carcinomas than in adenomas (our data) (21,24) and in high grade tumors (22). In any case, the hypermethylation profile of concurrent adenomas and carcinomas is fluctuating and probably reflects the concomitant implication of multiple factors including heterogeneity and the diversity of markers analyzed.

Because we are simultaneously detecting two opposite phenomena (hypermethylation and hypomethylation) in the same experiment, an apparent inverse correlation is obtained between the two indices of hypomethylation and hypermethylation; this result may indicate the alternative prevalence of one of the two converse processes in a group of tumors (the tails of the distribution). Nevertheless, the presence of both types of changes in all the tumors and the continuity of the hypermethylation/hypomethylation ratio distribution (Fig. 2B) suggests that gains and losses of DNA methylation are governed by different mechanisms and selective pressures

Table 2. Molecular and phenotypic characteristics of tumors classified by the DNA methylation profile

Parameter	Categories	Cluster 1 ($n = 47$)	Cluster 2 ($n = 46$)	P-value[a]
Hypermethylation index	—	0.116 ± 0.066	0.076 ± 0.047	0.001
Hypomethylation index	—	0.098 ± 0.057	0.196 ± 0.071	<0.001
DMI	—	0.214 ± 0.070	0.272 ± 0.081	<0.001
Dukes' stage	A–B	19	30	0.022
	C–D	28	16	
K-ras point mutation[b]	Transition	17	11	0.032
	Transversion	1	8	
	Negative	29	26	
p53 point mutation[c]	Transition at CpG	7	12	0.034
	Other point mutation	8	1	
	Negative	27	27	
Methylated genes[d]	<3	26	34	0.076
	≥3	7	2	

[a]Two tailed *t*-test, Fisher's exact test or Chi-square as appropriate.
[b]Mutations at codons 12 and 13.
[c]Seven tumors showing insertions or deletions in the coding sequence of the *p53* gene were not included.
[d]Six genes were included in the analysis: *hMLH1*, *APC*, *p16*, *p14*, *MGMT* and *LKB1*.

and are therefore independent. Other studies have also noted the independent contribution of both processes to tumorigenesis in colorectal (21) and Wilms tumors (29).

Profiles of DNA methylation associate with molecular and clinicopathological features

We have defined groups of carcinomas by hierarchical clustering of the AIMS profiles. Tree-type classification of the tumors delineated two main branches that came up from the differential methylation of 30 tags. Tumors in each group showed, in addition to predictable differences in the hypermethylation/hypomethylation ratio, striking differences in the mutation profile of the *K-ras* and *p*53 genes. The hypermethylated tumors showed almost exclusively transition mutations (G>A) at codons 12 and 13 of the *K-ras* gene (Table 2). The association of MGMT promoter methylation with G>A transitions in the *K-ras* gene has been previously reported (30–32). In our series, the *MGMT* gene was also more frequently methylated in cluster 1 (39%) than in cluster 2 (22%), but differences did not reach statistical significance ($P = 0.099$). Hence, our data expand the association between the type of mutation in the *K-ras* gene and the methylation of MGMT promoter to a specific DNA methylation signature characterized by extensive hypermethylations. Preceding findings also sustain a relationship between the DNA methylation profile and the spectrum of mutations in the *p53* gene. Transitions at non-CpG sites (more frequent in cluster 1) have also been linked to MGMT promoter hypermethylation (31,33,34). In addition, the prevalence of transitions at CpG sites in hypomethylating tumors suggests that endogenous mechanisms (called as defective repair of spontaneously deamynated 5mC) are likely to play a major role in p53 mutagenesis in this group of tumors (35–38). Although our results are insufficient to sustain a categorization of tumors based on their DNA methylation profiles, the distinctive molecular associations here reported strongly support the involvement of hypomethylation and hypermethylation in alternative processes related to malignant transformation.

This analysis also provides a list of candidate targets showing generalized hypermethylations (Fig. 4, bands of class 3) or hypomethylations (bands of class 4), together with targets selectively affected in one or another cluster of tumors (classes 1 and 2). Ongoing studies in our laboratory are focused on the characterization and functional analysis of different recurrent alterations with a potential specific involvement in colorectal carcinogenesis.

DNA methylation and survival

To our knowledge, this is the first study investigating the prognostic value of global hypomethylation and hypermethylation in colorectal cancer. Although none of the indices of differential DNA methylation appears to have prognostic utility in itself, the alternative association of the hypermethylation and hypomethylation indices with patient outcome in each one of the clusters is consistent with the independent roles of hypermethylation and hypomethylation in tumor initiation and progression (39). The attainment of high levels of hypomethylation already in premalignant lesions together with its maintenance throughout tumor progression (18,21) suggests that this factor may play a key role in conferring the malignant potential since early stages.

In summary, the interplay of DNA hypermethylation and hypomethylation demonstrates two independent roles with significant associations with molecular and clinicopathological parameters in colorectal cancer. Characterization of DNA methylation signatures in tumors should be instrumental not only in the identification of markers with a potential applicability in diagnosis and prognosis, but also in the definition of the pathways of progression. Further studies should clarify the implications of genetic and epigenetic profiles in tumor management and treatment.

MATERIALS AND METHODS

Samples

A total of 98 colorectal carcinomas, with their paired non-adjacent areas of normal colonic mucosa, and 11 colorectal adenomas, synchronous with carcinomas included in the former series, were collected as fresh-frozen tissues within 2 h of removal and then stored at -80°C. All samples were obtained from the Hospital de la Santa Creu i Sant Pau (Barcelona, Spain). The study protocol was approved by the Ethics Committee. Colorectal carcinomas used in this study were characterized previously for microsatellite instability (MSI) (40), mutations in the *p53* and *K-ras* genes (41), and the methylation status of the promoter region of the genes *hMLH1*, *APC*, *p16*, *p14*, *MGMT* and *LKB1* by methylation-specific PCR (MSP) (19). Detailed individual data are available in Supplementary Material (Appendix B).

Analysis of differential DNA methylation by AIMS

AIMS method is based on the differential cleavage of isoschizomers with distinct methylation sensitivity and the selective amplification of the sequences flanked by two methylated *Sma*I (CCCGGG) sites that are ligated to an adaptor and a specific 3–4 nucleotide sequence (adjacent to the *Sma*I site) arbitrarily chosen by the investigator. Lack of methylation at either site prevents amplification of the band. A detailed description of the method may be found in Frigola *et al.* (12). All samples were analyzed in three independent AIMS experiments with different primer sets (sets A, B and C) using conditions previously described (12). In a preceding setting, four normal–tumor pairs were analyzed in quadruplicate to assess reproducibility of all three AIMS experiments. Only sharp bands that were reproducible and clearly distinguishable from the background were tagged and assessed for differential methylation in all the samples. Faint bands with inconsistent display due to small variations in gel electrophoresis quality were not included in the analysis. Double bands consisting of two strands of the same sequence where considered as a single tagged band. Because of the polymorphic display of some bands in the normal mucosa, we have defined three different types of bands according to their nature: non-polymorphic (bands present in all normal tissues), low polymorphic (present in $>90\%$ of the samples) and finally, high polymorphic (present in $<90\%$ of the samples). Referring to the last type, we studied a putative correlation with age. Tagged bands showing an age-related display in the normal tissue were not used for the calculation of indices of hypermethylation and hypomethylation in the tumor when compared with the normal tissue.

Tagged bands behavior

Differences in the intensity of tagged bands between the tumor and its paired normal tissue were ascertained by direct visual inspection of the film. Densitometric analysis was performed in a limited subset of experiments to validate band intensity differences (data not shown), but was considered unnecessary in normal–tumor comparisons as only clear changes were taken into account and considered as qualitative events. Therefore, a 'behavior' could be scored for all tagged bands in every comparison between the normal and the tumor. Three different behaviors were defined: 'hypermethylation' (increased intensity in the tumor), 'hypomethylation' (decreased intensity in the tumor) and 'no change' (no substantial differences of intensity). Selected DNA methylation changes detected by AIMS have been confirmed by bisulfite sequencing (12,13) (unpublished data).

DNA methylation indices

Indices of hypomethylation and hypermethylation in the tumor were calculated as the number of hypomethylated and hypermethylated tagged bands in the tumor (when compared to the normal pair) divided by the total number of tagged bands considered. A third index reflecting the sum of both indices (differential methylation index) was also calculated.

Statistical analysis

All results are expressed as mean $\pm$ SD. Statistical differences between variables were analyzed with unpaired/paired *t*-tests or analysis of variance (ANOVA), as appropriate. Contingency tables were analyzed by the Chi-square or Fisher's exact test. Survival curves were traced according to the Kaplan–Meier method using the 50th percentile as cutoff for groups of low and high indices of abnormal DNA methylation. The statistical significance between curves was tested using the log-rank test. Univariate and multivariate analyses were performed using Cox's proportional hazards model. Hazard ratios and their 95% confidence interval (CI) were derived from Cox's proportional models. All *P*-values are calculated from two-sided statistical tests. Hierarchical clustering using Euclidean distance between observations and complete linkage as agglomeration method was performed to analyze the presence of subsets of tumors with comparable patterns of methylation changes. Only tags with differential methylation in $>25\%$ of the tumors were included in cluster analysis.

SUPPLEMENTARY MATERIAL

Supplementary Material is available at HMG Online.

ACKNOWLEDGEMENTS

We thank Gemma Aiza and Mar Muñoz for excellent technical help. This work was supported by a grant from the Spanish Ministry of Education and Science (SAF2003/5821). J.F. was recipient of an FPU fellowship from the Ministry of Education and Science at the Universitat Autònoma de Barcelona.

REFERENCES

1. Fearon, E.R. and Vogelstein, B. (1990) A genetic model for colorectal tumorigenesis. *Cell*, **61**, 759–767.
2. Bird, A.P. (1986) CpG-rich islands and the function of DNA methylation. *Nature*, **321**, 209–213.
3. Plass, C. (2002) Cancer epigenomics. *Hum. Mol. Genet.*, **11**, 2479–2488.

4. Feinberg, A.P., Gehrke, C.W., Kuo, K.C. and Ehrlich, M. (1988) Reduced genomic 5-methylcytosine content in human colonic neoplasia. *Cancer Res.*, **48**, 1159–1161.
5. Ehrlich, M. (2002) DNA methylation in cancer: too much, but also too little. *Oncogene*, **21**, 5400–5413.
6. Eden, A., Gaudet, F., Waghmare, A. and Jaenisch, R. (2003) Chromosomal instability and tumors promoted by DNA hypomethylation. *Science*, **300**, 455.
7. Jones, P.A. and Baylin, S.B. (2002) The fundamental role of epigenetic events in cancer. *Nat. Rev. Genet.*, **3**, 415–428.
8. Esteller, M. (2002) CpG island hypermethylation and tumor suppressor genes: a booming present, a brighter future. *Oncogene*, **21**, 5427–5440.
9. Feinberg, A., Cui, H. and Ohlsson, R. (2002) DNA methylation and genomic imprinting: insights from cancer into epigenetic mechanisms. *Semin. Cancer Biol.*, **12**, 389.
10. Huang, T.H., Perry, M.R. and Laux, D.E. (1999) Methylation profiling of CpG islands in human breast cancer cells. *Hum. Mol. Genet.*, **8**, 459–470.
11. Costello, J.F., Fruhwald, M.C., Smiraglia, D.J., Rush, L.J., Robertson, G.P., Gao, X., Wright, F.A., Feramisco, J.D., Peltomaki, P., Lang, J.C. *et al.* (2000) Aberrant CpG-island methylation has non-random and tumour-type-specific patterns. *Nat. Genet.*, **24**, 132–138.
12. Frigola, J., Ribas, M., Risques, R.A. and Peinado, M.A. (2002) Methylome profiling of cancer cells by amplification of inter-methylated sites (AIMS). *Nucleic Acids Res.*, **30**, e28.
13. Paz, M.F., Wei, S., Cigudosa, J.C., Rodriguez-Perales, S., Peinado, M.A., Huang, T.H. and Esteller, M. (2003) Genetic unmasking of epigenetically silenced tumor suppressor genes in colon cancer cells deficient in DNA methyltransferases. *Hum. Mol. Genet.*, **12**, 2209–2219.
14. Sadikovic, B., Haines, T.R., Butcher, D.T. and Rodenhiser, D.I. (2004) Chemically induced DNA hypomethylation in breast carcinoma cells detected by the amplification of intermethylated sites. *Breast Cancer Res.*, **6**, 30.
15. Ahuja, N., Li, Q., Mohan, A.L., Baylin, S.B. and Issa, J.P. (1998) Aging and DNA methylation in colorectal mucosa and cancer. *Cancer Res.*, **58**, 5489–5494.
16. Esteller, M., Corn, P.G., Baylin, S.B. and Herman, J.G. (2001) A gene hypermethylation profile of human cancer. *Cancer Res.*, **61**, 3225–3229.
17. Issa, J.P. (2002) Epigenetic variation and human disease. *J. Nutr.*, **132**, 2388S–2392S.
18. Goelz, S.E., Vogelstein, B., Hamilton, S.R. and Feinberg, A.P. (1985) Hypomethylation of DNA from benign and malignant human colon neoplasms. *Science*, **228**, 187–190.
19. Esteller, M., Fraga, M.F., Guo, M., Garcia-Foncillas, J., Hedenfalk, I., Godwin, A.K., Trojan, J., Vaurs-Barriere, C., Bignon, Y.J., Ramus, S. *et al.* (2001) DNA methylation patterns in hereditary human cancers mimic sporadic tumorigenesis. *Hum. Mol. Genet.*, **10**, 3001–3007.
20. Paz, M.F., Avila, S., Fraga, M.F., Pollan, M., Capella, G., Peinado, M.A., Sanchez-Cespedes, M., Herman, J.G. and Esteller, M. (2002) Germ-line variants in methyl-group metabolism genes and susceptibility to DNA methylation in normal tissues and human primary tumors. *Cancer Res.*, **62**, 4519–4524.
21. Bariol, C., Suter, C., Cheong, K., Ku, S.L., Meagher, A., Hawkins, N. and Ward, R. (2003) The relationship between hypomethylation and CpG island methylation in colorectal neoplasia. *Am. J. Pathol.*, **162**, 1361–1371.
22. Hawkins, N., Norrie, M., Cheong, K., Mokany, E., Ku, S.L., Meagher, A., O'Connor, T. and Ward, R. (2002) CpG island methylation in sporadic colorectal cancers and its relationship to microsatellite instability. *Gastroenterology*, **122**, 1376–1387.
23. Laghi, L., Bianchi, P. and Malesci, A. (2003) Gender difference for promoter methylation pattern of hMLH1 and p16 in sporadic MSI colorectal cancer. *Gastroenterology*, **124**, 1165–1166.
24. Toyota, M., Ahuja, N., Ohe-Toyota, M., Herman, J.G., Baylin, S.B. and Issa, J.P. (1999) CpG island methylator phenotype in colorectal cancer. *Proc. Natl Acad. Sci. USA*, **96**, 8681–8686.
25. van Rijnsoever, M., Grieu, F., Elsaleh, H., Joseph, D. and Iacopetta, B. (2002) Characterisation of colorectal cancers showing hypermethylation at multiple CpG islands. *Gut*, **51**, 797–802.
26. Yamashita, K., Dai, T., Dai, Y., Yamamoto, F. and Perucho, M. (2003) Genetics supersedes epigenetics in colon cancer phenotype. *Cancer Cell*, **4**, 121–131.
27. Sieber, O.M., Heinimann, K. and Tomlinson, I.P. (2003) Genomic instability—the engine of tumorigenesis? *Nat. Rev. Cancer*, **3**, 701–708.
28. Wynter, C.V., Walsh, M.D., Higuchi, T., Leggett, B.A., Young, J. and Jass, J.R. (2004) Methylation patterns define two types of hyperplastic polyp associated with colorectal cancer. *Gut*, **53**, 573–580.
29. Ehrlich, M., Jiang, G., Fiala, E., Dome, J.S., Yu, M.C., Long, T.I., Youn, B., Sohn, O.S., Widschwendter, M., Tomlinson, G.E. *et al.* (2002) Hypomethylation and hypermethylation of DNA in Wilms tumors. *Oncogene*, **21**, 6694–6702.
30. Esteller, M., Toyota, M., Sanchez-Cespedes, M., Capella, G., Peinado, M.A., Watkins, D.N., Issa, J.P., Sidransky, D., Baylin, S.B. and Herman, J.G. (2000) Inactivation of the DNA repair gene O6-methylguanine-DNA methyltransferase by promoter hypermethylation is associated with G to A mutations in *K-ras* in colorectal tumorigenesis. *Cancer Res.*, **60**, 2368–2371.
31. Kim, S.G., Chan, A.O., Wu, T.T., Issa, J.P., Hamilton, S.R. and Rashid, A. (2003) Epigenetic and genetic alterations in duodenal carcinomas are distinct from biliary and ampullary carcinomas. *Gastroenterology*, **124**, 1300–1310.
32. Lees, N.P., Harrison, K.L., Hall, C.N., Margison, G.P. and Povey, A.C. (2004) Reduced MGMT activity in human colorectal adenomas is associated with *K-ras* GC > AT transition mutations in a population exposed to methylating agents. *Carcinogenesis*, **25**, 1243–1247.
33. Esteller, M., Risques, R.A., Toyota, M., Capella, G., Moreno, V., Peinado, M.A., Baylin, S.B. and Herman, J.G. (2001) Promoter hypermethylation of the DNA repair gene O(6)-methylguanine-DNA methyltransferase is associated with the presence of G : C to A : T transition mutations in *p53* in human colorectal tumorigenesis. *Cancer Res.*, **61**, 4689–4692.
34. Yin, D., Xie, D., Hofmann, W.K., Zhang, W., Asotra, K., Wong, R., Black, K.L. and Koeffler, H.P. (2003) DNA repair gene O6-methylguanine-DNA methyltransferase: promoter hypermethylation associated with decreased expression and G : C to A : T mutations of *p53* in brain tumors. *Mol. Carcinog.*, **36**, 23–31.
35. Tornaletti, S. and Pfeifer, G.P. (1995) Complete and tissue-independent methylation of CpG sites in the *p53* gene: implications for mutations in human cancers. *Oncogene*, **10**, 1493–1499.
36. Schmutte, C., Yang, A.S., Nguyen, T.T., Beart, R.W. and Jones, P.A. (1996) Mechanisms for the involvement of DNA methylation in colon carcinogenesis. *Cancer Res.*, **56**, 2375–2381.
37. Schmutte, C., Yang, A.S., Beart, R.W. and Jones, P.A. (1995) Base excision repair of U : G mismatches at a mutational hotspot in the *p53* gene is more efficient than base excision repair of T : G mismatches in extracts of human colon tumors. *Cancer Res.*, **55**, 3742–3746.
38. Laird, P.W. and Jaenisch, R. (1994) DNA methylation and cancer. *Hum. Mol. Genet.*, **3**, 1487–1495.
39. Gaudet, F., Graeme, J.G., Eden, A., Jackson-Grusby, L., Dausman, J., Gray, J.W., Leonhardt, H. and Jaenisch, R. (2003) Induction of tumors in mice by genomic hypomethylation. *Science*, **300**, 489–492.
40. Gonzalez-Garcia, I., Moreno, V., Navarro, M., Marti-Rague, J., Marcuello, E., Benasco, C., Campos, O., Capella, G. and Peinado, M.A. (2000) Standardized approach for microsatellite instability detection in colorectal carcinomas. *J. Natl Cancer Inst.*, **92**, 544–549.
41. Tortola, S., Marcuello, E., Gonzalez, I., Reyes, G., Arribas, R., Aiza, G., Sancho, F.J., Peinado, M.A. and Capella, G. (1999) *p53* and *K-ras* gene mutations correlate with tumor aggressiveness but are not of routine prognostic value in colorectal cancer. *J. Clin. Oncol.*, **17**, 1375–1381.

Age-dependent association of DNA hypomethylation with cumulated genomic damage and tumor aggressiveness in human colorectal cancer.

Jordi Frigola, Rosa-Ana Risques, Victor Moreno, Gabriel Capellà, Miguel A. Peinado

Sotmès a Human Molecular Genetics

CAPÍTOL 3

La correlació entre hipometilació i inestabilitat genòmica sempre ha estat objecte d'un intens debat. Un dels principals motius d'aquesta discussió és la dificultat tècnica per avaluar tant les pèrdues de metilació com la inestabilitat genòmica. La principal dificultat tècnica per mesurar la hipometilació *in vitro* és la manca de viabilitat dels *knock out* de les diferents DNMTs en ratolins. Els treballs *in vivo* es troben molt limitats pel número de tècniques capaces de fer una valoració global dels nivells d'hipometilació. Respecte de la inestabilitat genòmica, donat que es tracta d'un concepte de canvi o alteració en relació al temps, és difícil fer-ne una estimació correcta.

A partir de la familiarització del nostre grup amb les tècniques de *fingerprint*, es va realitzar un càlcul del dany genòmic present en el genoma tumoral, mitjançant la tècnica d'AP-PCR. De manera molt esquemàtica, aquesta tècnica ens permet obtenir informació de guanys i pèrdues genòmiques presents a diferents regions cromosòmiques, d'una manera no dirigida o prèviament seleccionada. A partir d'aquestes dades, es va elaborar un índex de dany genòmic que representa una estimació no esbiaixada del nivell d'alteracions estructurals. Paral·lelament, la tècnica AIMS ens permet fer una anàlisi o estimació no esbiaixada del grau d'hipometilació. En aquest capítol, es presenten els resultats que sorgeixen de la correlació entre els nivells d'hipometilació, mesurats per AIMS, i els de dany genòmic, mesurats per AP-PCR, en una sèrie llarga de càncer colorectals (n=83).

Age-dependent association of DNA hypomethylation with cumulated genomic damage and tumor aggressiveness in human colorectal cancer.

Jordi Frigola[1], Rosa-Ana Risques[1], Victor Moreno[2], Gabriel Capellà[2], Miguel A. Peinado[1]

[1] IDIBELL-Institut de Recerca Oncològica, L'Hospitalet, Barcelona, Spain

[2] IDIBELL-Institut Català d'Oncologia, L'Hospitalet, Barcelona, Spain

Correspondence: Miguel A. Peinado,
IDIBELL - Institut de Recerca Oncològica,
Hospital Duran i Reynals,
Granvia km 2.7,
08907 L'Hospitalet, Barcelona, Spain.
email: mpeinado@iro.es
Tel 34-93 2607464
Fax 34-93 2607466

Abbreviations: AIMS, Amplification of Inter-Methylated Sites; AP-PCR, Arbitrarily Primed Polymerase Chain Reaction; GDF, Genomic Damage Fraction; HR, hazard ratio

Note: RAR present address: Department of Pathology, University of Washington, Seattle, Washington 98195-7705, USA.

ABSTRACT

Cancer cells undergo concurrent genome-wide demethylation and regional hypermethylation of CpG islands. While both processes are evenly common in cancer, hypomethylation has been oftenly overlooked given the current predominant focus on promoter hypermethylation and epigenetic silencing of tumor suppressor genes. A link between DNA demethylation and chromosomal instability in carcinogenesis is supported by consistent although scarce evidences. All colorectal cancers show DNA hypomethylation although its extent is highly variable. The impact of the different levels of hypomethylation in cancer biology and chromosomal instability is unknown. In order to shed some light into this issue we have performed a comprehensive assessment of DNA methylation (by Amplification of Intermethylated Sites, AIMS) and chromosomal instability (by Arbitrarily Primed PCR, AP-PCR) in a series of colorectal carcinomas (n=83) and their paired normal tissue. A positive correlation between hypomethylation and genomic damage was observed ($p=0.022$) reinforcing the relationship between alterations at genomic and epigenomic level. This correlation was stronger in younger patients (≤67). Furthermore, the hypomethylation level was an independent prognostic factor in older patients (>67), and specially in those with advanced Dukes' stage tumors. These results suggest that the parallelism in the accumulation of both genetic and epigenetic alterations is age-dependent and that their implications are also age-related and different. Our data provide relevant information that supports a critical role of genome-wide hypomethylation in colorectal carcinogenesis. Moreover we believe that hypomethylation levels should be taken into account in the interpretation of the response to therapies using demethylating agents.

INTRODUCTION

Most of the colorectal cancers display some form of genomic instability in early stages, including subtle DNA sequence alterations, gross chromosomal rearrangements, aneuploidy and gene amplification (1). The wide heterogeneity of these aberrations suggests that a variety of different cellular processes might be affected. Specific functional defects can be associated with a characteristic pattern of genomic instability (2). In colorectal cancer, this is illustrated by the phenotype of postreplicative mismatch repair system (reviewed in (3)). However, the underlying causes of the others genetics aberrations are less clear.

It has been known for a long time that tumor cells are hypomethylated in comparison to normal cells (4, 5). These methylation changes constitute a hallmark even in early stages of colorectal cancer (6, 7). Hypomethylation of DNA has multiple mechanistic implications. It has been suggested that the hypomethylation of non-promoter regions of DNA and of structural elements, such as centromeric DNAs, might cause genomic instability (reviewed in (8)). Defects in DNA methylation have been linked to the chromosomal instability observed in aneuploid human colorectal cancer cell lines (9). Indeed, mitogen-stimulated cells from individuals affected with immunodeficiency, centromere instability and facial anomalies (ICF syndrome) show increased chromosomal rearrangements in hypomethylated centromeric regions (10). Moreover, an increased rate of mutation owing to DNMT1 deficiency has been observed in murine embryonic stem (ES) cells (11) and in murine somatic cells (12, 13).

Besides these evidences, the relationship between genome-wide hypomethylation and chromosomal instability has not been addressed form a quantitative point of view. This is critical taking into account the wide variation in the levels of the cumulated genetic (14-18) and epigenetic (19) alterations among human colorectal cancers. Moreover, it is still unclear the contribution of DNA hypomethylation to the biological and clinical properties of the tumor cell and how it interacts with other genetic factors, including the extent of chromosomal instability, in conferring specific behaviors. To address this issue we have obtained estimates of genomic disruption at chromosomal and DNA methylation level in a large series of colorectal carcinomas.

The extent of chromosomal alterations was assessed by Arbitrarily Primed PCR (AP-PCR). AP-PCR fingerprints obtained from normal and tumor DNA may be easily compared allowing the detection and characterization of genetic differences and the obtention of unbiased estimates of global genomic disruption (reviewed in (20)). The extent of DNA hypermethylation and hypomethylation was assessed by the Amplification of Intermethylated Sites (AIMS) technique (21). AIMS profiles represent unique sequences flanked by two methylated CpG sites. Differences in the display of AIMS amplified bands between paired

normal and tumor tissue correspond to changes in the methylation status of specific sequences (21-23). An estimate of the degree of DNA hypomethylation and hypermethylation in the tumor relative to the corresponding normal tissue has been obtained by combination of three independent AIMS experiments in a series of colorectal adenomas and carcinomas (19).

The correlates of the indices of genetic and epigenetic alterations with other genetic and clinical features of the tumors have been investigated, together with the possible interactions among them.

MATERIAL AND METHODS

Patients and tumor samples

A total of 83 patients were included in this study based on the availability of high-quality DNA from paired normal and tumor tissue. All the patients were diagnosed with colorectal cancer at the Hospital de la Santa Creu i Sant Pau (Barcelona, Catalonia, Spain) and prospectively included in a study designed to evaluate the prognostic value of specific genetic and epigenetic alterations. The Ethics Committee approved the study protocol. Briefly, the most important characteristics of the 83 cases included in the study were: 46 males and 37 females; mean age 67 $\pm$ 12 years (range, 33-96 years). Twenty tumors were located in the right colon and 63 in the left colon, including the rectum. The distribution of the carcinomas according to the modified Dukes' classification was: A+B, n=44; C, n=26 and D, n=13). It is of note that tumors exhibiting microsatellite instability (MSI) were not included in the study because it has been clearly established that this group constitutes a well differentiated entity with specific profiles of genetic and epigenetic alterations and distinctive biological features (reviewed in (24-26)). Analysis of MSI was performed as previously described (27). Transformed cell content was above 75% in most tumor specimens as assessed by histological examination. DNA from normal and tumor tissue was obtained by standard procedures.

Estimation of the Genomic Damage Fraction

Genetics alterations at chromosomal and subchromosomal level were assessed using the DNA fingerprinting technique Arbitrarily Primed PCR (AP-PCR). The AP-PCR is based on the amplification by PCR of genomic DNA using primers of arbitrarily chosen sequence and initial cycles of low stringency. Because the primer anneals to multiple sites, many PCR products are generated and result in a reproducible fingerprint when analyzed by gel

electrophoresis (28). Three independent experiments were performed for each sample. An index of cumulated alterations (Genomic Damage Fraction, GDF) was calculated as the number of bands with differential display in the tumor in regard to the paired normal tissue divided by the total number of bands visualized. Assay conditions and main associations of the GDF with genetic and clinical features of the tumors have been described in detail elsewhere (17).

Quantification of the degree of hypermethylation and hypomethylation

Comparative fingerprints representing the methylome of the tumor and the normal tissue were obtained by Amplification of Intermethylated Sites (AIMS). AIMS bands correspond to selected genomic sequences flanked by two methylated Sma I sites (CCCGGG). Lack of methylation at either site prevents amplification of the band. A total of 193 sequences generated in three independent experiments were scored for differential methylation between the normal and the tumor tissue. The index of hypomethylation was calculated as the number of hypomethylated sequences (bands with a decreased intensity in the tumor as compared to the normal tissue) divided by the total number of bands analyzed. Alternatively, the index of hypermethylation represented the fraction of hypermethylated sequences (bands with an increased intensity in the tumor as compared to the normal tissue). Assay conditions and technical validation of the approach has been described before (21). Main associations of the hypomethylation and hypermethylation indices with genetic and clinical features of the tumors have been also described in detail elsewhere (19).

Statistical analysis

All results are expressed as a mean ± SD. Statistical differences between variables were analyzed with unpaired/paired t tests or analysis of variance (ANOVA), and regression tests, as appropriate. Contingency tables were analyzed by the Chi-square or Fisher's exact test. Survival curves for quantitative variables (GDF and hypomethylation index) were traced according to the Kaplan-Meier method using the percentile 50% as cutoff for groups of low and high indices. The statistical significance between curves was tested using the log-rank test. Univariate and multivariate analyses were performed using the Cox proportional hazards model. Hazard ratios and their 95% confidence interval (CI) were derived from Cox's proportional models. All p values are calculated from two-sided statistical tests.

RESULTS

Relationship between the degree of genomic damage and hypomethylation

The GDF was 0.172±0.085 (range 0.015-0.389) per tumor. In other words, 17% of the genomic sequences represented in the three AP-PCR experiments were altered in the average tumor. As reported previously (17), higher levels of GDF were observed in tumors with p53 mutations (p=0.007). No differences regarding age, sex, Dukes' stage or K-ras mutations were observed. The index of hypomethylation was 0.149±0.082 (range, 0.005-0.356) and the hypermethylation 0.096±0.062 (range, 0.010-0.338). Hypomethylation and hypermethylation indices displayed different associations with genetic and clinicopathological characteristics of the tumors that have been described in detail (19).

A correlation between GDF and the hypomethylation index, but not hypermethylation index was observed (Figure 1A-B). In order to get insights into the nature and implications of the association between GDF and hypomethylation, we investigated the interaction GDF/hypomethylation with different characteristics of the tumors, including genetic profiles (mutations in the K-ras and p53 genes), patient's sex and age, tumor stage and patient's survival (Table 1). The most striking interaction was observed between age and GDF. Younger patients (≤67) showed a stronger association between GDF and hypomethylation (Figure 1C). This correlation was not maintained in older patients (>67).

As shown in previous studies, the GDF and hypomethylation index are indicators of poor prognosis when considered separately and in specific subgroups of colorectal cancers (17, 19). To assess if this association was independent we used multivariate Cox regression models to analyze overall survival. To simplify the presentation of the results, quantitative variables were dichotomized using the mean as the cutoff value. Therefore the hypomethylation index and the GDF were tagged as High (above the mean) and Low (below the mean). In a first analysis considering all patients (n=83), neither the hypomethylation index nor the GDF were independent prognostic factors when compared to Dukes' stage (Table 2). Due to the reported differentiated correlation between hypomethylation and GDF we considered a separated analysis of patients based on age. Interestingly, in older patients in which the hypomethylation index and the GDF do not correlate, the hypomethylation index appeared as an independent prognostic factor with predictive capacity equivalent to Dukes' stage (Table 2). As shown in Kaplan-Meier survival curves (Figure 2), high hypomethylation levels were indicative of very bad outcome in patients above 67 and in Dukes stages C or D.

DISCUSSION

Although DNA hypomethylation is a hallmark of colorectal cancer, the mechanistic implication in tumorigenesis is poorly understood (29). Besides the activation of specific genes (reviewed in (8)), probably the main consequence of generalized demethylation is genetic instability (8). In fact, much of the DNA hypomethylation occurs in highly and moderately repeated DNA sequences including heterochromatic DNA repeats, dispersed retrotranposons and endogenous retroviral elements. As described above different kind of studies support this association (11-13). Nevertheless, the scenario is probably more complex, because it has been also reported that a decrease of DNMT1 activity correlates with the reduction in the number of intestinal adenomas formed in the mice (30) and results in opposite effects on the development of two different types of tumor (31). Furthermore, limiting DNA methylation did not appear to increase either point mutations nor genomic rearrangements in transgenes of exogenous origin in murine ES cells (32). These inconsistencies raise questions about the nature and extent of this association and the biological implications that may have in carcinogenesis.

In order to shed some light into this issue and after a specific study to discern the role of DNA hypermethylation and hypomethylation in colorectal cancer, we have explored the association between genome-wide demethylation and chromosomal instability in a large series of human colorectal carcinomas. We have used DNA fingerprinting techniques to obtain global estimates of both genomic alterations (AP-PCR) and DNA hypomethylation (AIMS). This has the advantage of using techniques that may be applied to samples obtained in clinical settings. Moreover, the data generated are of similar nature and therefore common criteria can be applied to its analysis.

In previous studies we and other have demonstrated the feasibility of AP-PCR to detect tumor specific genetic alterations including chromosomal losses and gains (33-42). The application of this technique to series of colorectal cancers was also instrumental in the discovery of ubiquitous microsatellite instability in a subset of tumors (43). Furthermore, due to its capacity to simultaneously screen for multiple alterations genome-wide in an unbiased manner, it has also been applied to the assessment of cumulated genomic damage in colorectal (44, 45), lung (46) and stomach (47) cancers.

On the other hand, the DNA methylation has been evaluated by AIMS technique. This technique constitutes a sensitive and unbiased approach to screen for methylation changes in the methylome of cancer cell. Noteworthy, both types of DNA methylation changes (hyper- and hypomethylations) can be evaluated independently in the same experiment. As reported

before, we have generated two different methylation indices reflecting the extent of hypermethylation and hypomethylation changes. Because the amplified sequences are distributed genome wide but are preferentially located in gene-rich regions (21), the indices are likely to represent the overall trend in functional sequences.

To our knowledge, there are no previous studies comparing the degree of genomic damage with global estimates of hypermethylation and hypomethylation. In a previous study we have shown that hypermethylation increases through tumor progression (19), nevertheless this increase is not parallel to the accumulation of chromosomal alterations, indicating the independence of both processes.

In agreement with previous studies, hypomethylation levels correlated with the index of genomic alterations, although a wide variability was observed (Figure 1). A deeper examination of the data revealed that this correlation was much stronger in younger patients (Figure 1). Because DNA hypomethylation is an early event already present in benign adenomas (6, 19), these results suggest that it is in this subgroup of patients were DNA hypomethylation may play a more important role in genome instabilization. While age-dependent hypermethylation of specific loci has been reported (48), the total level of methylated cytosines diminishes in aging (49). Therefore, it can be hypothesized that the mechanisms and perhaps the nature and the consequences of the epigenetic changes occurring in the elderly may be distinct from those appearing in the younger patient. Characterization of the sequences undergoing tumor demethylation in young and old patients together with those that undertake age-dependent hypomethylation should contribute to clarify this issue.

We have previously reported a trend of high hypomethylation with poorer survival. Here we have analyzed the possible interaction of hypomethylation with genomic damage in modifying the outcome. While either GDF and the hypomethylation index add little information to a simplified Dukes' stage classification system when considering the whole collection, differences have been also observed when separating the samples according to the patient's age. In this case, high hypomethylation levels were an indicator of poor prognosis and independent of Dukes' stage (Table 2 and Figure 2). While this study is too preliminary to propose the application of the analysis of hypomethylation levels as a prognostic factor, we believe that our data provide relevant information that supports a critical role of genome-wide hypomethylation in colorectal carcinogenesis.

New therapies based on the reactivation of silenced tumor suppressor genes by using demethylating agents appear as promising alternatives (reviewed in (8, 50)). Based in our findings, we anticipate that opposite responses might be expected in patients with different

epigenetic profiles. We suggest that hypomethylation levels in normal and tumor tissue may condition the response to such treatments and therefore they should be taken into account to interpret the results. Future studies should elucidate the mechanisms involved in the age- and tumor-related hypomethylation and contribute to the design of more effective and personalized treatments.

ACKNOWLEDGEMENTS

We thank Gemma Aiza and Mar Muñoz for excellent technical help. This work was supported by a grant from the Spanish Ministry of Education and Science (SAF2003/5821). JF was recipient of a fellowship from the Ministry of Education and Science at the Universitat Autònoma de Barcelona. RAR was recipient of a fellowship from the Comissió Interdepartamental de Recerca i Innovació Tecnològica (CIRIT).

REFERENCES

1. Schar, P. (2001) Spontaneous DNA damage, genome instability, and cancer - when DNA replication escapes control. *Cell,* **104**, 329-332.
2. Lengauer, C., Kinzler, K.W. and Vogelstein, B. (1998) Genetic instabilities in human cancers. *Nature,* **396**, 643-649.
3. Jiricny, J. (1998) Replication errors: cha(lle)nging the genome. *EMBO J.,* **17**, 6427-6436.
4. Gama-Sosa, M.A., Slagel, V.A., Trewyn, R.W., Oxenhandler, R., Kuo, K.C., Gehrke, C.W. and Ehrlich, M. (1983) The 5-methylcytosine content of DNA from human tumors. *Nucleic Acids Res.,* **11**, 6883-6894.
5. Feinberg, A.P. and Vogelstein, B. (1983) Hypomethylation distinguishes genes of some human cancers from their normal counterparts. *Nature,* **301**, 89-92.
6. Goelz, S.E., Vogelstein, B., Hamilton, S.R. and Feinberg, A.P. (1985) Hypomethylation of DNA from benign and malignant human colon neoplasms. *Science,* **228**, 187-190.
7. Feinberg, A.P., Gehrke, C.W., Kuo, K.C. and Ehrlich, M. (1988) Reduced genomic 5-methylcytosine content in human colonic neoplasia. *Cancer Res.,* **48**, 1159-1161.
8. Feinberg, A.P. and Tycko, B. (2004) The history of cancer epigenetics. *Nat. Rev. Cancer,* **4**, 143-153.
9. Lengauer, C., Kinzler, K.W. and Vogelstein, B. (1997) DNA methylation and genetic instability in colorectal cancer cells. *Proc. Natl. Acad. Sci. U. S. A.,* **94**, 2545-2550.
10. Xu, G.L., Bestor, T.H., Bourc'his, D., Hsieh, C.L., Tommerup, N., Bugge, M., Hulten, M., Qu, X., Russo, J.J. and Viegas-Pequignot, E. (1999) Chromosome instability and immunodeficiency syndrome caused by mutations in a DNA methyltransferase gene. *Nature,* **402**, 187-191.
11. Chen, R.Z., Pettersson, U., Beard, C., Jackson-Grusby, L. and Jaenisch, R. (1998) DNA hypomethylation leads to elevated mutation rates. *Nature,* **395**, 89-93.
12. Eden, A., Gaudet, F., Waghmare, A. and Jaenisch, R. (2003) Chromosomal instability and tumors promoted by DNA hypomethylation. *Science,* **300**, 455.
13. Gaudet, F., Graeme, J.G., Eden, A., Jackson-Grusby, L., Dausman, J., Gray, J.W., Leonhardt, H. and Jaenisch, R. (2003) Induction of tumors in mice by genomic hypomethylation. *Science,* **300**, 489-492.
14. Dutrillaux, B. (1995) Pathways of chromosome alteration in human epithelial cancers. *Adv. Cancer Res.,* **67**, 59-82.
15. Stoler, D.L., Chen, N., Basik, M., Kahlenberg, M.S., Rodriguez-Bigas, M.A., Petrelli, N.J. and Anderson, G.R. (1999) The onset and extent of genomic instability in

sporadic colorectal tumor progression. *Proc. Natl. Acad. Sci. U. S. A.,* **96**, 15121-15126.

16. Hawkins, N.J., Tomlinson, I., Meagher, A. and Ward, R.L. (2001) Microsatellite-stable diploid carcinoma: a biologically distinct and aggressive subset of sporadic colorectal cancer. *Br. J. Cancer,* **84**, 232-236.
17. Risques, R.A., Moreno, V., Ribas, M., Marcuello, E., Capella, G. and Peinado, M.A. (2003) Genetic pathways and genome-wide determinants of clinical outcome in colorectal cancer. *Cancer Res.,* **63**, 7206-7214.
18. Giaretti, W., Venesio, T., Sciutto, A., Prevosto, C., Geido, E. and Risio, M. (2003) Near-diploid and near-triploid human sporadic colorectal adenocarcinomas differ for KRAS2 and TP53 mutational status. *Genes. Chromosomes Cancer,* **37**, 207-213.
19. Frigola, J., Sole, X., Paz, M.F., Moreno, V., Esteller, M., Capella, G. and Peinado, M.A. (2005) Differential DNA hypermethylation and hypomethylation signatures in colorectal cancer. *Hum. Mol. Genet.,* **14**, 319-326.
20. Risques, R.A., Ribas, M. and Peinado, M.A. (2003) Assessment of cumulated genetic alterations in colorectal cancer. *Histol. Histopathol.,* **18**, 1289-1299.
21. Frigola, J., Ribas, M., Risques, R.A. and Peinado, M.A. (2002) Methylome profiling of cancer cells by amplification of inter- methylated sites (AIMS). *Nucleic Acids Res.,* **30**, e28.
22. Paz, M.F., Wei, S., Cigudosa, J.C., Rodriguez-Perales, S., Peinado, M.A., Huang, T.H. and Esteller, M. (2003) Genetic unmasking of epigenetically silenced tumor suppressor genes in colon cancer cells deficient in DNA methyltransferases. *Hum. Mol. Genet.,* **12**, 2209-2219.
23. Sadikovic, B., Haines, T.R., Butcher, D.T. and Rodenhiser, D.I. (2004) Chemically induced DNA hypomethylation in breast carcinoma cells detected by the amplification of intermethylated sites. *Breast Cancer Res,* **6**, 30.
24. Atkin, N.B. (2001) Microsatellite instability. *Cytogenet. Cell Genet.,* **92**, 177-181.
25. Peltomaki, P. (2003) Role of DNA mismatch repair defects in the pathogenesis of human cancer. *J. Clin. Oncol.,* **21**, 1174-1179.
26. Popat, S., Hubner, R. and Houlston, R.S. (2005) Systematic review of microsatellite instability and colorectal cancer prognosis. *J. Clin. Oncol.,* **23**, 609-618.
27. Gonzalez-Garcia, I., Moreno, V., Navarro, M., Marti-Rague, J., Marcuello, E., Benasco, C., Campos, O., Capella, G. and Peinado, M.A. (2000) Standardized approach for microsatellite instability detection in colorectal carcinomas. *J. Natl. Cancer Inst.,* **92**, 544-549.
28. Welsh, J. and McClelland, M. (1990) Fingerprinting genomes using PCR with arbitrary primers. *Nucleic Acids Res.,* **18**, 7213-7218.

29. Ehrlich, M. (2002) DNA methylation in cancer: too much, but also too little. *Oncogene,* **21**, 5400-5413.
30. Laird, P.W., Jackson-Grusby, L., Fazeli, A., Dickinson, S.L., Jung, W.E., Li, E., Weinberg, R.A. and Jaenisch, R. (1995) Suppression of intestinal neoplasia by DNA hypomethylation. *Cell,* **81**, 197-205.
31. Trinh, B.N., Long, T.I., Nickel, A.E., Shibata, D. and Laird, P.W. (2002) DNA methyltransferase deficiency modifies cancer susceptibility in mice lacking DNA mismatch repair. *Mol. Cell. Biol.,* **22**, 2906-2917.
32. Chan, M.F., van Amerongen, R., Nijjar, T., Cuppen, E., Jones, P.A. and Laird, P.W. (2001) Reduced rates of gene loss, gene silencing, and gene mutation in Dnmt1-deficient embryonic stem cells. *Mol. Cell. Biol.,* **21**, 7587-7600.
33. Peinado, M.A., Malkhosyan, S., Velazquez, A. and Perucho, M. (1992) Isolation and characterization of allelic losses and gains in colorectal tumors by arbitrarily primed polymerase chain reaction. *Proc. Natl. Acad. Sci. U. S. A.,* **89**, 10065-10069.
34. Kohno, T., Morishita, K., Takano, H., Shapiro, D.N. and Yokota, J. (1994) Homozygous deletion at chromosome 2q33 in human small-cell lung carcinoma identified by arbitrarily primed PCR genomic fingerprinting. *Oncogene,* **9**, 103-108.
35. Achille, A., Biasi, M.O., Zamboni, G., Bogina, G., Magalini, A.R., Pederzoli, P., Perucho, M. and Scarpa, A. (1996) Chromosome 7q allelic losses in pancreatic carcinoma. *Cancer Res.,* **56**, 3808-3813.
36. Okazaki, T., Takita, J., Kohno, T., Handa, H. and Yokota, J. (1996) Detection of amplified genomic sequences in human small-cell lung carcinoma cells by arbitrarily primed-PCR genomic fingerprinting. *Hum. Genet.,* **98**, 253-258.
37. Saitoh, Y., Bruner, J.M., Levin, V.A. and Kyritsis, A.P. (1998) Identification of allelic loss on chromosome arm 6p in human astrocytomas by arbitrarily primed polymerase chain reaction. *Genes. Chromosomes Cancer,* **22**, 165-170.
38. Arribas, R., Risques, R.A., Gonzalez-Garcia, I., Masramon, L., Aiza, G., Ribas, M., Capella, G. and Peinado, M.A. (1999) Tracking recurrent quantitative genomic alterations in colorectal cancer: allelic losses in chromosome 4 correlate with tumor aggressiveness. *Lab. Invest.,* **79**, 111-122.
39. Scarpa, A., Taruscio, D., Scardoni, M., Iosi, F., Paradisi, S., Ennas, M.G., Rigaud, G., Moore, P.S. and Menestrina, F. (1999) Nonrandom chromosomal imbalances in primary mediastinal B-cell lymphoma detected by arbitrarily primed PCR fingerprinting. *Genes. Chromosomes Cancer,* **26**, 203-209.
40. Yamada, T., Kohno, T., Navarro, J.M., Ohwada, S., Perucho, M. and Yokota, J. (2000) Frequent chromosome 8q gains in human small cell lung carcinoma detected

by arbitrarily primed-PCR genomic fingerprinting. *Cancer Genet. Cytogenet.,* **120**, 11-17.

41. Anami, Y., Takeuchi, T., Mase, K., Yasuda, J., Hirohashi, S., Perucho, M. and Noguchi, M. (2000) Amplotyping of microdissected, methanol-fixed lung carcinoma by arbitrarily primed polymerase chain reaction. *Int. J. Cancer,* **89**, 19-25.
42. Piao, Z., Lee, K.S., Kim, H., Perucho, M. and Malkhosyan, S. (2001) Identification of novel deletion regions on chromosome arms 2q and 6p in breast carcinomas by amplotype analysis. *Genes. Chromosomes Cancer,* **30**, 113-122.
43. Ionov, Y., Peinado, M.A., Malkhosyan, S., Shibata, D. and Perucho, M. (1993) Ubiquitous somatic mutations in simple repeated sequences reveal a new mechanism for colonic carcinogenesis. *Nature,* **363**, 558-561.
44. Arribas, R., Capella, G., Tortola, S., Masramon, L., Grizzle, W.E., Perucho, M. and Peinado, M.A. (1997) Assessment of genomic damage in colorectal cancer by DNA fingerprinting: prognostic applications. *J. Clin. Oncol.,* **15**, 3230-3240.
45. Malkhosyan, S., Yasuda, J., Soto, J.L., Sekiya, T., Yokota, J. and Perucho, M. (1998) Molecular karyotype (amplotype) of metastatic colorectal cancer by unbiased arbitrarily primed PCR DNA fingerprinting. *Proc. Natl. Acad. Sci. U. S. A.,* **95**, 10170-10175.
46. de Juan, C., Iniesta, P., Vega, F.J., Peinado, M.A., Fernandez, C., Caldes, T., Massa, M.J., Lopez, J.A., Sanchez, A., Torres, A.J. *et al.* (1998) Prognostic value of genomic damage in non-small-cell lung cancer. *Br. J. Cancer,* **77**, 1971-1977.
47. Suzuki, K., Ohnami, S., Tanabe, C., Sasaki, H., Yasuda, J., Katai, H., Yoshimura, K., Terada, M., Perucho, M. and Yoshida, T. (2003) The genomic damage estimated by arbitrarily primed PCR DNA fingerprinting is useful for the prognosis of gastric cancer. *Gastroenterology,* **125**, 1330-1340.
48. Issa, J.P. (2002) Epigenetic variation and human disease. *J. Nutr.,* **132**, 2388S-2392S.
49. Richardson, B.C. (2002) Role of DNA methylation in the regulation of cell function: autoimmunity, aging and cancer. *J. Nutr.,* **132**, 2401S-2405S.
50. Jaenisch, R. and Bird, A. (2003) Epigenetic regulation of gene expression: how the genome integrates intrinsic and environmental signals. *Nat. Genet.,* **33 Suppl**, 245-254.

Table 1. Correlation between GDF and the hypomethylation index in colorectal cancers classified according to genetic and clinicopathological features

Variable	Category	Correlation (Pearson)	p
All tumors		0.250	**0.022**
K-ras mutation	WT (n=49)	0.0173	0.234
	Mutated (n=33)	0.372	**0.033**
p53 mutation	WT (n=46)	0.263	0.077
	Mutated (n=33)	0.177	0.323
Age	≤67 (n=36)	0.519	**0.001**
	>67 (n=47)	0.057	0.715
Sex	Female (n=37)	0.241	0.151
	Male (n=46)	0.293	**0.048**
Dukes' stage	A-B (n=44)	0.185	0.228
	C-D (n=39)	0.313	0.052
Localization	Left (n=20)	0.399	0.081
	Right	0.218	0.086

Table 2. Multivariate Cox analysis

All patients (n=83)

Covariables	Categories	HR (95% CI)	p
Dukes' stage	C-D vs A-B	4.7 (2.1-10.5)	**<0.001**
Hypomethylation index	High vs Low[1]	1.9 (0.9-4.1)	0.123
GDF	High vs Low[1]	0.5 (0.2-1.1)	0.073

Younger patients (≤67 y.o., n=36)

Covariables	Categories	HR (95% CI)	p
Dukes' stage	C-D vs A-B	9.7 (2.0-46.6)	**0.004**
Hypomethylation index	High vs Low[1]	0.7 (0.2-2.7)	0.644
GDF	High vs Low[1]	0.4 (0.1-2.2)	0.400

Older patients (>67 y.o., n=47)

Covariables	Categories	HR (95% CI)	p
Dukes' stage	C-D vs A-B	3.1 (1.2-8.0)	**0.017**
Hypomethylation index	High vs Low[1]	3.5 (1.3-9.1)	**0.012**
GDF	High vs Low[1]	0.5 (0.2-1.3)	0.136

[1] High and Low are defined as above and below the mean (Hypomethylation index: 0.149; GDF: 0.172).

FIGURE LEGENDS

Figure 1

Scatter plot of the distribution of the Genomic Damage Fraction against the Hypermethylation (box A) and the Hypomethylation Index (box B) in 83 colorectal carcinomas. A statistically significant correlation was observed only for the Hypomethylation index (box B). When patients were classified according to their age, the correlation was strengthened in younger patients (box C, ≤67 y.o.), and lost in older patients (box D, >67 y.o.).

Figure 2

Kaplan-Meier overall survival curves in colorectal cancer patients. Older patients (panel A, >67 y.o.) displayed a poorer survival but it did not reach statistical significance. When only old patinets were considered, a high hypomethylation index was indicator of poorer prognosis (panel B), although the strongest differences were observed in Dukes' stages C and D (panel C).

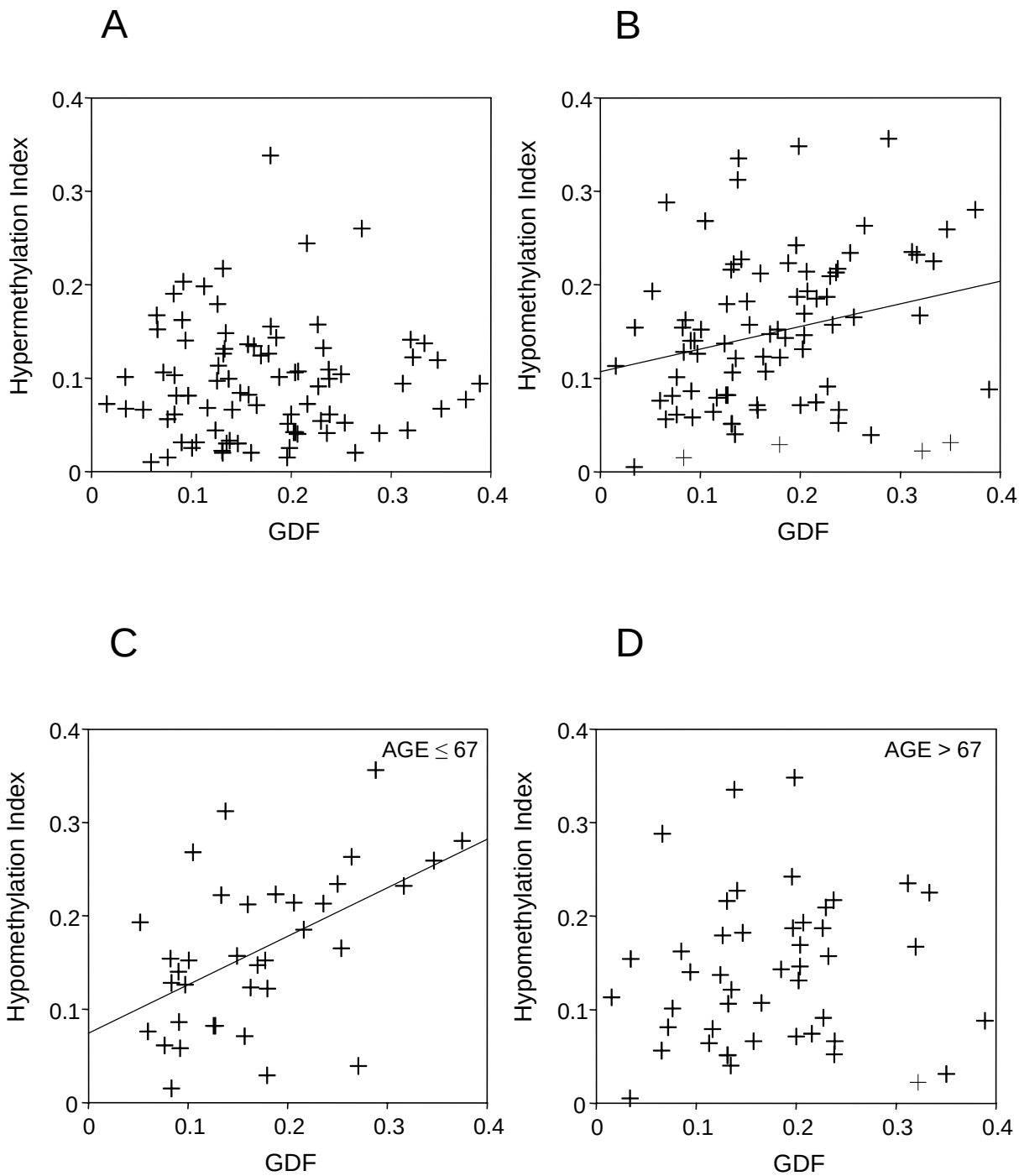
A
B
C
D
Hypermethylation Index
Hypomethylation Index
GDF
AGE ≤ 67
AGE > 67
0
0.1
0.2
0.3
0.4

Figure 1

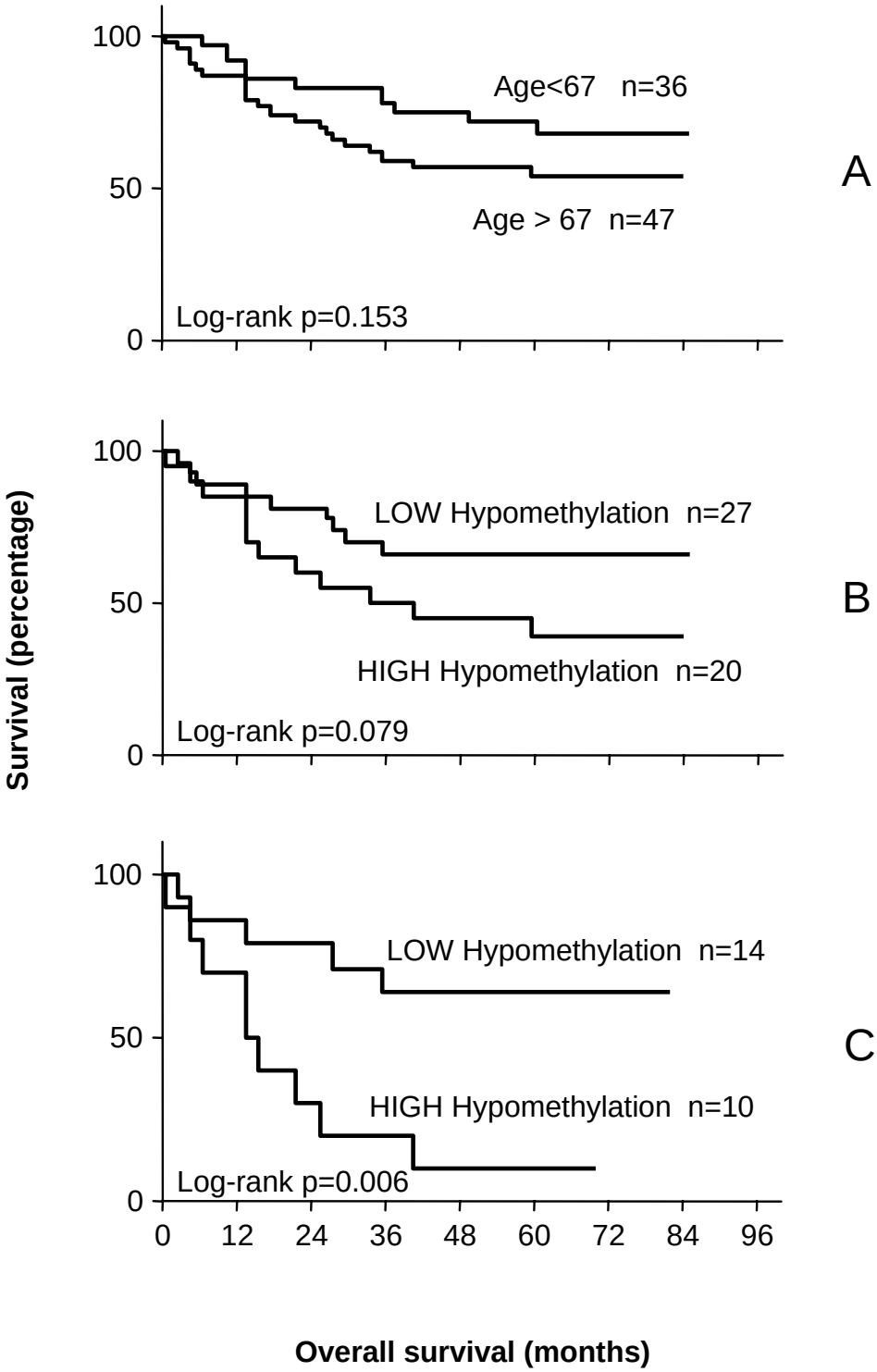
100
50
0
Age<67 n=36
Age > 67 n=47
Log-rank p=0.153
A
100
50
0
LOW Hypomethylation n=27
HIGH Hypomethylation n=20
Log-rank p=0.079
B
Survival (percentage)
100
50
0
LOW Hypomethylation n=14
HIGH Hypomethylation n=10
Log-rank p=0.006
C
0
12
24
36
48
60
72
84
96
Overall survival (months)

Figure 2

Hypermethylation of the prostacyclin synthase (PTGIS) promoter is a frequent event in colorectal cancer and associated with aneuploidy

Frigola J, Muñoz M, Clark SJ, Moreno V, Capellà G, Peinado MA

Sotmès a Oncogene

CAPÍTOL 4

A partir de l'estudi global descrit en els darrers dos capítols, es van poder identificar i caracteritzar tota una sèrie de canvis específics recurrents. En aquest treball es mostra la identificació i posterior caracterització en un d'aquests canvis recurrents. Concretament, es tracta d'un fragment que, a partir dels *fingerprints* de l'AIMS, es mostrava clarament hipermetilat en un nombre elevat de tumors. A la bibliografia, la hipermetilació específica en tumors s'ha descrit àmpliament com a mecanisme de silenciament gènic. En aquest cas, es tractava de l'enzim encarregat de la síntesi de la prostaglandina PGI_2 (PTGIS). La hipermetilació d'aquest gen no s'havia descrit en cap tipus de càncer. Tanmateix, sí que s'havia observat una participació directa de PGI_2 en l'activació de la via d'apoptosi a través del receptor PPARδ, suggerint un paper rellevant del silenciament d'aquest gen en el càncer colorectal. Aleshores, en aquest treball es mostra la identificació i posterior caracterització del silenciament per hipermetilació del promotor del gen PGIS en càncer colorectal. Es discuteix també la possible contribució d'aquest silenciament en el procés tumoral.

Hypermethylation of the prostacyclin synthase (PTGIS) promoter is a frequent event in colorectal cancer and associated with aneuploidy

Frigola J[1], Muñoz M[1], Clark SJ[2], Moreno V[3,4], Capellà G[3], Peinado MA[1]

[1] IDIBELL-Institut de Recerca Oncològica, L'Hospitalet, Barcelona, Spain

[2] The Garvan Institute of Medical Research, Darlinghurst NSW 2010, Australia

[3] IDIBELL-Institut Català d'Oncologia, L'Hospitalet, Barcelona, Spain

[4] Laboratori de Bioestadistica i Epidemiologia, Facultat de Medicina, Universitat Autonoma de Barcelona, Cerdanyola, Barcelona, Spain

Running title: PTGIS hypermethylation in colorectal cancer

Key words: colorectal cancer, tumor progression, cancer marker, cancer epigenetics, genetic instability

Correspondence: Miguel A. Peinado,
Institut de Recerca Oncològica,
Granvia km 2.7,
08907 L'Hospitalet, Barcelona,
Spain.
email: mpeinado@iro.es
Tel 34-932607464
Fax 34-932607426

ABSTRACT

Inactivation of specific tumor suppressor genes by transcriptional silencing aasociated with hypermethylation of the promoter is a common event in cancer. We have applied the Amplification of Intermethylated Sites (AIMS) technique to a 100 human colorectal cancers and seven cell lines to identify recurrent alterations that may unveil silenced tumor suppressor genes. Bisulfite sequencing was used to confirm differential DNA methylation results. Gene expression analysis was performed by Real-Time RT-PCR. An AIMS band recurrently displayed in tumors but not in normal tissues was isolated and identified as part of the CpG island of the prostacyclin synthase (PTGIS) gene promoter. PTGIS promoter was hypermethylated in 43 out of 100 colorectal cancers and in all cell lines. Bisulfite sequencing and clonal analysis confirmed the results obtained by AIMS and demonstrated biallelic hypermethylation of PTGIS promoter. Hypermethylation of the PTGIS promoter was associated with diminished gene expression, that was restored after treatment with demethylating and histone deacetylases inhibitor agents. PTGIS hypermethylation was associated with aneuploidy and p53 mutations. In the adjusted model, PTGIS methylation, but not p53 mutation, maintained the association with aneuploidy. We conclude that epigenetic inactivation of the PTGIS gene is a recurrent alteration in colorectal carcinogenesis.

INTRODUCTION

Aberrant hypermethylation in the promoter region of different genes is a common feature of most cancers and appears associated with transcriptional silencing of the contiguous gene (Jones & Baylin, 2002). Epigenetic inactivation is involved through different elements in all the signaling pathways disrupted in human carcinogenesis (Jones & Baylin, 2002). Therefore, the characterization of the methylome in normal and pathologic tissues is one of the most demanding challenges in human genome projects and will be instrumental for the development of diagnostic tools and the design of specific therapies. Amplification of Inter-Methylated Sites (AIMS) (Frigola et al., 2002) generates methylome fingerprints by the simultaneous screening of a large number of selectively amplified methylated sequences. When series of cases including normal and colorectal tumor samples are analyzed, the characterization of recurrently altered sequences may help in unveiling novel targets relevant to human carcinogenesis. Characterization of one of the AIMS-generated sequences showing recurrent differential representation between normal and tumor tissue revealed the frequent methylation of the Prostacyclin Synthase (PTGIS) gene promoter in neoplastic samples, indicating its putative epigenetic silencing associated with malignant transformation.

A key regulatory step in the synthesis of prostaglandins is the enzymatic conversion of arachidonic to PGH2 by COX1 and COX2, the latter frequently overexpressed in human colorectal tumors. Inhibition of the COX pathway has been considered a prime target in multiple preventive and therapeutic designs, mainly in colorectal tumors (Brown & DuBois, 2005). PGH2 is subsequently converted to distinct prostaglandins. The synthesis of one of these prostagladins, the prostacyclin or PGI_2, is catalyzed by PTGIS. PGI_2 appears to exert antiproliferative effects (Lim & Dey, 2002) and to have chemopreventive properties (Brown & DuBois, 2005). Furthermore, intracellular PGI_2 has been shown to promote apoptosis by activating the endogenous PPARδ receptor (Hatae et al., 2001; Lim & Dey, 2002). We have pursued further characterization of the methylation profile of the PTGIS gene in a series of cell lines and colorectal cancers and its association with the clinical and molecular features of the tumors.

RESULTS

AIMS screening

From the fingerprints obtained by AIMS, we identified a double band (tagged T1) that showed a consistent over-representation in tumors as compared to the respective normal

tissues (Figure 1A), indicating differential hypermethylation. Specifically, 40 out of 90 tumors (44%) and 3 out of 10 adenomas (30%) showed a noticeable increase in the intensity of the band when compared to the paired normal tissue. T1 band was also clearly present in all the colorectal cell lines analyzed suggesting that this sequence was strongly methylated. The doublet was isolated, cloned, sequenced and identified by BLAST alignment as a DNA fragment comprising part of the CpG island located in the PTGIS promoter. Only one of the two SmaI sites flanking the T1 band was inside of the CpG island (Figure 1B).

High resolution methylation analysis of the PTGIS promoter

The methylation profile of the CpG island located at the 5' end the PTGIS gene was characterized by bisulfite sequencing in two adenomas (one displaying T1 band and one lacking T1 band in the AIMS fingerprints), five carcinomas (three displaying T1 band and two lacking T1 band), together with the respective paired normal mucosa (all without T1 band), and seven colon cancer cell lines. First, a 316 bp region (Fragment A) spanning 21 CpGs at the 3' end of the CpG island and including part of the AIMS T1 band was amplified by PCR (Figure 1B). Ten different clones from each sample were sequenced. CpGs outside the CpG island were methylated in all normal tissues, but the 16 CpGs within the CpG island were sparsely methylated. These CpGs were densely methylated in tumors exhibiting hypermethylation of PTGIS gene as revealed by AIMS, but not in tumors with no change in the AIMS fingerprint as compared to normal tissue (Figure 1C), demonstrating that AIMS differential display was associated with changes in the DNA methylation of the CpG island. Therefore the relative increase in the intensity of the AIMS T1 band detected in 40 tumors and 3 adenomas was interpreted as an indicator of methylation of the CpG island.

To confirm this interpretation we analyzed an inner fragment of the CpG island. A 412 bp long sequence spanning 40 CpG sites (Fragment B) was amplified by PCR, cloned and sequenced (Figure 1B). The CpG methylation profiles of five normal-tumor pairs and two adenomas are shown in Figure 2. Dense hypermethylation was clearly evidenced in carcinomas 138T, 99T and 72T and adenoma A2, all of them with a clear display of the T1 band in the AIMS fingerprint. Carcinomas 69T and 127T and adenoma A1, lacking T1 band, were unmethylated. In summary, a perfect correlation between the differential representation of the AIMS T1 band and the methylation profile of the CpG island ascertained by bisulfite sequencing was found in all the samples analyzed. The sequencing of the CpG island also allowed the genotyping of a polymorphism consisting in four or six repetitions of a 9 nucleotide sequence (Amano et al., 2004). As illustrated in figure 2, the sequencing of cloned PCR products confirmed the methylated status of the two alleles in heterozygous samples

(99T and A2). Moreover, bisulfite sequencing revealed dense methylation (75-100%) of almost all CpG sites in all cell lines analyzed (Figure 3).

Analysis of PTGIS expression

We determined if hypermethylation of the PTGIS promoter was associated with a down-regulation of expression. PTGIS expression levels were determined by real time RT-PCR in 15 normal-tumor pairs including the samples we had previously performed a detailed characterized of the CpG island methylation profile. Four tumors with unmethylated PTGIS CpG island showed up-regulated expression when compared to normal tissue (Figure 4A), suggesting that cell transformation enhances PTGIS gene expression. Down-regulation of PTGIS expression was observed in tumors showing extensive promoter hypermethylation, except for one case that was up-regulated (Figure 4A). Moreover, PTGIS expression was undetectable in the four cell lines analyzed (Figure 4A).

Restoration of PTGIS expression in colon cancer cells

Colorectal cancer cell line HCT116 that showed complete hypermethylation and undetectable levels of PTGIS expression was cultured with the demethylating agent 5Aza and the histone deacetylase inhibitor TSA. Interestingly, either treatment was able to induce the reexpression of the PTGIS, but the highest levels of gene expression were observed when the cell line was cultured with both agents (Figure 4B). PTGIS associated CpG island demethylation was complete in cells treated with both agents, but partial in cells treated for 24h with 5Aza alone (see Supplementary material).

PTGIS hypermethylation and clinicopathological and molecular features

The possible association of the PTGIS promoter methylation status with different characteristics of the tumors was investigated. No significant differences were found regarding age, sex, tumor location, Dukes' stage, K-ras mutation or microsatellite instability (Table 1). Noteworthy, there was a highly significant association between hypermethylation of the PTGIS promoter and p53 mutations and aneuploidy (Table 1). The association between p53 mutations and aneuploidy was weaker (p=0.062). When a multivariate adjusted model was analyzed, PTGIS methylation retained its association with aneuploidy (odds-ratio 3.23, CI95% 1.08-9.70, p=0.03) but not p53 mutation (odds-ratio 1.76, CI95% 0.60-5.20, p=0.30) , pointing out a prevalent role of PTGIS inactivation in genomic instabilization.

DISCUSSION

In a previous study, the application of the methylome fingerprinting technique AIMS allowed us to detect hypomethylation and hypermethylation signatures in a large series of colorectal carcinomas when compared to their paired normal colonic mucosas (Frigola et al., 2005). Moreover, because the AIMS generated markers can be isolated and individually characterized, this approach is also suitable for the identification of recurrent epigenetic alterations in cancer (Frigola et al., 2002; Paz et al., 2003; Sadikovic et al., 2004). Here we describe the PTGIS promoter hypermethylation in colorectal cancer as a paradigm of one of these epigenetic changes. PTGIS hypermethylation has been confirmed by bisulfite sequencing, its functional implications demonstrated at gene expression level, and its involvement in colorectal tumorigenesis unveiled by the differential features of tumors with and without epigenetic inactivation of the PTGIS gene.

The bisulfite characterization of the DNA region represented in AIMS revealed that, although the SmaI site restricting the differential amplification is in the boundary of the CpG island, the quantitative nature of the AIMS technique allows the detection of differences in the density of CpG methylation. The analysis of the CpG island core including the transcription start site of PTGIS gene confirmed the perfect association between quantitative changes detected by AIMS and qualitative hypermethylation events. The presence of polymorphisms in this region allowed the demonstration of the biallelic extent of the PTGIS promoter hypermethylation.

Gene expression analyses revealed that hypermethylation of the PTGIS promoter was associated with downregulation of the transcript, as expected. On the contrary, tumors with unmethylated CpG island showed an enhanced expression of the PTGIS gene. A discordant result was also found in one tumor (Figure 4A, case 15), with an increased expression of PTGIS in spite of exhibiting a heavily methylated promoter. This result may be explained by contamination by normal tissue, heterogeneity in the tumor, monoallelic inactivation and a gene expression normalization problem. Colon cancer cell lines exhibited undetectable levels of the transcript in a context of a very dense hypermethylation. The link between promoter hypermethylation and epigenetic silencing of the PTGIS gene was directly tackled by demonstrating that treatment with the demethylating drug 5Aza and TSA, a specific inhibitor of the histone deacetylases, also resulted in the reactivation of PTGIS. The combined treatment with the two agents was highly synergistic in inducing the PTGIS expression as it has been demonstrated for other genes (Cameron et al., 1999; Yang et al., 2001; Ghoshal et al., 2002), and supports the notion that both DNA and histone modifications participate in the regulation of gene expression. Altogether, these results suggest that methylation of the PTGIS promoter is likely to play a important role in colorectal cancer.

Different investigations have highlighted the importance of the PTGIS expression in preventing tumor growth and progression (Keith et al., 2002; Pradono et al., 2002; Cutler et al., 2003; Keith et al., 2004). It has been suggested that some of the protective effects of PTGIS overexpression may be attributable to apoptosis activation mediated by PPARδ (Hatae et al., 2001). Recent studies have also reported that PPARδ may promote intestinal adenoma growth (Gupta et al., 2004), revealing the important, but also complex, involvement of this pathway in colorectal cancer. In our setting we found that PTGIS promoter hypermethylation was strongly associated with the presence of p53 mutations, as well as, aneuploidy (Table 1). The association between p53 mutations and aneuploidy was weaker, pointing out that PTGIS epigenetic silencing may be a direct effector in the induction or facilitation of chromosomal instability in cancer cells. Available data are insufficient to ascertain the molecular mechanisms underlying the observed correlations, but it is possible that PTGIS is involved in the cell's response to genomic damage, probably by resistance to apoptosis mediated by PPARδ (Hatae et al., 2001). The relevance of PTGIS inactivation in colorectal cancer is further reinforced by its early occurrence in tumor progression, its age-independent nature and the strong tumor specificity of the methylation process. Full understanding of the causes and implications of PTGIS inactivation in colorectal cancer requires a comprehensive study of the different elements of the COX-2 pathway, their interactions and their consequences on cell's biology.

In conclusion, we have shown the suitability of the AIMS approach to discover new epigenetic targets in cancer. For the first time, we report the hypermethylation of the PTGIS promoter as a common event in colorectal cancer. The PTGIS promoter methylation profile has been characterized by AIMS and bisulfite sequencing and the functional implications, namely transcriptional silencing, have been demonstrated in primary tumors and cell lines Furthermore, this inactivation is strongly associated with p53 mutation and aneuploidy. Therefore, we propose that PTGIS gene inactivation may play an important role in colorectal cancer progression with putative direct implications in chromosomal instability and avoidance of apoptosis. It is obvious that after these results, a new line of therapeutic strategies based in the reactivation of PTGIS activity or the administration of prostacyclin analogues can be hypothesized in an important subset of colorectal cancers. Future studies should elucidate the relevance of this approach.

MATERIAL AND METHODS

Samples

Ninety colorectal carcinomas, with their paired nonadjacent areas of normal colonic mucosa, and 10 colorectal adenomas, synchronous with carcinomas included in the former series, were collected as fresh-frozen tissues within 2 h of removal and then stored at -80ºC. All samples were obtained from the Hospital de la Santa Creu i Sant Pau (Barcelona, Spain). The study protocol was approved by the Ethics Committee. Ninety colorectal carcinomas used in this study were characterized previously for mutations in the p53 and K-ras genes (Tortola et al., 1999), and aneuploidy (Risques et al., 2001). Human colorectal carcinoma cell lines were obtained from the American Type Culture Collection (ATCC, Manassas, VA).

AIMS screening

We used the AIMS method to screen for tumor-specific alterations. AIMS method is based on the differential cleavage of isoschizomers with distinct methylation sensitivity and the selective amplification of short sequences (up to ~1 Kb long) flanked by two methylated SmaI (CCCGGG) sites that are ligated to an adaptor and a specific 3-4 nucleotide sequence (adjacent to the SmaI site) arbitrarily chosen by the investigator. Lack of methylation at either site prevents amplification of the band. The AIMS generated sequences can be tagged, isolated and individually characterized. All samples were analyzed using the set of primers (set A) and conditions described previously (Frigola et al., 2002). An illustrative example is shown in Figure 1A. A sequence (displayed as a double band) appearing differentially methylated in AIMS fingerprints was excised from a fresh dried polyacrylamide gel, reamplified, cloned and sequenced to ascertain the unique identity of the isolated band.

Methylation analysis

To confirm the methylation status of the PTGIS gene promoter we performed genomic bisulfite sequencing under conditions described previously (Clark et al., 1994). On the basis of the functional promoter sequence (Yokoyama et al., 1996), two different fragments of the CpG island (857 bp) were amplified by nested PCR. Fragment A was located at the 3'end of the PTGIS gene CpG island and included one of the SmaI sites from the AIMS sequence. Fragment B covered the first exon of the gene and the central part of the CpG island (Figure 1). Primers sequence is described in Table 2. PCR conditions may be obtained from the authors. Ten individual clones were sequenced from each PCR reaction.

Gene expression analysis

RNA was extracted using the phenol-chloroform method. Quantitative real time PCR was performed in a LightCycler apparatus (Roche Diagnostics S.L. Applied Science). Reaction was performed using primers covering exons 5 and 6 of the PTGIS gene (Table 2), and the LCFastStart DNA Master SYBR Green I reagent set (Roche Diagnostics S.L. Applied Science) according to the manufacturer's instructions. The reaction was performed in triplicate. The amplified products were sequenced to confirm the identity. The expression levels of PTGIS gene in normal-tumor pairs were normalized according to the average of 18s rRNA, β2-microglobuline and cyclophilin expression levels. However, cyclophilin expression was modified by TSA treatment and was not considered in the normalization of PTGIS expression in TSA treatment. A relative calibration curve was constructed for each gene with use of five serial dilutions starting with 100 ng of RNA.

Restoration of PTGIS expression in HCT116 colon cancer cells

Cells were treated for 24 h with 0.5 m 5-Aza-2'-deoxycytidine (5Aza) (Sigma, St. Louis, MO). After the treatment the medium was replaced with fresh medium and the cells cultured for a further 48 h before harvesting. Cells were treated for 24 h with trichostatin A (TSA) (Sigma) at 25, 50 and 100 nmol/l or an identical volume of ethanol. For co-treatment, cells were treated with 5Aza for 24 h, after which, medium was removed and TSA was added for a further 24 h. The concentrations and the treatment conditions used were chosen based on preliminary studies showing optimal reactivation of gene expression.

Statistical analysis

Statistical differences between variables were analyzed with unpaired/paired t tests or analysis of variance (ANOVA), as appropriate. Contingency tables were analyzed by the Chi-square or Fisher's exact test, as appropriate. Logistic regression models were used for multivariate analyses of binary traits. Two-tailed P values below 0.05 were considered to be statistically significant.

ACKNOWLEDGEMENTS

We thank Gemma Aiza for excellent technical help and Jenny Song and Clare Stirzaker for the 5Aza and TSA treatment of the cells. Grant support: Ministerio de Educación y Ciencia (SAF2003/5821, SAF2004/07579), Fondo de Investigaciones Sanitarias (FIS PI030114), Network of Cooperative Research on Cancer (C03/10) and Epidemiology and Public Health (C03/09), and NH&MRC (293810). JF was recipient of a fellowship from the Ministry of Education and Science at the Universitat Autònoma de Barcelona.

REFERENCES

Amano, S., Tatsumi, K., Tanabe, N., Kasahara, Y., Kurosu, K., Takiguchi, Y., Kasuya, Y., Kimura, S. & Kuriyama, T. (2004). *Respirology*, **9,** 184-9.

Brown, J.R. & DuBois, R.N. (2005). *Journal of Clinical Oncology*, **23,** 2840-2855.

Cameron, E.E., Bachman, K.E., Myohanen, S., Herman, J.G. & Baylin, S.B. (1999). *Nat Genet*, **21,** 103-7.

Clark, S.J., Harrison, J., Paul, C.L. & Frommer, M. (1994). *Nucleic Acids Res*, **22,** 2990-7.

Cutler, N.S., Graves-Deal, R., LaFleur, B.J., Gao, Z., Boman, B.M., Whitehead, R.H., Terry, E., Morrow, J.D. & Coffey, R.J. (2003). *Cancer Res*, **63,** 1748-51.

Frigola, J., Ribas, M., Risques, R.A. & Peinado, M.A. (2002). *Nucleic Acids Res*, **30,** e28.

Frigola, J., Sole, X., Paz, M.F., Moreno, V., Esteller, M., Capella, G. & Peinado, M.A. (2005). *Hum Mol Genet*, **14,** 319-26.

Ghoshal, K., Datta, J., Majumder, S., Bai, S., Dong, X., Parthun, M. & Jacob, S.T. (2002). *Mol Cell Biol*, **22,** 8302-19.

Gupta, R.A., Wang, D., Katkuri, S., Wang, H., Dey, S.K. & DuBois, R.N. (2004). *Nat Med*, **10,** 245-7.

Hatae, T., Wada, M., Yokoyama, C., Shimonishi, M. & Tanabe, T. (2001). *J Biol Chem*, **276,** 46260-7.

Jones, P.A. & Baylin, S.B. (2002). *Nat Rev Genet*, **3,** 415-28.

Keith, R.L., Miller, Y.E., Hoshikawa, Y., Moore, M.D., Gesell, T.L., Gao, B., Malkinson, A.M., Golpon, H.A., Nemenoff, R.A. & Geraci, M.W. (2002). *Cancer Res*, **62,** 734-40.

Keith, R.L., Miller, Y.E., Hudish, T.M., Girod, C.E., Sotto-Santiago, S., Franklin, W.A., Nemenoff, R.A., March, T.H., Nana-Sinkam, S.P. & Geraci, M.W. (2004). *Cancer Res*, **64,** 5897-904.

Lim, H. & Dey, S.K. (2002). *Endocrinology*, **143,** 3207-10.

Paz, M.F., Wei, S., Cigudosa, J.C., Rodriguez-Perales, S., Peinado, M.A., Huang, T.H. & Esteller, M. (2003). *Hum Mol Genet*, **12,** 2209-19.

Pradono, P., Tazawa, R., Maemondo, M., Tanaka, M., Usui, K., Saijo, Y., Hagiwara, K. & Nukiwa, T. (2002). *Cancer Res*, **62,** 63-6.

Risques, R.A., Moreno, V., Marcuello, E., Petriz, J., Cancelas, J.A., Sancho, F.J., Torregrosa, A., Capella, G. & Peinado, M.A. (2001). *Lab Invest*, **81,** 307-15.

Sadikovic, B., Haines, T.R., Butcher, D.T. & Rodenhiser, D.I. (2004). *Breast Cancer Res*, **6,** 30.

Tortola, S., Marcuello, E., Gonzalez, I., Reyes, G., Arribas, R., Aiza, G., Sancho, F.J., Peinado, M.A. & Capella, G. (1999). *J Clin Oncol*, **17,** 1375-81.

Yang, X., Phillips, D.L., Ferguson, A.T., Nelson, W.G., Herman, J.G. & Davidson, N.E. (2001). *Cancer Res*, **61,** 7025-9.

Yokoyama, C., Yabuki, T., Inoue, H., Tone, Y., Hara, S., Hatae, T., Nagata, M., Takahashi, E.I. & Tanabe, T. (1996). *Genomics*, **36,** 296-304.

Table 1. Clinicopathological and molecular correlates of PTGIS methylation in colorectal cancer

Parameter	PTGIS unmethylated n=50	PTGIS methylated n=40	p[a]
Age (mean±SD)	66.2±13.1	63.9±13.1	0.413
Sex			0.525
Female	20	19	
Male	30	21	
Location			0.252
Right	17	9	
Left	33	31	
Dukes' stage			0.817
A	9	6	
B	17	14	
C	15	15	
D	9	5	
p53 mutation			**0.001**
No	37	15	
Yes	12	22	
K-ras mutation			0.829
No	29	24	
Yes	21	15	
Ploidy[b]			**0.006**
Diploid	21	6	
Aneuploid	28	33	

[a] Two-tailed Student t-test, Fisher's exact test or Chi-square test as appropriate

[b] One case showing hypodiplody and unmethylated PTGIS has not been included in the statistical analysis.

Table 2. Primers sequence

Purpose	Sequence (5'-3')
AIMS ligation (MCF and Blue primers)	CCGGTCAGAGCTTTGCGAAT ATTCGCAAAGCTCTGA
AIMS (PCR), Set A	ATTCGCAAAGCTCTGACCGGGCTA ATTCGCAAAGCTCTGACCGGGTGG
PTGIS promoter, Fragment A, Bisulfite sequencing, first PCR	GTTTTTTTTGTTAAGAAGGTGT ATAAATAATTCCAAAACATAATCAAA
PTGIS promoter, Fragment A, Bisulfite sequencing, nested PCR	TTAAGAAGGTGTAAGGTGGG AACACTCCCATCTATATAATAA
PTGIS promoter, Fragment B, Bisulfite sequencing, first PCR	TTTTAAARTGGGTTGGGGTGGG CCTTCCCACCTTACACCTTCTTA
PTGIS promoter, Fragment B, Bisulfite sequencing, nested PCR	GGAATTTTATTTGGGAGTGGGTT CACCTTCTTAACAAAAAAAAC
PTGIS expression by Real Time RT-PCR	CCGTGGCTCCCTGTCAGT GCAGCTTCCACAGGCGAC

FIGURE LEGENDS

Figure 1

(A) Detail of the fingerprint generated by AIMS in six Normal (N)–Tumor (T) pairs. The AIMS double band (tagged T1) and corresponding to the PTGIS sequence is indicated. Three tumors showing a clear increase in the intensity of the T1 band are marked with an up-arrowhead at the bottom. (B) The relative position of the AIMS band, the PTGIS associated CpG island (each vertical bar indicates a CpG site) including the first exon of the PTGIS gene (box), and the two fragments (A and B) of the PTGIS CpG island analyzed by bisulfite sequencing are shown. Sequence is oriented 5'-3' in regard to the PTGIS gene. (C) Bisulfite sequencing of the fragment A amplified from a normal tissue and its paired tumor tissue. Results of ten independent clones fo each sample are shown. Empty dots indicate unmethylated CpG sites, black dots indicate methylated CpG sites. The 3' boundary of the CpG island showed unmethylation of the CpG sites closer to the exon but methylation of those more external in nomral tissueisland was unmethylated in The normal tissue showed dense methylation of the CpG sites in the 3' boundary of the CpG island, that was unmethylated in CpG sites closer to the . Tumor tissue showed dense methylation of all CpGs.

Figure 2

Bisulfite sequencing of the central part of the PTGIS associated CpG island (amplified fragment B). The results obtained in ten sequenced clones and corresponding to the CpG methylation profile of five paired normal and tumor tissues and two adenomas are represented. Empty dots indicate unmethylated CpG sites, black dots indicate methylated CpG sites. PTGIS CpG island was unmethylated in all normal tissues and adenoma A1 and carcinomas 69 and 127. PTGIS CpG island was hypermethylated in adenoma A2 and carcinomas 72, 99 and 138.

Figure 3

DNA methylation profile of the central part of PTGIS promoter region CpG island in seven colon cancer cell lines (amplified as fragment B). Squares represent individual CpG sites and the fill-in code corresponds to the percentage of methylation. Cell line SK-CO-1 contains an additional CpG site (no 29) due to a single nucleotide polymorphism. All cell lines displayed dense methylation of the PTGIS CpG island.

Figure 4

(A) Relative expression of PTGIS in fifteen normal-tumor tissues (case numebr is shown at the bottom) and four cell lines as determined by real time RT-PCR. Expression ratios (Y axis) were calculated after normalization using control genes (seee Material and methods) and are represented as logarithms. Black bars indicate tumors with heavy methylation of the PTGIS promoter, gray bars indicate tumors with partial methylation (probably due to heteregeneity of the sample), white bars indicate unmethylated tumors. Error bars indicate standard deviation. PTGIS expression levels were undetectable in cell lines and the relative expression value has been represented arbitrarily. (B) Expression of PTGIS in HCT116 cells after treatment with the 5Aza and TSA. Y-axis represents relative expression values in arbitrary units calculated after normalization using control genes (see Material and Methods).

A

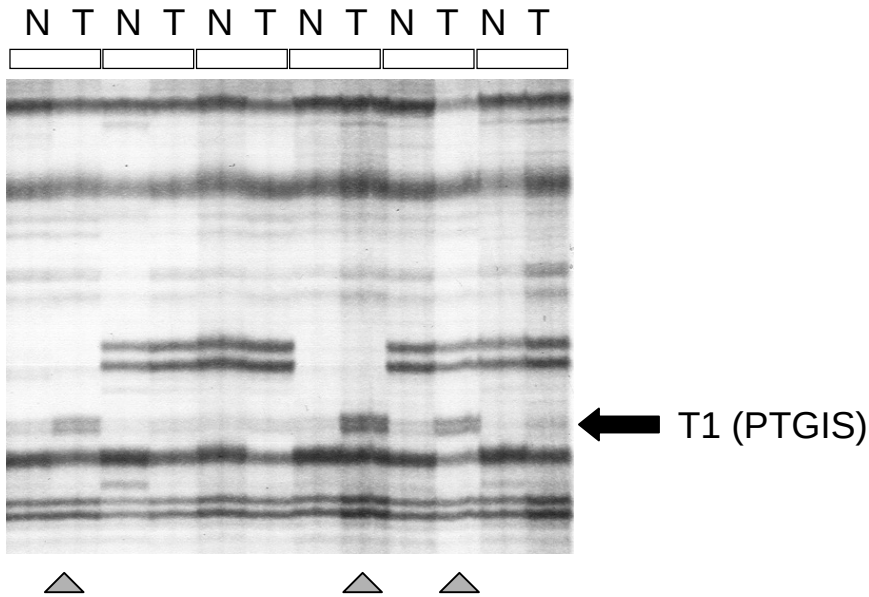
N T N T N T N T N T N T
T1 (PTGIS)

B

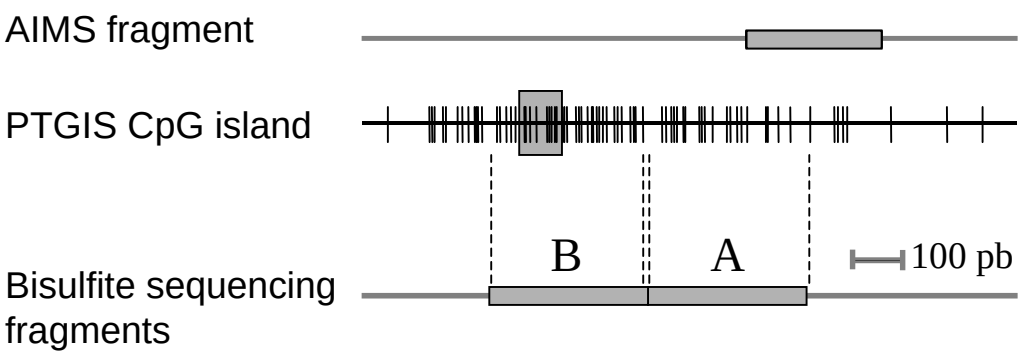
AIMS fragment
PTGIS CpG island
B
A
100 pb
Bisulfite sequencing fragments

C

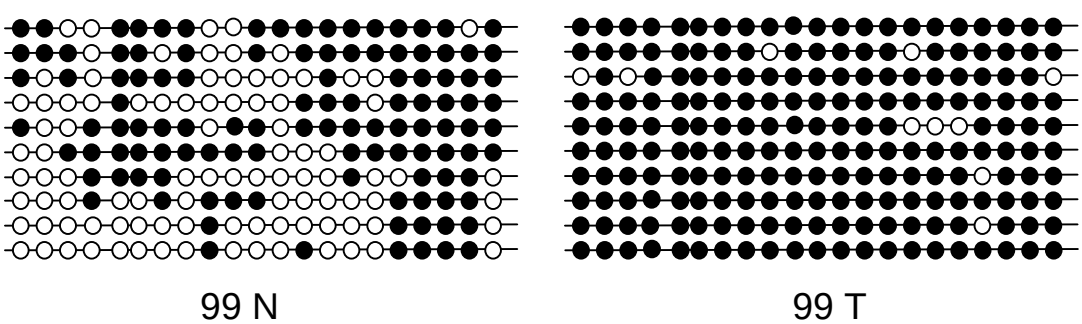
99 N
99 T

Figure 1

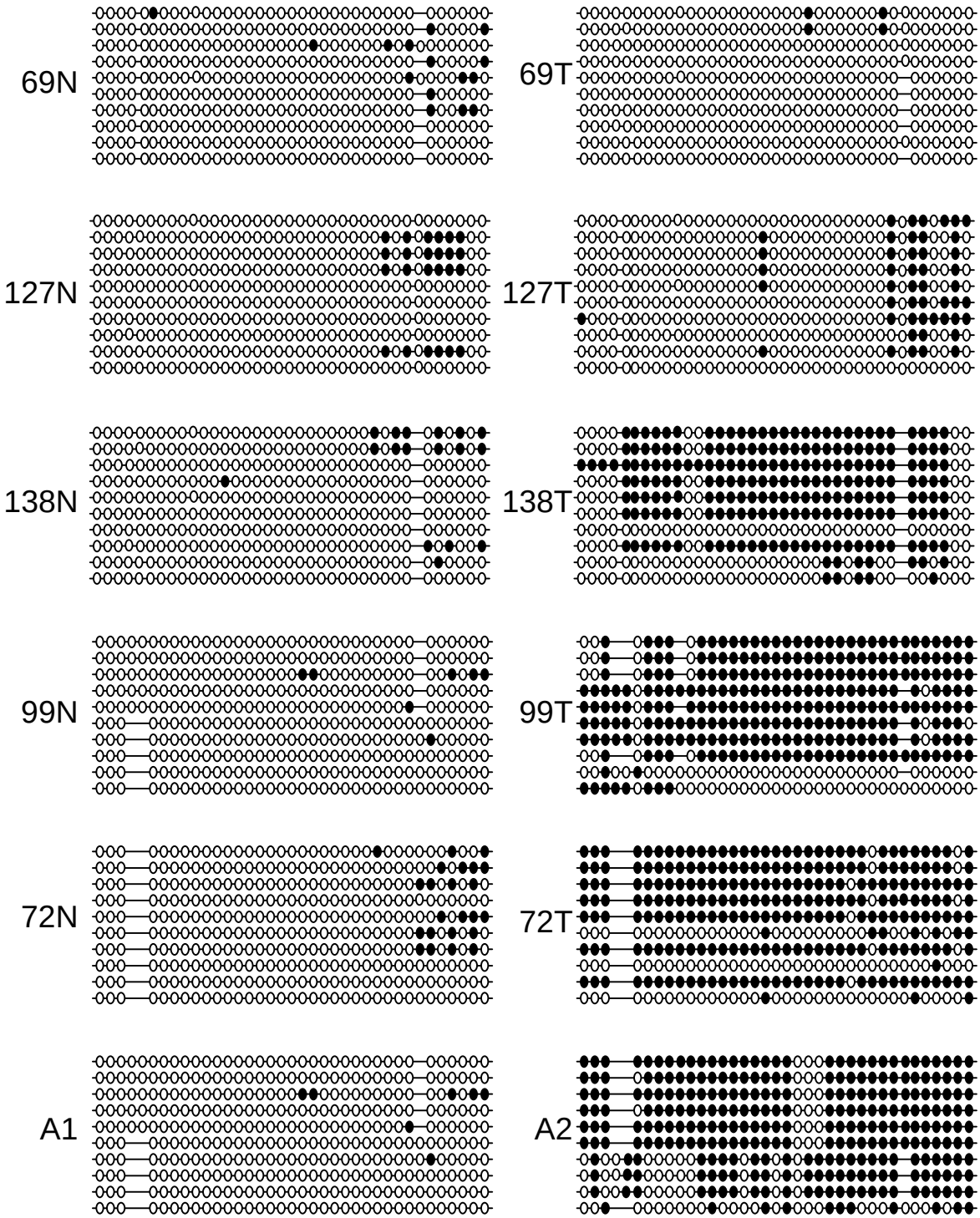

Figure 2

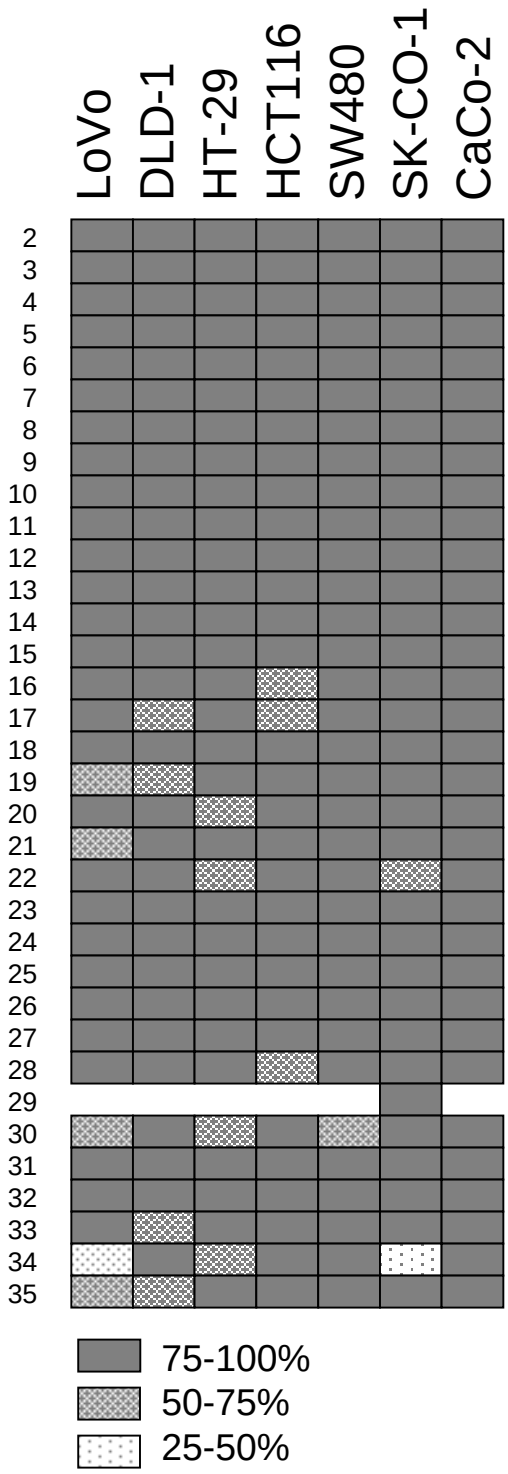
LoVo
DLD-1
HT-29
HCT116
SW480
SK-CO-1
CaCo-2
2
3
4
5
6
7
8
9
10
11
12
13
14
15
16
17
18
19
20
21
22
23
24
25
26
27
28
29
30
31
32
33
34
35
75-100%
50-75%
25-50%

Figure 3

A

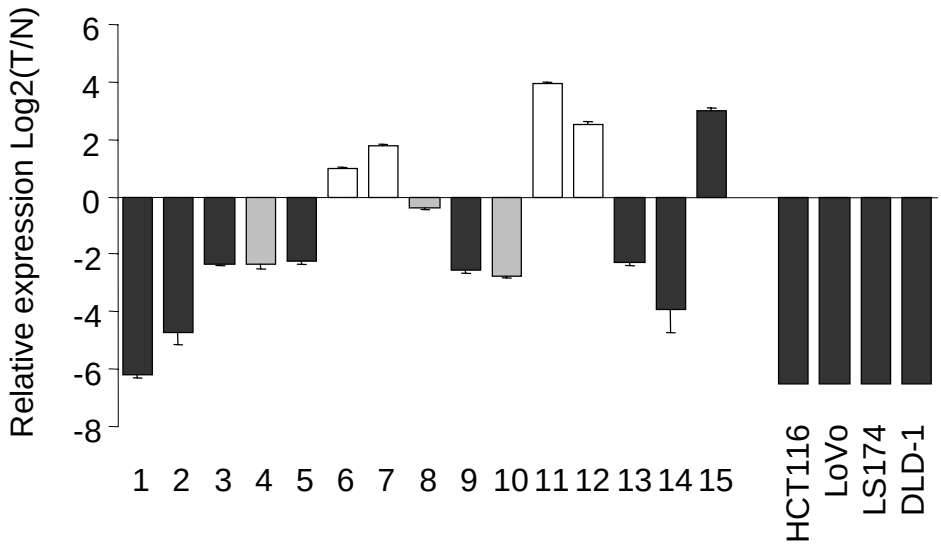
Relative expression Log2(T/N)
6
4
2
0
-2
-4
-6
-8
1 2 3 4 5 6 7 8 9 10 11 12 13 14 15
HCT116
LoVo
LS174
DLD-1

B

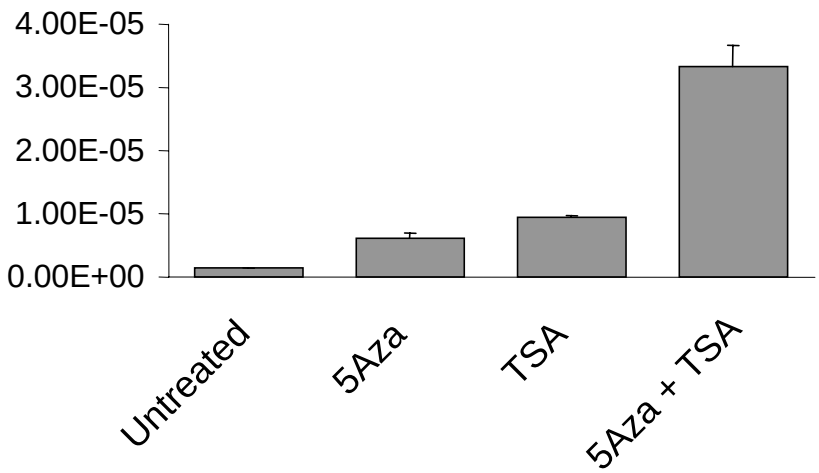
4.00E-05
3.00E-05
2.00E-05
1.00E-05
0.00E+00
Untreated
5Aza
TSA
5Aza + TSA

Figure 4

DNA hypermethylation in cancer: beyond the boundaries of a CpG island.

Jordi Frigola, Jenny Song, Clare Stirzaker, Miguel A. Peinado & Susan J. Clark

Sotmès a Nature Genetics

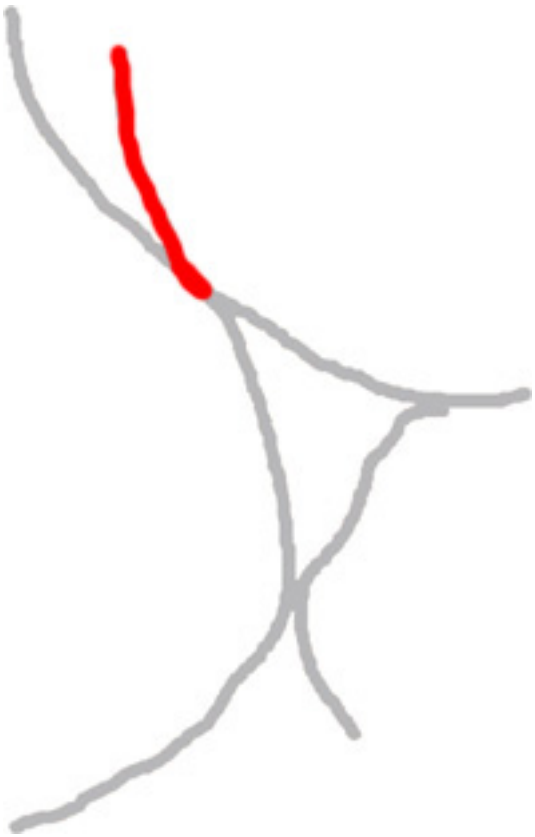

CAPÍTOL 5

La hipermetilació associada al procés tumoral sempre s'ha descrit com un tipus d'alteració molt localitzada i que afectava a un sol gen.

A partir de la tècnica AIMS es va identificar una hipermetilació recurrent, el fragment Z. La localització d'aquest fragment presentava dues característiques importants: (1) no estava associat a un gen determinat, i (2) estava relativament a prop d'una regió rica en illes CpG. Aquestes característiques ens van portar a l'anàlisi de la metilació genòmica i posterior caracterització de l'estructura cromatínica, al voltant del fragment original. En aquest capítol exposem la caracterització d'una regió que presenta la hipermetilació sincrònica de quinze illes CpG que s'estenen al llarg d'una Mb de longitud. Aquestes dades representen per primera vegada, la hipermetilació com una alteració cromosòmica amb un abast més enllà de l'illa CpG.

DNA hypermethylation in cancer: beyond the boundaries of a CpG island.

[1,2]Jordi Frigola, [2]Jenny Song, [2]Clare Stirzaker, [1]Miguel A. Peinado & [2*]Susan J. Clark

[1] IDIBELL-Institut de Recerca Oncologica,
Hospital Duran i Reynals
Granvia km 2,7
08907 L'Hospitalet, Barcelona Barcelona, Spain

[2] Garvan Institute of Medical Research,
384 Victoria St, Darlinghurst
Sydney, 2010, NSW, Australia

Corresponding Author: *Susan J. Clark
Telephone: 61-2-92958315
Fax: 61-2-92958316
E-mail: s.clark@garvan.org.au

Address for Correspondence:
Garvan Institute of Medical Research,
384 Victoria St, Darlinghurst
Sydney, 2010, NSW, Australia,

Key words: CpG island, DNA methylation, colorectal cancer.

Deregulation of the genomic DNA methylation profile is a hallmark of cancer DNA with hypermethylation and silencing of discrete CpG island associated genes being commonly observed. We now show hypermethylation in colorectal cancer of genomic DNA spanning a 1 Mb contiguous region that includes 15 CpG islands, and two known genes, *Engrailed-1* and *MARCO* and multiple Expression Sequence Tags (ESTs). Expansive hypermethylation of neighbouring CpG islands has not been reported before in cancer. This data provides evidence for a new paradigm that aberrant DNA methylation of large chromosomal regions is under co-ordinate control potentially leading to concomitant epigenetic silencing of multiple linked genes and transcribed regions in cancer cells.

Studies to date, using either candidate gene approaches or global array surveys have demonstrated that multiple, but discrete promoter-associated CpG islands can be methylated concurrently in any one cancer cell [1 2]. Using a global methylation approach AIMS (Amplification of Inter-Methylated Sites) [3 4] we identified a pair of *Sma*I sites, encompassing a 196bp fragment (Z), that was differentially methylated in 71 out of 112 (63%) colorectal tumours matched/normal pairs (Fig 1A). The Z fragment itself was not part of a definitional CpG island (bp:196bp, GC:47%, CpG O/E: 0.7) but was located 1.2kb downstream from a CpG rich region on chromosome 2q14.2 (Fig1B&C). The CpG rich region spanned 25kb and contained 11 discrete CpG islands (Genome Browser July 2003 CpG island predictor) including the CpG island with 128 CpG sites (CpG 128) that spanned the promoter of the developmentally regulated gene *Engrailed- 1* (*En1*) (Fig 1C). To determine if this extensive cluster of CpG islands was also differentially methylated in colorectal cancer, we used direct bisulphite PCR sequencing and methylation clonal sequencing analysis to determine the methylation status of 6 of the CpG islands (CpG104, CpG103, CpG128, CpG41, CpG173, CpG48) spanning 25kb downstream of the Z fragment in two colorectal cell lines HCT116 and SW480 and in 2 tumour/normal matched pairs 9N/T and 165N/T. The CpG sites in the Z fragment and in all 6 CpG islands including the En1 promoter (CpG128) were shown to be extensively methylated in the two colorectal cancer cell lines and in the 2 cancer DNA samples relative to methylation in the matched normal samples (Fig 2A&B). In fact both alleles are subject to hypermethylation, as CpG48 has an informative polymorphism (rs1438850) and both the A and T allele were shown to

be hypermethylated in HCT116 cells (supplementary S1). The presence of bi-allelic methylation suggests that the region is possibly subject to trans-regulatory control.

We extended the direct PCR DNA methylation sequencing analysis upstream and downstream to define the length of the differentially methylated region and to define the boundaries of CpG island methylation in the colorectal cancer samples. We found contiguous hypermethylation in the colorectal cancer cell lines and in the cancer samples relative to the matched normal samples in a region that spanned nearly 1Mb on chromosome 2q14.2, from CpG island (CpG61) 610kb upstream of the Z fragment, to CpG island (CpG 229) 325kb downstream. Flanking CpG islands CpG41.2 and CpG85 that codes for *TSAP6*, were unmethylated in both cancer and normal DNA, defining the left and right boundaries respectively of the differentially methylated region (Fig 2B). In addition to the 15 CpG islands, CpG depleted sequences were also examined. As well as the CpG depleted Z-fragment, a region 20kb upstream from the Z fragment (20kb) (bp=182, GC%= 63 CpG o/e = 0.6) was also found to be differentially methylated in cancer cells in comparison to the matched normal samples (Fig 2B). This data suggests that aberrant hypermethylation in cancer is not just restricted to the CpG island regions but extends into neigbouring CpG depleted regions as well.

Two known genes encoding *Engrailed-1* (*En1*) and *MARCO* (macrophage receptor with collagenous domain), and a putative gene encoding a C1q-domain protein (*C1QL2*), as well as multiple ESTs are located across the differentially methylated 1Mb region (Fig 2 B&C). *En1* is a homeobox transcription factor and interacts directly with the canonical Wnt signaling pathway through repression of Wnt7a and plays an essential role in development[5]. CpG island (CpG128) spans the promoter of *En1* and was shown to be differentially methylated in the colorectal cell lines and in the 2 cancer samples (6T & 165T) but not in the matched normal samples (Fig 2A). By direct PCR sequencing CpG128 was also found to be hypermethylated in 18/26 (70%) colorectal cancers versus matched normal samples (Fig 2C). Hypermethylation of *En1* promoter was found to be independent of sex, age, and Dukes stage, indicating it may be an early event in colorectal cancer. *MARCO* is a type II transmembrane protein of class A scavenger receptor family and plays a role in anti-microbial host defense [6]. *MARCO* expression has been reported to be downregulated by up to 90 fold during colon cell maturation [7]. The promoter of *MARCO* is not associated with a CpG island [8] and in fact contains only 4 CpG sites in the promoter

region and these 4 sites were not differentially methylated in the cell lines or the normal or tumour tissues (supplementary S2).

Consistent with previous array analysis [7] the expression of *En1* and *MARCO* is normally undetectable or very low (basal levels) in colorectal epithelial cells and we found by quantitative RT-PCR that it is even further reduced in the HCT116 cells and cancer samples relative to the matched normal colorectal cells (Fig 3A). Intriguingly treatment of the HCT116 cells with demethylating agent 5-Aza-2'-deoxycytidine (5Aza-C) results in dramatic activation of *En1* expression and this is further enhanced by treatment with an inhibitor of histone deacetylase trichostatin A (TSA) (Fig3B). Addition of 5Aza-C to HCT116 cells had only a minor effect on the activation of *MARCO* whereas the addition of 5Aza-C in combination with TSA led to significant activation of expression of *MARCO* (Fig3B), indicating a major role of chromatin modification in repression of *MARCO*. We used a Chromatin immunoprecipation (ChIP) assay to analyse histone H3 lysine methylation (H3-K9) in the promoter regions of *En1* and *MARCO* in HCT116 cells. For both promoters a marked reduction in H3-K9 immunoprecipitation was observed following treatment with TSA or 5-Aza-C (Fig3C), indicating significant lysine methylation in HCT116 cells. The data indicate transcriptional repression of the linked region in cancer cells by both DNA and histone methylation and chromatin remodelling.

The significance of silencing of this region in colorectal cancer is unclear but it is clear that it is a common event, and an event that occurs on both chromosomes. *MARCO* and *En1* have not been indicated as tumour suppressor genes, this region is not reported to be commonly deleted in colorectal cancer and we found no evidence of LOH in the cell lines or colorectal samples studied (data not shown). However chromatin remodelling encompassing the promoter of *MARCO* would ensure its inability to respond to bacterial Infections of the colon thereby reducing the potential innate immune response in the cancer cells. *En1* is a transcription factor that directly interacts with the Wnt signaling pathway [9] and therefore its inactivation could clearly play a significant role in colorectal cancer progression.

Hypermethylation of the DNA and chromatin of individual CpG associated genes is a common signature in cancer cells. In this study we show that this signature can span more than just the promoters of individual genes and in fact can extend across at least 1Mb of DNA. Such widespread methylation can result in the inactivation of all the incumbent genes regardless of whether the gene promoters are CpG rich or CpG depleted and

suggests the existence of an epigenetic regulatory mechanism extending across a broad region. The existence of long-range epigenetic regulation has previously been identified in the specific cases of X-chromosome inactivation and imprinted genes but has not been recognised more generally. In summary, we propose that epigenetic inactivation spanning large chromosomal regions provides a global gene silencing mechanism with equivalent implications to LOH as the genes and noncoding transcripts within the region would all be inactivated.

ACKNOWLEDGEMENTS

We thank Jairo Rodriguez for LOH analysis. This work was supported in part by a grant from NH&MRC (293810) and a grant from the Spanish Ministry of Education and Science (SAF2003/5821). JF is a fellow of the Spanish Ministry of Education and Science (FPU program) at the Universitat Autonoma de Barcelona and SJC is a principal research fellow of NH&MRC (293811).

MATERIAL AND METHODS

Samples

One hundred and twelve colorectal carcinomas, with their paired non adjacent areas of normal colonic mucosa were collected as fresh-frozen tissues within 2 hours of removal and stored at –80C. All samples were obtained from the Hospital de la Santa Creu i Sant Pau (Barcelona Spain). The study protocol was approved by the Ethics committee. Human colorectal carcinoma cell lines were obtained from the American Type culture Collection (ATCC, Manassas, VA).

AIMS screening

We used AIMS method to screen for tumour-specific alterations. AIMS method is based on the differential cleavage of isoschizomers with distinct methylation sensitivity and the selective amplification of short sequences flanked by two SmaI (CCCGGG) sites that are ligated to an adaptor and a specific 3-4 nucleotide sequence. Lack of methylation at either site prevents amplification of the band. The AIMS generated fragments were isolated and sequenced. All samples were analysed using the set of primers (set B) and the conditions previously described [3]. Results on global profiles of DNA methylation have been described elsewhere [4].

5-Aza-2'-deoxycytidine and TSA treatment of cells

The colon cancer cell line HCT116 was cultured in D-MEM/F12 (Gibco /BRL) medium supplemented with MEM sodium pyruvate and L-Glutamine and 10% foetal calf serum. 100mm tissue culture dishes were seeded with $0.5x10^6$ cells and treated 24 h later with 0.5μM 5-Aza-2'-deoxycytidine (5-Aza-dC) (Sigma) for 24 hours and cultured with fresh medium for a further 48 h. Cells were treated with Trichostatin A (TSA) (Sigma) at 100 nM for 24 h. For co-treatment of cells with 5-Aza-dC and TSA, 5-Aza-dC was added initially for 24 h, after which it was removed and TSA was added for a further 24h.

RNA extraction and Quantitative Real-Time RT-PCR

RNA was extracted from tumour and matched normal samples, as well as from the cell lines using Trizol reagent (Invitrogen) and cDNA was reverse transcribed from 2μg of total RNA using SuperScript™ III RNase H - Reverse Transcriptase (Invitrogen Life

Technologies), according to the manufacturer's instructions. The reaction was primed with 200ng of random hexamers **(**Roche). The reverse transcription reaction was diluted 1:20 with sterile H_20 before addition to the RT-PCR. Expression was quantitated using a flourogenic real-time detection method using the ABI Prism 7000 Sequence Detection System. 5µl of the reverse transcription reaction was used in the quantitative real-time PCR reaction using 2x SYBR Green 1 Master Mix (P/N 4309155) with 50ng of each primer. The primers used for amplification are listed in Table 1. To control for the amount and integrity of the RNA, the Human 18S ribosomal RNA (rRNA) kit (P/N 4308329) (Applied Biosystems), containing the rRNA forward and reverse primers and rRNA VIC^{TM} probe, was used. 5µl of the reverse transcription was used in a 20µl reaction in TaqMan Universal PCR Master Mix (P/N 4304437) with 1µl of the 20xHuman 18S rRNA mix. The reactions were performed in triplicate and the standard deviation was calculated using the Comparative method (ABI PRISM 7700 Sequence Detection system User Bulletin #2, 1997 P/N 4303859). The cycle number corresponding to where the measured fluorescence crosses a threshold is directly proportional to the amount of starting material. The mean expression levels are represented as the ratio between each gene and 18S rRNA expression.

Genomic Bisulphite Sequencing

DNA was extracted from the HCT116/SW480 cells using the Puregene extraction kit (Gentra Systems) and Trizol reagent (Invitrogen) from the cancer/normal samples according to the manufacturer's protocol. The bisulphite reaction was carried out on 2µg of restricted DNA for 16 h at 55°C under conditions as previously described [10] [11]. Three independent PCR reactions were performed and pooled to ensure a representative methylation profile. The primers used for the bisulphite PCR amplifications are listed in Table 1. Pooled PCR fragments were directly purified using the Wizard PCR DNA purification system and cloned into the pGEM^{R} -T-Easy Vector (Promega) using the Rapid Ligation Buffer System (Promega). Approximately 12 individual clones were sequenced from the pooled PCR reactions using the Dye Terminator cycle sequencing kit with AmpliTaq DNA polymerase, FS (Applied Biosystems) and the automated 373A NA Sequencer (Applied Biosystems). Direct Sequencing of the pooled PCR products was also obtained using the reverse primer of the PCR amplification in the Dye Terminator cycle sequencing kit with AmpliTaq DNA polymerase, and the automated 3730 DNA analyser with KB^{TM} basecaller in Sequence analysis v5.1 (Applied Biosystems). The degree of

methylation was calculated by comparing the peak height of the cytosine residues with the peak of the thymine residues as described in Melki *et al* [1].

Chromatin Immunoprecipitation (ChIP) Assays

ChIP assays were carried out according to the manufacturer (Upstate Biotechnology). Briefly, ~ 1 x 10^6 HCT116 cells, in a 10cm dish, were fixed by adding formaldehyde at a final concentration of 1% and incubating for 10 minutes at 37°C. The cells were washed twice with ice cold PBS containing protease inhibitors (1mM phenylmethylsulfonyl fluoride (PMSF), 1μg/ml aprotinin and 1μg/ml pepstatin A), harvested and treated with SDS lysis buffer for 10 min on ice. The resulting lysates were sonicated to shear the DNA to fragment lengths of 200 to 500 basepairs. The complexes were immunoprecipitated with an antibodiy specific for dimethyl-histone H3(lys9) (#07-212))from Upstate Biotechnology. 10μl of antibody were used for each immunoprecipitation according to the manufacturer. No antibody controls were also included for each ChIP assay and no precipitation was observed. The antibody/protein complexes were collected by salmon sperm DNA/protein A agarose slurry and washed several times following the manufacturer's instructions. The immune complexes were eluted with 1% SDS and 0.1 M $NaHCO_3$ and the crosslinks were reversed by incubation at 65°C for 4 hours in the presence of 200mM NaCl. The samples were treated with proteinase K for 1 hour and the DNA was purified by phenol/chloroform extraction, ethanol precipitation and resuspended in 30μl H_2O.

*Quantitative Real-Time PCR Analysis***.**

The amount of target that was immunoprecipitated, was measured by Real-Time PCR using the ABI Prism 7900HT Sequence Detection System. Amplification primers for En1 nd MARCO are listed in Table 1. PCR reactions were set up according to the SDS compendium (ver 2.1) for the 7900HT Applied Biosystems Sequence Detector as described previously [11]. Either immunoprecipitated DNA, no-antibody control or input chromatin were used in each PCR and the PCRs were set up in triplicate. Standard deviation was calculated using the Comparative method (ABI PRISM 7700 Sequence Detection System User Bulletin #2, 1997 (P/N 4303859). For each sample an average C_T value was obtained for immunoprecipitated material and for the input chromatin. The difference in C_T values (delta C_T) reflects the difference in the amount of material that was immunopreciptated relative to the amount of input (ABI PRISM 7700 Sequence Detection system User Bulletin #2, 1997 (P/N 4303859).

REFERENCES

1. Melki, J.R., Vincent, P.C. & Clark, S.J. Concurrent DNA hypermethylation of multiple genes in acute myeloid leukemia. *Cancer Res* **59**, 3730-40. (1999).
2. Rush, L.J. et al. Epigenetic profiling in chronic lymphocytic leukemia reveals novel methylation targets. *Cancer Res* **64**, 2424-33. (2004).
3. Frigola, J., Ribas, M., Risques, R.A. & Peinado, M.A. Methylome profiling of cancer cells by amplification of inter-methylated sites (AIMS). *Nucleic Acids Res* **30**, e28. (2002).
4. Frigola, J. et al. Differential DNA hypermethylation and hypomethylation signatures in colorectal cancer. *Hum Mol Genet* **14**, 319-26. Epub 2004 Dec 1. (2005).
5. Adamska, M., MacDonald, B.T., Sarmast, Z.H., Oliver, E.R. & Meisler, M.H. En1 and Wnt7a interact with Dkk1 during limb development in the mouse. *Dev Biol* **272**, 134-44. (2004).
6. Sankala, M. et al. Characterization of recombinant soluble macrophage scavenger receptor MARCO. *J Biol Chem* **277**, 33378-85. Epub 2002 Jul 03. (2002).
7. Mariadason, J.M. et al. A gene expression profile that defines colon cell maturation in vitro. *Cancer Res* **62**, 4791-804. (2002).
8. Kangas, M. et al. Structure and chromosomal localization of the human and murine genes for the macrophage MARCO receptor. *Genomics* **58**, 82-9. (1999).
9. Moon, R.T., Kohn, A.D., De Ferrari, G.V. & Kaykas, A. WNT and beta-catenin signalling: diseases and therapies. *Nat Rev Genet* **5**, 691-701. (2004).
10. Clark, S.J., Harrison, J., Paul, C.L., & Frommer, M. High sensitivity mapping of methylated cytosines. *Nucl. Acids Res.* **22**, 2990-2997 (1994).
11. Stirzaker, C., Song, J.Z., Davidson, B. & Clark, S.J. Transcriptional gene silencing promotes DNA hypermethylation through a sequential change in chromatin modifications in cancer cells. *Cancer Res* **64**, 3871-7. (2004).

FIGURE LEGENDS

Figure 1

Hypermethylation of a 1Mb region in colorectal cancer on chromosome 2q12.4. **(a)** An example from 15 sets of cancer and matched normal colorectal samples of differential methylation of a 196bp *Sma*I fragment (Z) generated by AIMS. The 196bp *Sma*I fragment, named the Z fragment, indicated by an arrow, was excised from a fresh dried polyacrylamide gel, reamplified, cloned and sequenced to ascertain the identity of the isolated band. **(b)** Chromosomal location on 2q14.2 of the differentially methylated Z fragment sequence (*) in context of the location of the CpG islands and ESTs identified via Genome Brower (July 2003). Dark lines represent CpG islands greater than 300bp in length and light grey lines CpG islands less than 300bp. The differentially methylated region covers a 1Mb region encompasses 15 CpG islands from base position 11900000 to 12000000. The CpG number indicates the number of CpG sites per island. **(c)** Expanded view of the Z fragment relative to the surrounding CpG islands on chromosome 2q14.2. The location of the CpG islands relative to the Z fragment are indicated in Kb. The black arrows indicate the known genes in the region and the grey arrow represents the predicted genes based on SWISS-PROT.

Figure 2

Examples of bisulphite DNA methylation sequencing analysis. **(a)** Sequence analysis of 10-12 clones derived from a pool of 3 independent PCR fragments containing the Z fragment and CpG island 128 (*En-1* promoter) from two colorectal cell lines HCT116 and SW480 and two paired cancer (T) matched normal (N) samples. Methylated CpG sites are indicated by black squares and unmethylated CpG sites are white. **(b)** Summary of the DNA methylation profile by direct PCR sequencing of the CpG islands and CpG depleted regions across a 1Mb region of chromosome 2q14.2 in 2 colorectal cell lines and 2 pairs of cancer and matched normal samples. The coordinates from Genome Browser Human (July 2003) and the distance in kilobases (Kb) from the Z fragment are indicated. Each CpG island that is associated with a gene is shown. CpG I denotes presence or absence of a CpG island. **(d)** DNA methylation of the CpG 128 En1 promoter by direct PCR sequencing is summarised in 26 colorectal samples. The sample number, age, sex and

Duke stage is indicated. Methylation of the *En1* promoter is showing in black and the lack of methylation is shown in white.

Figure 3

Expression and Chromatin immunoprecipitation (ChIP) studies show the effect of chromatin suppression of *Engrailed-1* (*En1*) and *MARCO* in colorectal cancer cells. **(a)** Suppression of *Engrailed-1* (*En1*) and *MARCO* expression in cancer cells. The level of expression of *En1* and *MARCO* was assayed by quantitative real-time PCR and normalised using 18S RNA expression from RNA isolated from 10 pooled tumour samples and 10 matched normal samples and HCT116 cells. **(b)** The level of expression of *En1* and *MARCO* was also compared between HCT116 cells that were untreated (-) compared to treatment with 5-Aza-2' deoxycytidine (Aza), TSA or a combination of TSA and 5-Aza-2' deoxycytidine (Aza/TSA). Error bars show standard errors of three independent experiments. **(c)** Chromatin from HCT116 cell lines, untreated (-) or treated with 5-Aza-2' deoxycytidine (Aza), TSA or a combination of TSA and 5-Aza-2' deoxycytidine (Aza/TSA) were immunoprecipitated with antibodies to anti-methylated Histone H3 (lysine 9). The amount of immunoprecipitated DNA from the *Engrailed* (*En1*) promoter associated CpG island 128 and the *MARCO* promoter was quantified by real-time PCR and the amount of immunoprecipitated DNA plotted was calculated as a ratio of immunoprecipitated DNA to the total amount of input DNA in the PCR reaction. Errors bars show standard errors of three independent experiments.

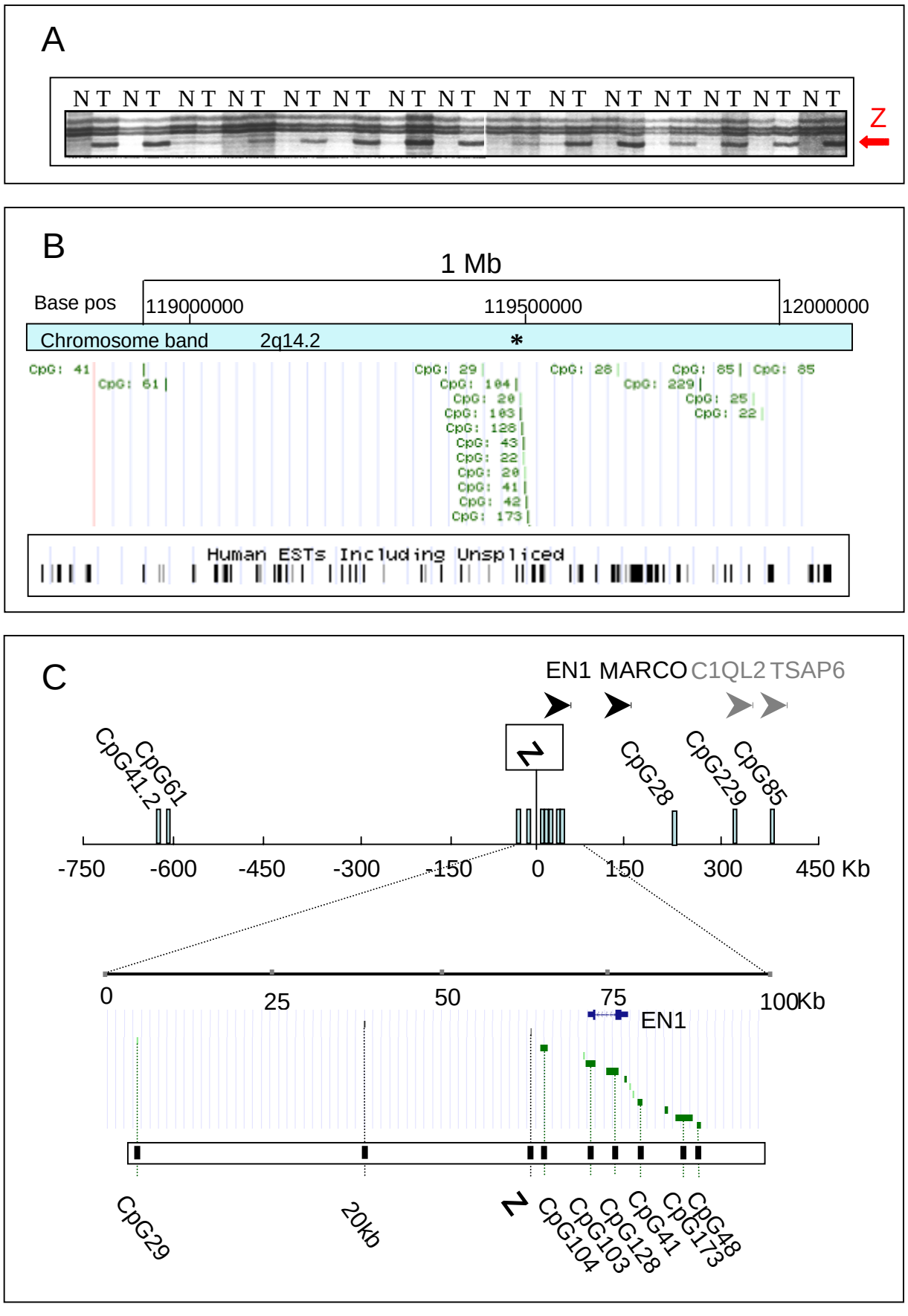
A
N T N T N T N T N T N T N T N T N T N T N T N T N T N T N T
Z
B
1 Mb
Base pos
119000000
119500000
12000000
Chromosome band
2q14.2
*
CpG: 41
CpG: 61
CpG: 29
CpG: 104
CpG: 20
CpG: 103
CpG: 128
CpG: 43
CpG: 22
CpG: 20
CpG: 41
CpG: 42
CpG: 173
CpG: 28
CpG: 85
CpG: 229
CpG: 25
CpG: 22
CpG: 85
Human ESTs Including Unspliced
C
EN1 MARCO C1QL2 TSAP6
CpG41.2
CpG61
Z
CpG28
CpG229
CpG85
-750
-600
-450
-300
-150
0
150
300
450 Kb
0
25
50
75
100Kb
EN1
CpG29
20kb
Z
CpG104
CpG103
CpG128
CpG41
CpG173
CpG48

Figure 1

A

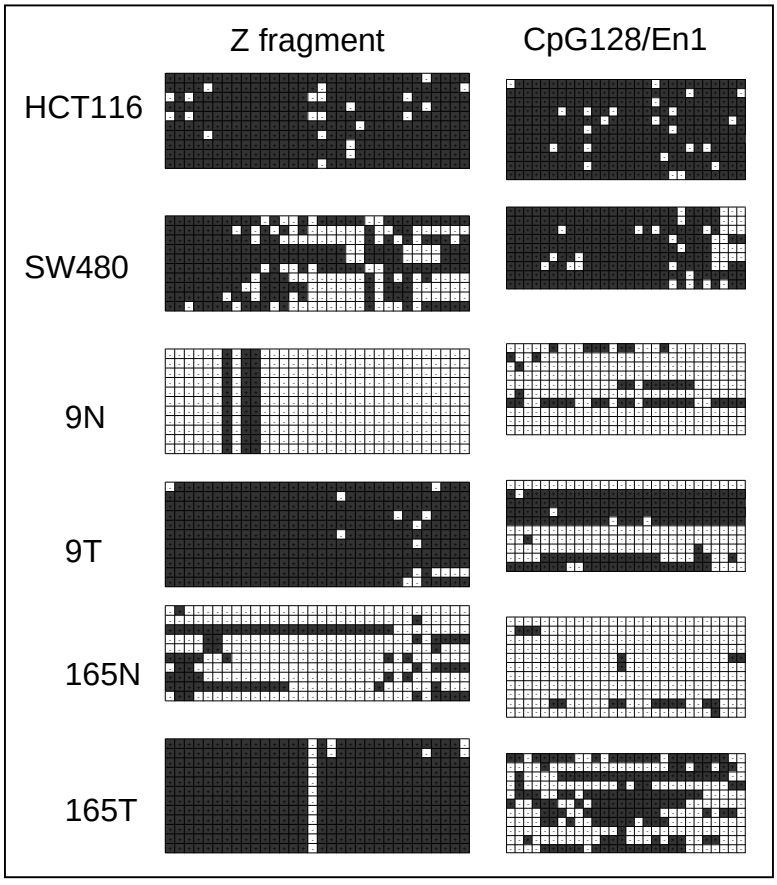

C

CASE	CpG128	AGE	SEX	DUKE'S
17	■	31	W	C2
127		31	W	C2
143	■	37	W	C1
175		46	W	B2
19		49	W	B1
69	■	52	M	B2
108		62	M	C2
122	■	62	M	C1
78	■	62	M	B2
103	■	66	M	B2
9	■	67	M	B2
21	■	68	W	B2
144		72	W	B2
72	■	73	M	C2
113	■	73	W	B2
63	■	74	W	C2
223	■	75	M	B2
147	■	76	W	C2
165	■	76	M	C2
75	■	77	M	B2
102	■	77	M	B2
151	■	79	M	B2
138		80	W	B2
171	■	85	M	C2
74		87	M	C2
90		88	W	C2

B

NAME	CpGi	Co-ord	Dis.(Kb)	GENE	HCT	SW	9N	9T	165N	165T
CpG41.2	Yes	119038970-119039344	-650	-						
CpG61	Yes	119076916-119077611	-610	-	■	■		■		
CpG29	Yes	119627212-119627460	-58	-	■	■		■		■
20Kb	No	119661213-119661555	-20	-	■	■		■		■
Z	No	119686319-119686515	0	-	■	■		■		■
CpG104	Yes	119687749-119688990	3	-	■	■		■		■
CpG103	Yes	119694605-119696111	8	-	■	■		■		■
CpG128	Yes	119697763-119699631	15	EN1	■	■		■		■
CpG41	Yes	119702525-119703055	18		■	■		■		■
CpG173	Yes	119708178-119710710	23	-	■	■		■		■
CpG48	Yes	119711280-119711971	25	-	■	■		■		■
5'-MARCO	No	119595459-119823428	110	MARCO	■	■	■	■	■	■
CpG229	Yes	120009273-120011808	325	C1QL2	■	■		■		■
CpG85	Yes	120076226-120076963	390	TSAP6						

Figure 2

Expression

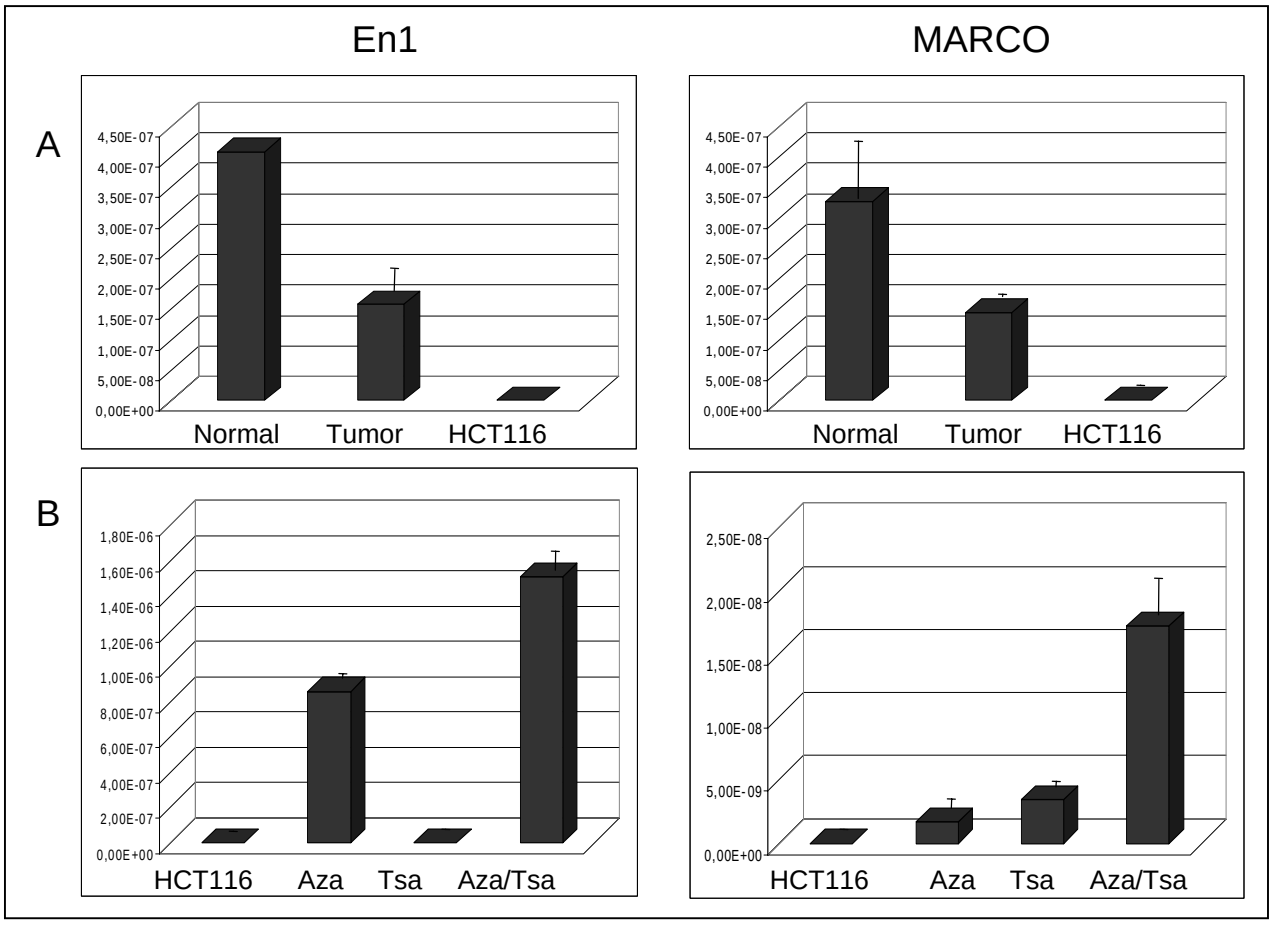

Chromatin Immunoprecipitation

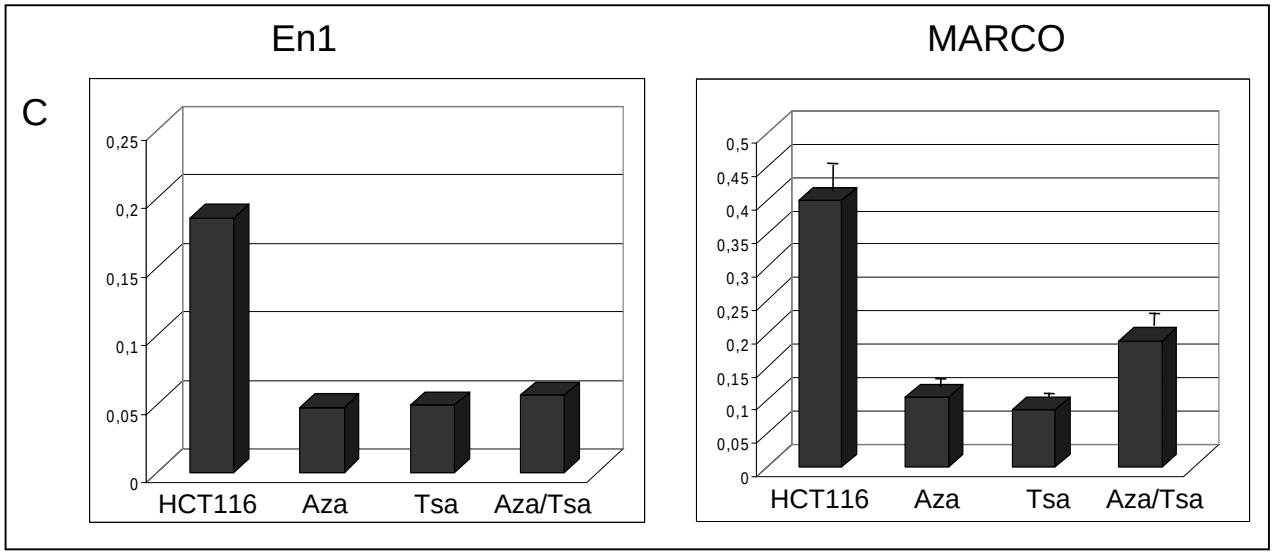

Figure 3

Clone	SNPa	1	2	3	4	5	6	7	8	9	10	11	12	13	14
1	T	-	+	-	+	+	+	+	+	+	+	+	+	+	+
2	T	+	+	+	+	-	+	+	+	+	+	+	+	+	+
3	A	+	+	+	+	+	+	+	+	+	+	+	+	+	+
4	T	-	+	-	+	+	+	+	+	+	+	+	+	+	+
5	A	+	-	-	+	-	+	+	+	+	+	+	+	+	+
6	A	+	-	+	+	+	+	+	+	+	+	+	+	+	+
7	T	+	+	+	+	+	+	+	+	+	+	-	+	+	+
9	A	+	-	+	+	+	+	+	+	+	+	+	+	+	+
10	T	-	-	+	+	+	+	+	+	+	+	+	+	+	+
11	T	-	+	-	+	+	+	+	+	+	+	+	+	+	+
12	T	+	+	+	+	+	+	+	+	+	+	+	+	+	+

Supplementary S1

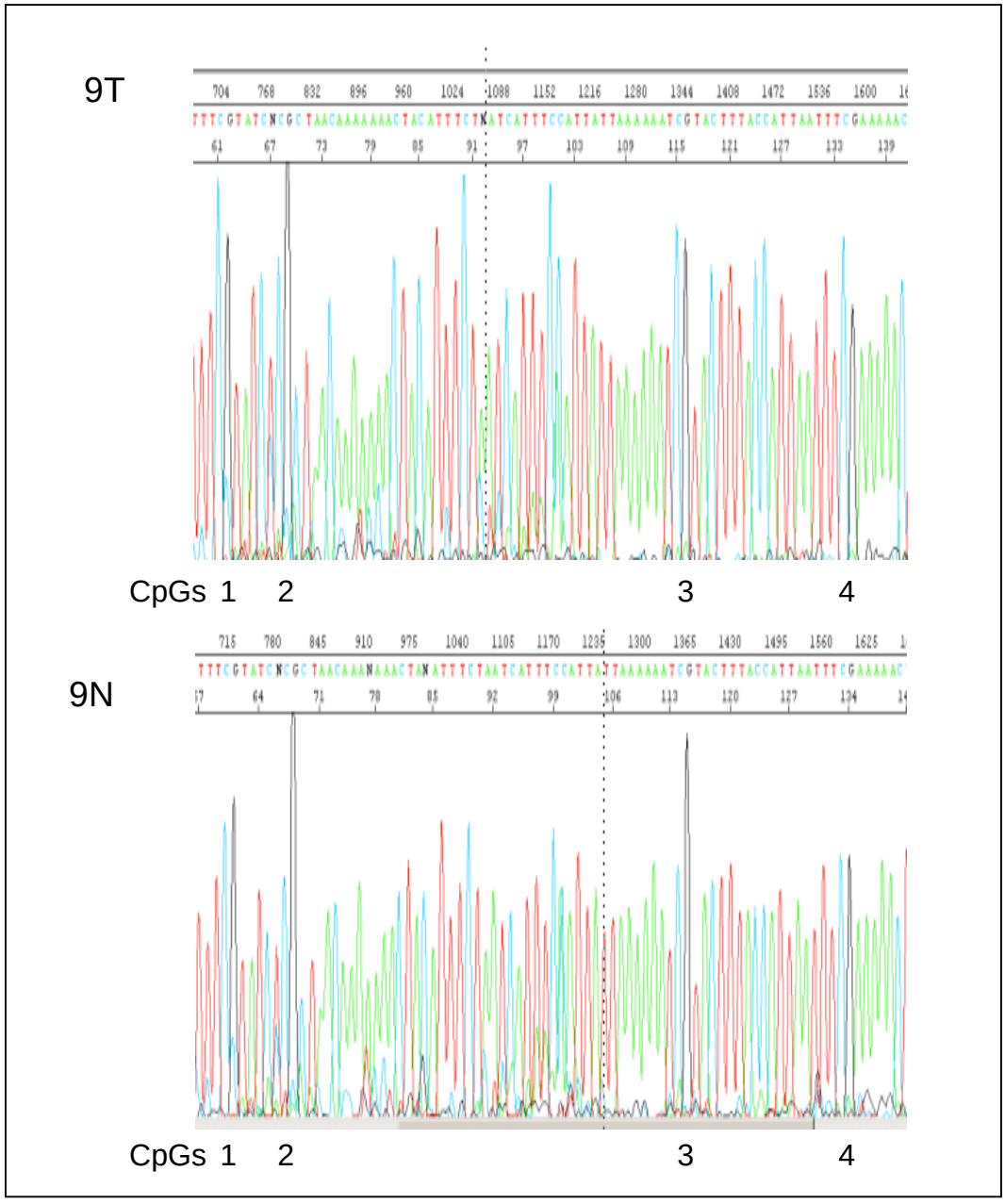

Supplementary S2

Table 1

Bisulphite primers

Sequence	Genebank	GI	Forward Primer Outer (5' -3')	Reverse Primer Outer (5'-3')	Forward Primer Inner (5'-3')	Rev
CpG41.2	AC093901	18497267	AGTTGTAGTGTTGAGGATTT, CpG 41-2 L3(58808-58827)	TAAATCCTTAACAAAATAAA, CpG 41-2 R3(59129-59110)	TGTAAGGTAGAAATATTAA, CpG 41-2 L4(58849-58867	AA
CpG61	AC093901	18497267	GAAAGTAGATTTAGTTTTTG, CpG 61 L1(97188-97207)	CCCATTAAAAACTATTTATTA, CpG 61 R1(97515-97495)	TTGTTAATTTTTGGGTAATT, CpG 61 L2(97212-97231)	AC
CpG29	AC018686	11038588	ATTGTTTTGGTGTAAAGTAT, CpG 29 L1(189607-189626)	CCTCTACTTATATTAACTAA, CpG 29 R1(189943-189924)	TGAATTTATAGTTTTTAGTT, CpG 29 L2(189630-18964	AT
20Kb	AC012665	14589661	TTTAGTTTGGATTTAGATTT, 20 Kb Z L1	CCTCAATCCTAATATATTTA, 20 Kb Z R1	ATTTAGGGTTGAGGGTTTTT, 20 Kb Z L2	AT
Z	AC012665	14589661	AAAAATTATTTAAAAACTCCCC-Z3L	ATAAGTATAGAATTTTAGGG-Z1R	AAAATTTAACCCACCAATCCTA-Z4L	TA
CpG104	AC012665	14589661	TTTAGTTTTTATTGGAGAGA-CpG104(II)-L1	TAAAAAACTATTATCCCTCC-CpG104(II)-R1	TTTAGTTTTTATTGGAGAGA- CpG104(II)-L1	TA
CpG103	AC012665	14589661	AATTAGATTTTGATTTGGGAT, CpG 103 L1(34867-34887)	ATAATCTAATAAAAAACACTT, CpG 103 R1(35263-35243)	TTGAGTTTTTGGGTTAGGGTT, CpG 103 L2(34897-3491	CC
CpG128	AC012665	14589661	AGAATAATAAAGATAAGAGAT, CpG 128 L1(37815-37835)	ACTATCCTACTTATAAACTC, CpG 128 R1(38225-38206)	GTTTTAGGGATTTAGAGTTT, CpG 128 L2(37843-37862	CT
CpG41	AC012665	14589661	GAAGATAATTTATAGGTTTTA, CpG 41 L1(41698-41718)	ATCCCATTACTATAACAAAT, CpG 41 R1	ATAGGTTTGTGAATAAAATT, CpG 41 L2	AA
CpG173	AC012665	14589661	AGGGATTGGAGGTTTTATTA, CpG 173 L1	CAAATAACAACTAACCCCAA, CpG 173 R1	TGAGTAGTTTTTTGAATATTA, CpG 173 L2	CC
CpG48-rv	AC012665	14589661	GGGATTAGTGGAATTATGTT, CpG 48 –rv-L1	AAAAACAAAACCCAACCTTC, CpG 48 –rv-R1	ATGTTGGTTTTTAGTTATTTT, CpG 48 –rv-L2	TC
5'-MARCO	AC013457	14589667	TGAGAAATAAGAAAATTTTT, Marco L1	AAAAATTCCAAATTAAAACA, Marco R1	GTTTTTGAGTGAGATTTAAT, Marco L2	AA
CpG229	AC016673	11038558	AGAGAAAGGAGGTTGGTTT, CpG 229 L3	ATAAATCTCAAAAACCCCCA, CpG 229 R3	GAGTGTAGGGGTTATTGAT, CpG 229 L4	AC
TSAP6	AC016673	11038558	GTTTAGAGGTTATTTTGGTT, TSAP6 L3	AAAAAATACACTCACCTCTA, TSAP6 R3	GAGTTTTGTTTATTTTAGT, TSAP6 L4	AA

T-PCR primers

Sequence	Genebank	GI	Forward Primer	Reverse Primer
CpG128	AC012665	14589661	TGGGTGTACTGCACACGTTATTC (EN1_EXP_L1)	CTTGTCCTCCTTCTCGTTCTTCTT (EN1_EXP_R1)
5'-MARCO	AC013457	14589667	GCTGCAGCGGGTAGACAACT (F1)	GCCTTGTTCACCTTTGATTCTGA (R1)

ChIP primers

Sequence	Genebank	GI	Forward Primer	Reverse Primer
CpG128	AC012665	14589661	CAGAGGCCAGGATCGCAT (EN1-Ch-F) (37927-37944)	TCACCCCAGTTCCAGTCACA (EN1-Ch-R) (37983-37964)
5'-MARCO	AC013457	14589667	GAAAATTCTCAAGGAGGACGAGC (MARCO-Ch-F) (10075-1	TGCAATTTGGTGAAAAGCAGC (MARCO-Ch-R) (10138-10118)

Chromatin remodelling and DNA methylation results in co-ordinate gene suppression across the entire human chromosome 2q14.2 in colorectal cancer

Jordi Frigola, Jenny Song, Clare Stirzaker, Miguel A. Peinado & Susan J. Clark

En preparació.

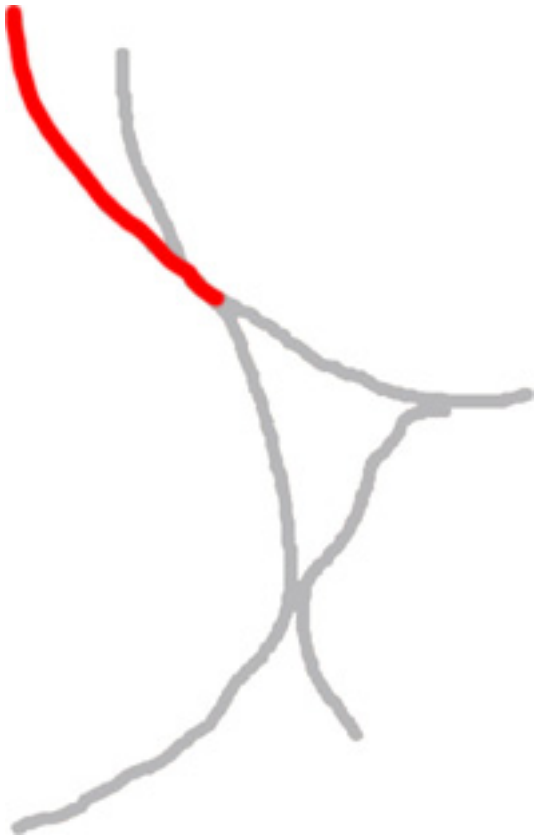

CAPÍTOL 6

La presència de grans canvis estructurals en la cromatina associats al procés tumoral representa un mecanisme de control en l'expressió gènica de grans regions cromosòmiques. Aquest tipus d'alteracions no s'ha descrit mai en la bibliografia.

Aquest treball és una extensió de la caracterització presentada en el capítol 5. Concretament, presentem els resultats obtinguts en la caracterització de la metilació genòmica, així com de l'estructura cromatínica de la banda citogenètica 2q14.2, lloc d'origen del fragment Z.

Actualment, s'està elaborant aquest treball i com a conseqüència, no es disposa de la discussió en format article. Tanmateix, els resultats presentats en aquest capítol són ampliament tractats al llarg de la discussió d'aquesta tesis.

Chromatin remodelling and DNA methylation results in co-ordinate gene suppression across the entire human chromosome 2q14.2 in colorectal cancer

[1,2]Jordi Frigola, [2]Jenny Song, [2]Clare Stirzaker, [1]Miguel A. Peinado & [2*]Susan J. Clark

[1]IDIBELL-Institut de Recerca Oncologica,
Hospital Duran i Reynals
Granvia km 2,7
08907 L'Hospitalet, Barcelona Barcelona, Spain

[2]Garvan Institute of Medical Research,
384 Victoria St, Darlinghurst
Sydney, 2010, NSW, Australia

Corresponding Author: *Susan J. Clark
Telephone: 61-2-92958315
Fax: 61-2-92958316
E-mail: s.clark@garvan.org.au

Address for Correspondence:
Garvan Institute of Medical Research,
384 Victoria St, Darlinghurst
Sydney, 2010, NSW, Australia,

Key words: CpG island, DNA methylation, colorectal cancer.

INTRODUCTION

Cancer is a disease of the DNA with both genetic and epigenetic lesions contributing to changes in gene expression. Genetic changes that are associated with cancer include gene mutation in critical tumour-associated genes, as well as gene deletion or loss of heterozygosity (LOH) of larger regions harbouring tumour suppressor genes. In addition to genetic changes it is clear that epigenetic changes are also a common hallmark of cancer DNA, with changes in both DNA methylation and chromatin remodelling of CpG island associated tumour suppressor genes. Since these epigenetic changes are associated with gene silencing, it is clear that hypermethylation and chromatin modification of individual tumour suppressor genes plays a key role in the pathogenesis of cancer. One of the major questions still to be resolved is the mechanism responsible for epigenetic change in cancer, in particular what determines which genes are susceptible to hypermethylation in different cancer types (Stirzaker *et al*, 2004). Studies to date, using either candidate gene approaches or global array surveys have demonstrated that multiple unlinked genes can be methylated concurrently in any one cancer cell. Using a global methylation approach AIMS (Amplification of Inter-Methylated Sites) (Frigola *et al*, 2002) we now show that epigenetic changes in cancer are not just restricted to individual CpG island associated genes but can span an entire chromosome band resulting in global silencing of the region. We propose that epigenetic inactivation spanning large chromosomal regions may act as a gene silencing mechanism with equivalent implications to LOH in tumours.

RESULTS

Identification of a differentially methylated region in colorectal cancer using AIMS

Studies to date, using either candidate gene approaches or global array surveys have demonstrated that multiple, but discrete promoter-associated CpG islands can be methylated concurrently in any one cancer cell (Melki et al, 1999; Rush et al, 2004). Using a global methylation approach AIMS (Amplification of Inter-Methylated Sites) (Frigola et al, 2002; Frigola et al, 2005) (Fig1A) on 112 colorectal cancer samples we identified number of differentially methylated fragments in the cancer versus normal colon cells. Interestingly more hypomethylation was detected in the colorectal cancer versus the matched normal samples as shown in Figure1B. However, one fragment, termed the Z fragment, that encompassed a pair of *Sma*I sites (196bp apart) was found to be commonly hypermethylated in the colorectal cancer samples (Fig1B). In fact the Z fragment was differentially methylated in 71 out of 112 (63%) colorectal tumours versus matched normal pairs, as determined by AIMS amplification. The Z fragment was sequenced and found to be located on chromosome 2q14.2. The Z fragment encompassed a region that was not part of a definitional CpG island (bp:196bp, GC:47%, CpG O/E: 0.7) but was located 1.2kb downstream from a region that was extensively CpG rich. The downstream CpG rich region spanned 25kb and contained 11 discrete CpG islands (Genome Browser July 2003 CpG island predictor). Only one of the CpG islands in the 25kb region was associated with a gene and this CpG island with 128 CpG sites (CpG 128), contained the promoter of a developmentally regulated homeobox-containing gene *Engrailed-1* (*En1*) (Fig 2A).

DNA methylation of neighbouring CpG islands

To determine if the extensive cluster of CpG islands was also differentially methylated in colorectal cancer, we used direct bisulphite PCR sequencing and methylation clonal sequencing analysis to determine the methylation status of 6 of the CpG islands (CpG104, CpG103, CpG128, CpG41, CpG173, CpG48) and a spanning 25kb downstream of the Z fragment in two colorectal cell lines HCT116 and SW480 and in 2 tumour/normal matched pairs 9N/T and 165N/T. The CpG sites in the Z fragment and in a CpG depleted region 20kb upstream from the Z fragment (20kb) (bp=182, GC%= 63 CpG o/e = 0.6) and in all 6 CpG islands, including the *En1* promoter (CpG128), were shown to be extensively methylated in the two colorectal cancer cell lines and in the 2 cancer DNA samples relative to methylation in the matched normal samples (Fig

2B). The clonal analysis indicated in a low level of methylation in some molecules in the matched normal samples this could reflect either minor cancer cell contamination of the samples or a low level of methylation in the normal colon, whereas direct PCR sequencing which is less sensitive showed no detectable methylation in the normal samples (data not shown).

DNA methylation analysis across chromosome 2q14.2

The 14.2 cytogenetic band on chromosome 2, is rich in genes and associated CpG islands, and spans a 4Mb region (Fig3A). The location of the defined and putative genes and associated CpG islands is shown in Figure3B. We extended the direct PCR DNA methylation sequencing analysis upstream and downstream of the 25kb CpG rich sequence, adjacent to the Z fragment, to define the length of the differentially methylated region and to define the boundaries of CpG island methylation across the 4Mb region of chromosome 2q14.2 in the colorectal cancer samples.

Figure3C summarises the DNA methylation state across the 4Mb region of chromosome 2q14.2 in the colorectal cancer cell lines and in the cancer tissue samples relative to the matched normal samples. The clones analysis from selected CpG islands is showed in supplemental data (S1). In the cancer cells we found contiguous hypermethylation of the neighbouring CpG islands in a region that spanned nearly 1Mb from CpG island (CpG61) 610kb upstream of the Z fragment, to CpG island (CpG 229), 325kb downstream. The hypermethylated 1Mb region contained 15 CpG islands but only two CpG128 and CpG229 were associated with either a known gene (En1) or a predicted gene (LOC165257 encoding a C1q-domain containing protein). However this region is rich in ESTs suggesting the CpG islands may be associated with promoters for non coding RNAs.

Two further regions of hypermethylation were identified along the 14.2 cytogenetic band from chromosome 2 in the colorectal cancer cells (Fig3C). The first region is located 690Kb downstream of the Z fragment, and includes the CpG island (CpG67) spanning the promoter of the *SCTR* gene (coding for the secretin receptor). The second methylated region spans 650kb in length and is located 1.5-2.15 Mb downstream of the Z fragment and includes four CpG islands; (CpG285) spans the promoter of the *INHBB* gene (inhibin beta B), CpG 26 and CpG206 are not associated with gene promoter regions and CpG22 is located at the 3' end of the *3'GLI2* gene (encoding a C2H2-type zinc finger protein).

Each of the three hypermethylated regions, within the cytogeneic band 14.2 on chromosome 2, are flanked by unmethylated CpG islands. Three unmethylated CpG islands are located upstream of the 1Mb hypermethylated region, overlapping the junction to the 14.1 band, and include the CpG islands associated with the genes INSIG2 (encoding insulin induced protein 2) and DDX18 (encoding DEAD box polypeptide18) (Suppl). Similarly, the CpG islands that are located at the 14.3 band junction, remain unmethylated in the colorectal cancer cells and these islands are associated with two genes CLASP (encoding the CLIP-associating protein) and TSN (translin). Two sets of CpG island clusters between the three methylated regions, also remain unmethylated in both cancer cell lines and cancer tissue samples and normal colorectal DNA. The first set of these islands is associated with the genes *TSAP6* (coding for hypothetical protein *Dudulin2*) and *DBI* (encoding Diazepam Binding Inhibitor) and the second set is associated with the PTPN4 gene (encoding Protein tyrosine phosphatase, non-receptor type 4) and RALB (encoding a v-ral simian leukemia viral oncogene homolog B; ras related; GTP binding protein) (Fig3C).

There were only two genes across 2q14.2 that contained methylated CpG sites in the cancer and matched normal cells and these were *MARCO* (a type II transmembrane protein of class A scavenger receptor) and GLI2 (a GLI-Kruppel family member). However the promoters of both *MARCO* and GLI2 are not associated with CpG islands (Kangas et al, 1999). A CpG rich region was found however located at the 3'end of GLI2 (CPG22) and this region was found to also be methylated in the normal cells. (Fig3C).

Hypermethylation not restricted to one allele

To determine if the hypermethylation occurred in both alleles or was allelic specific similar to an imprinted region we performed clonal DNA methylation sequencing across two CpG islands that showed informative polymorphisms (CpG48 and CpG67 associated with the SCTR promoter). In both cases we found hypermethylation in each allele from the HCT116 cells (Fig4). The presence of bi-allelic methylation suggests that the region is possibly subject to trans-regulatory control.

DNA Methylation in Colorectal Tumours

To determine if the level of hypermethylation in colorectal cancer was as extensive across chromosome 2q14.2 as found for the Z fragment by AIMS (63%), we performed direct PCR sequencing of 3 promoter associated CpG islands En1(CpG128), SCTR (CpG67) and INHBB (CpG285), from DNA isolated from 26 matched colorectal cancers

versus matched normal samples. En1 was found to be hypermethylated in 18/26 (70%), *SCTR* in 23/26 (88%) and *INHBB* in 15/26 (58%) of colorectal cancers versus matched normal samples (Fig 5A). The degree of hypermethylation and number genes methylated was found to be independent of sex, age, and Dukes stage, indicating it may be an early event in colorectal cancer. The hypermethylation of all 3 genes was also observed in a variety of colorectal cell lines including HCT116, KM12sm, LS411N and LISP1 showing methylation of all three genes (Fig 5B).

Gene Expression across 2q14.2

To determine if hypermethylation of the CpG islands in the three hypermethylated regions across 2q14.2 correlated with gene suppression in the cancer cells we compared the expression of En1, SCTR and INHBB by real-time RT-PCR from the HCT116 cells to the expression levels from 10 colorectal tumour tissue samples (pooled) versus the corresponding 10 normal tissues. We found En1, SCTR and INHBB were all completely inactivated in HCT116 cells and the level of expression was suppressed in the cancer tissue samples relative to the normal level of expression in colorectal cells (Fig6A). We then determined the level of expression of the all the genes in the 14.2 cytogenetic band and found that regardless of the DNA methylation status of the associated CpG islands, all the genes were suppressed in the HCT116 cell lines relative to expression in the normal colorectal cells (Fig6B). Moreover the expression in the pooled tumour RNA was also reduced relative to the normal expression from the pooled matched normal samples. Interestingly, the level of expression varied across the region; the genes that were associated with CpG islands that remained unmethylated in the cancer cells (DDX18, INSIG, PTPN4, RALBB, TSN), expressed at a higher level in the normal colorectal cells whereas the CpG island associated genes that were hypermethylated in the cancer cells (En1, SCTR,INHBB) displayed minimal (basal) expression in normal cells.

Chromatin Modification across chromosome 2q14.2

To determine if the unmethylated CpG island associated genes were suppressed in the cancer cells due to the flanking CpG island methylation or chromatin modification, we treated HCT116 cells with the demethylating agent 5-Aza-2'-deoxycytidine (5Aza-C) and with an inhibitor of histone deacetylase trichostatin A (TSA). We found that for the genes that were methylated in HCT116 (En1, MARCO, SCTR and INHBB), treatment with 5Aza or TSA alone resulted in minimal reactivation of the genes (Fig7A), whereas a combination of 5Aza and TSA resulted in substantial reactivation of all these genes.

The CpG island associated genes that were unmethylated in the HCT116 also showed little reactivation after treatment with 5Aza or TSA alone but all showed some activation after treatment with a combination of 5Aza and TSA with the greatest activation being observed for the genes (INSIG2, PTPN4,RALB and GLI2) closest to the methylated regions and the weakest activation being associated with the genes (DDX and TSN), furthest from the methylated regions at either boundary of 2q14.2 (Fig7B). Therefore to determine if chromatin modification was contributing to the suppression of all the genes across the entire band in cancer, we performed ChIP analysis and real-time PCR to quantitate the level of methylated K9-H3 and acetylated K9-H3 in the HCT116 cells. We found that methylated K9-H3 histones were bound the promoter region of the methylated genes En1, MARCO, SCTR and INHBB but this binding was relieved by treatment with 5Aza and TSA (Fig8A). Similarily we found that methylated K9-H3 histones were also bound the promoter regions of the unmethylated genes DDX18, INSIG2, PTPN4, RALB, GLI3 and TSN (Fig 8B) and this binding was also relieved by treatment with 5Aza and TSA indicating that the entire region is associated with methylated histones regardless of the DNA methylation status of individual genes.

DISCUSSION

Vegeu pàgina de presentació del capítol 6 (pàg. 122).

MATERIALS AND METHODS

Samples

One hundred and twelve colorectal carcinomas, with their paired non adjacent areas of normal colonic mucosa were collected as fresh-frozen tissues within 2 hours of removal and stored at –80C. All samples were obtained from the Hospital de la Santa Creu i Sant Pau (Barcelona Spain). The study protocol was approved by the Ethics committee. Human colorectal carcinoma cell lines were obtained from the American Type culture Collection (ATCC, Manassas, VA).

AIMS screening

We used AIMS method to screen for tumour-specific alterations. AIMS method is based on the differential cleavage of isoschizomers with distinct methylation sensitivity and the selective amplification of short sequences flanked by two SmaI (CCCGGG) sites that are ligated to an adaptor and a specific 3-4 nucleotide sequence. Lack of methylation at either site prevents amplification of the band. The AIMS generated fragments were isolated and sequenced. All samples were analysed using the set of primers (set B) and the conditions previously described (Frigola *et al*, 2002). Results on global profiles of DNA methylation have been described elsewhere (Frigola *et al*, 2005).

5-Aza-2'-deoxycytidine and TSA treatment of cells

The colon cancer cell line HCT116 was cultured in D-MEM/F12 (Gibco /BRL) medium supplemented with MEM sodium pyruvate and L-Glutamine and 10% foetal calf serum. 100mm tissue culture dishes were seeded with $0.5x10^6$ cells and treated 24 h later with 0.5mM 5-Aza-2'-deoxycytidine (5-Aza-dC) (Sigma) for 24 hours and cultured with fresh medium for a further 48 h. Cells were treated with Trichostatin A (TSA) (Sigma) at 100 nM for 24 h. For co-treatment of cells with 5-Aza-dC and TSA, 5-Aza-dC was added initially for 24 h, after which it was removed and TSA was added for a further 24h.

RNA extraction and Quantitative Real-Time RT-PCR

RNA was extracted from tumour and matched normal samples, as well as from the cell lines using Trizol reagent (Invitrogen) and cDNA was reverse transcribed from 2mg of total RNA using SuperScript^{TM} III RNase H$^-$ Reverse Transcriptase (Invitrogen Life

Technologies), according to the manufacturer's instructions. The reaction was primed with 200ng of random hexamers **(**Roche). The reverse transcription reaction was diluted 1:20 with sterile H_20 before addition to the RT-PCR. Expression was quantitated using a flourogenic real-time detection method using the ABI Prism 7000 Sequence Detection System. 5ml of the reverse transcription reaction was used in the quantitative real-time PCR reaction using 2x SYBR Green 1 Master Mix (P/N 4309155) with 50ng of each primer. The primers used for amplification are listed in Table 1. To control for the amount and integrity of the RNA, the Human 18S ribosomal RNA (rRNA) kit (P/N 4308329) (Applied Biosystems), containing the rRNA forward and reverse primers and rRNA VIC^{TM} probe, was used. 5ml of the reverse transcription was used in a 20ml reaction in TaqMan Universal PCR Master Mix (P/N 4304437) with 1ml of the 20xHuman 18S rRNA mix. The reactions were performed in triplicate and the standard deviation was calculated using the Comparative method (ABI PRISM 7700 Sequence Detection system User Bulletin #2, 1997 P/N 4303859). The cycle number corresponding to where the measured fluorescence crosses a threshold is directly proportional to the amount of starting material. The mean expression levels are represented as the ratio between each gene and 18S rRNA expression.

Genomic Bisulphite Sequencing

DNA was extracted from the HCT116/SW480 cells using the Puregene extraction kit (Gentra Systems) and Trizol reagent (Invitrogen) from the cancer/normal samples according to the manufacturer's protocol. The bisulphite reaction was carried out on 2mg of restricted DNA for 16 h at 55°C under conditions as previously described (Clark *et al*, 1994; Stirzaker *et al*, 2004). Three independent PCR reactions were performed and pooled to ensure a representative methylation profile. The primers used for the bisulphite PCR amplifications are listed in Table 1. Pooled PCR fragments were directly purified using the Wizard PCR DNA purification system and cloned into the pGEM^{R} -T-Easy Vector (Promega) using the Rapid Ligation Buffer System (Promega). Approximately 12 individual clones were sequenced from the pooled PCR reactions using the Dye Terminator cycle sequencing kit with AmpliTaq DNA polymerase, FS (Applied Biosystems) and the automated 373A NA Sequencer (Applied Biosystems). Direct Sequencing of the pooled PCR products was also obtained using the reverse primer of the PCR amplification in the Dye Terminator cycle sequencing kit with AmpliTaq DNA polymerase, and the automated 3730 DNA analyser with KB^{TM} basecaller in Sequence analysis v5.1 (Applied Biosystems). The degree of methylation

was calculated by comparing the peak height of the cytosine residues with the peak of the thymine residues as described in Melki *et al* , 1999.

Chromatin Immunoprecipitation (ChIP) Assays

ChIP assays were carried out according to the manufacturer (Upstate Biotechnology). Briefly, ~ 1 x 10^6 HCT116 cells, in a 10cm dish, were fixed by adding formaldehyde at a final concentration of 1% and incubating for 10 minutes at 37_C. The cells were washed twice with ice cold PBS containing protease inhibitors (1mM phenylmethylsulfonyl fluoride (PMSF), 1mg/ml aprotinin and 1mg/ml pepstatin A), harvested and treated with SDS lysis buffer for 10 min on ice. The resulting lysates were sonicated to shear the DNA to fragment lengths of 200 to 500 basepairs. The complexes were immunoprecipitated with an antibodiy specific for dimethyl-histone H3(lys9) (#07-212))from Upstate Biotechnology. 10ml of antibody were used for each immunoprecipitation according to the manufacturer. No antibody controls were also included for each ChIP assay and no precipitation was observed. The antibody/protein complexes were collected by salmon sperm DNA/protein A agarose slurry and washed several times following the manufacturer's instructions. The immune complexes were eluted with 1% SDS and 0.1 M $NaHCO_3$ and the crosslinks were reversed by incubation at 65_C for 4 hours in the presence of 200mM NaCl. The samples were treated with proteinase K for 1 hour and the DNA was purified by phenol/chloroform extraction, ethanol precipitation and resuspended in 30ml H_2O.

Quantitative Real-Time PCR Analysis

The amount of target that was immunoprecipitated, was measured by Real-Time PCR using the ABI Prism 7900HT Sequence Detection System. Amplification primers for En1 and MARCO are listed in Table 1. PCR reactions were set up according to the SDS compendium (ver 2.1) for the 7900HT Applied Biosystems Sequence Detector as described previously (Stirzaker *et al*, 2004). Either immunoprecipitated DNA, no-antibody control or input chromatin were used in each PCR and the PCRs were set up in triplicate. Standard deviation was calculated using the Comparative method (ABI PRISM 7700 Sequence Detection System User Bulletin #2, 1997 (P/N 4303859). For each sample an average C_T value was obtained for immunoprecipitated material and for the input chromatin. The difference in C_T values (delta C_T) reflects the difference in the amount of material that was immunopreciptated relative to the amount of input (ABI PRISM 7700 Sequence Detection system User Bulletin #2, 1997 (P/N 4303859).

REFERENCES

Melki, J.R., Vincent, P.C. & Clark, S.J. Concurrent DNA hypermethylation of multiple genes in acute myeloid leukemia. *Cancer Res* **59**, 3730-40. (1999).

Rush, L.J. et al. Epigenetic profiling in chronic lymphocytic leukemia reveals novel methylation targets. *Cancer Res* **64**, 2424-33. (2004).

Frigola, J., Ribas, M., Risques, R.A. & Peinado, M.A. Methylome profiling of cancer cells by amplification of inter-methylated sites (AIMS). *Nucleic Acids Res* **30**, e28. (2002).

Frigola, J. et al. Differential DNA hypermethylation and hypomethylation signatures in colorectal cancer. *Hum Mol Genet* **14**, 319-26. Epub 2004 Dec 1. (2005).

Kangas, M. et al. Structure and chromosomal localization of the human and murine genes for the macrophage MARCO receptor. *Genomics* **58**, 82-9. (1999).

Clark, S.J., Harrison, J., Paul, C.L., & Frommer, M. High sensitivity mapping of methylated cytosines. *Nucl. Acids Res.* **22**, 2990-2997 (1994).

Stirzaker, C., Song, J.Z., Davidson, B. & Clark, S.J. Transcriptional gene silencing promotes DNA hypermethylation through a sequential change in chromatin modifications in cancer cells. *Cancer Res* **64**, 3871-7. (2004).

FIGURE LEGENDS

Figure 1. Identification of a differentially methylated region in colorectal cancer using AIMS**. (a)** Schematic diagram of AIMS technique. Genomic DNA is represented by a solid line, with seven CCCGGG recognition sites. Unmethylated (white boxes) and methylated sites (black boxes) are depicted. The unmethylated sites are cut in a first digestion using the methylation sensitive Sma1 restriction endonuclease that leaves blunt ends. A second digestion is performed using the isoschizomer PspA1 that leaves a CCGG overhang. Adaptors are ligated to the sticky ends. DNA fragments flanked by two ligated adaptors are amplified by PCR using specific primers that hybridize to the adaptor sequence plus the restriction site and one or more additional nucleotides that are arbitrarily chosen. **(b)** Distribution of the 193 AIMS bands identified in the previous study (Frigola et al, 2005). Tag's methylation status is represented by a distribution of all tags along two dimensions graph. The number of samples that showed changes (total samples =93) on y-axis and the ratio between hypermethylations/hypomethylation changes on x-axis (in logarithmic scale). Noteworthy, a fragment tagged Z showed the highest degree of hypermethylation in tumors.

Figure 2. DNA methylation profile of CpG islands neighboring En1. **(a)** Localization of the Z fragment within the 2q14.2 cytogenetic band (Genome Browser, http://genome.ucsc.edu, July 2003). CpG islands in a 25 Kb region downstream from Z fragment including one CpG island associated with the promoter of the Engrailed-1 (En1) gene were analyzed for methylation by clonal bisulfite sequencing. **(b)** Results of the methylation analysis of 5 CpG islands contained in this region are shown. Ten-twelve different clones derived from a pool of 3 independent PCR fragments for each one of CpG islands were sequenced. Two colorectal cell lines (HCT116 and SW480) and two pair cancer (T) matched normal (N) samples were analyzed. Red squares indicate a methylated CpG, green squares indicate unmethylated CpG.

Figure 3. DNA methylation profiles of chromosome band 2q14.2. **(a)** Scheme of the 2q14.2 cytogenetic band and the genes and CpG islands mapped in this region (Genome Browser, http://genome.ucsc.edu, July 2003). The genes are shown in blue and the CpG islands in green. **(b)** Defined and putative genes (in blue) and CpG islands associated (in green) present along cytogenetic band 2q14.2 (4 Mb long, approximately. **(c)** Summary of the DNA methylation profile by direct PCR sequencing

of the CpG islands and CpG depleted regions across 2q14.2 in 2 colorectal cell lines (HCT116 and SW480) and 2 pairs of cancer and matched normal samples. The coordinates from Human Genome Browser (July 2003) and the distance in Kb from Z fragment are indicated. Methylated sequences are represented in red and unmethylated sequences in green.

Figure 4. Results of clonal bisulfite sequencing analysis of two CpG islands that showed informative single nucleotide polymorphisms (SNP). Methylated and unmethylated CpG sites are shown in red and green, respectively.

Figure 5. DNA methylation of the EN1 (CpG128), SCTR and INHBB CpG island promoter by direct PCR sequencing in 26 colorectal samples **(a)** and 13 colon cancer cell lines **(b)**. The sample number or cell line name, age, sex and Duke's stage are indicated. Methylation of the promoter is shown in red and the lack of methylation is shown in green.

Figure 6. Gene expression across 2q14.2. **(a)** Expression of the genes EN1, SCTR and INHBB in 10 pooled tumor samples, 10 matched normal samples and HCT116 cells. The level of expression was assayed by quantitative real-time PCR and normalized according to 18S RNA levels. **(b)** Expression of the genes DDX18, INSIG2, PTPN4, RALBB and TSN (containing a CpG island) and genes MARCO and GLI2 (containing a depleted CpG promoter) in 10 pooled tumor samples, 10 matched normal samples and HCT116 cell. Y axis represents relative expression levels in arbitrary units.

Figure 7. Expression levels of genes mapping to 2q14.2 in HCT116 before (-) and after treatment with 5-Aza-2' deoxycytidine (Aza), TSA or a combination of TSA and 5-Aza-2' deoxycytidine (Aza/TSA). Error bars show standard errors of three independent experiments. EN-1, SCTR and INHBB contain methylated CpG islands. MARCO does not have CpG island. DDX18, INSIG2, PTPN4, RALBB, GLI2 and TSN contain unmethylated CpG islands.

Figure 8. Chromatin modification across chromosome band 2q14.2. DNA immunoprecipitated with antibodies to anti-methylated Histone H3 (lysine 9) was determined by real time PCR in HCT116 cells untreated (-), untreated or treated with 5-Aza-2' deoxycytidine (Aza), TSA or a combination of TSA and 5-Aza-2' deoxycytidine (Aza/TSA). The amount of immunoprecipitated DNA for each gene was calculated as a

ratio of immunoprecipitated DNA respect the total amount of input DNA in the PCR reaction. Errors bars show standard errors of three independent experiments. EN-1, SCTR and INHBB contain methylated CpG islands. MARCO does not have CpG island. DDX18, INSIG2, PTPN4, RALBB, GLI2 and TSN contain unmethylated CpG islands.

A

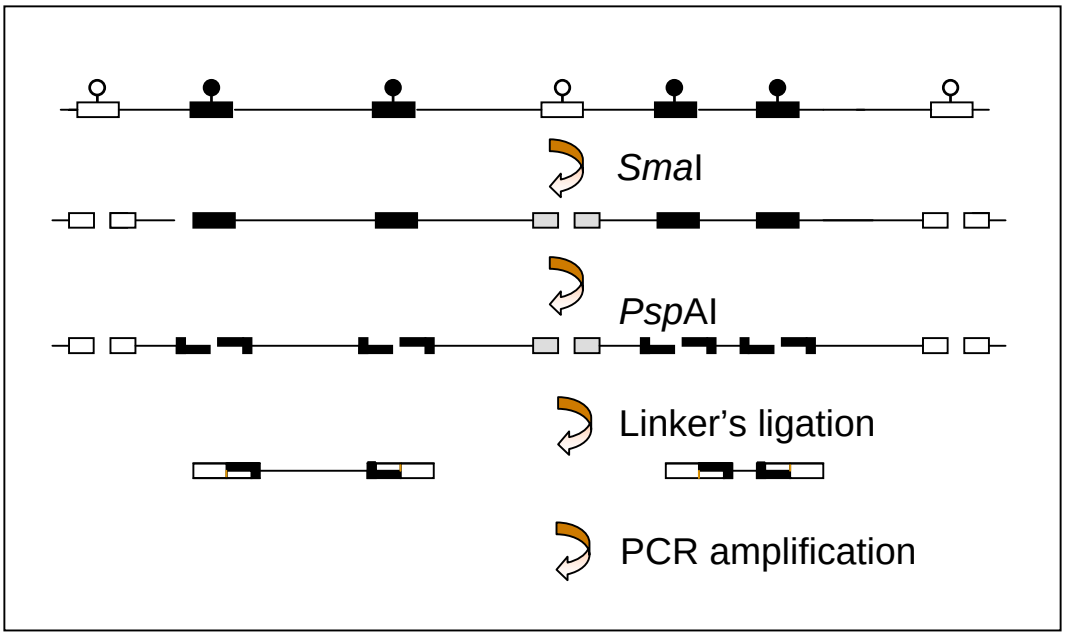
SmaI
PspAI
Linker's ligation
PCR amplification

B

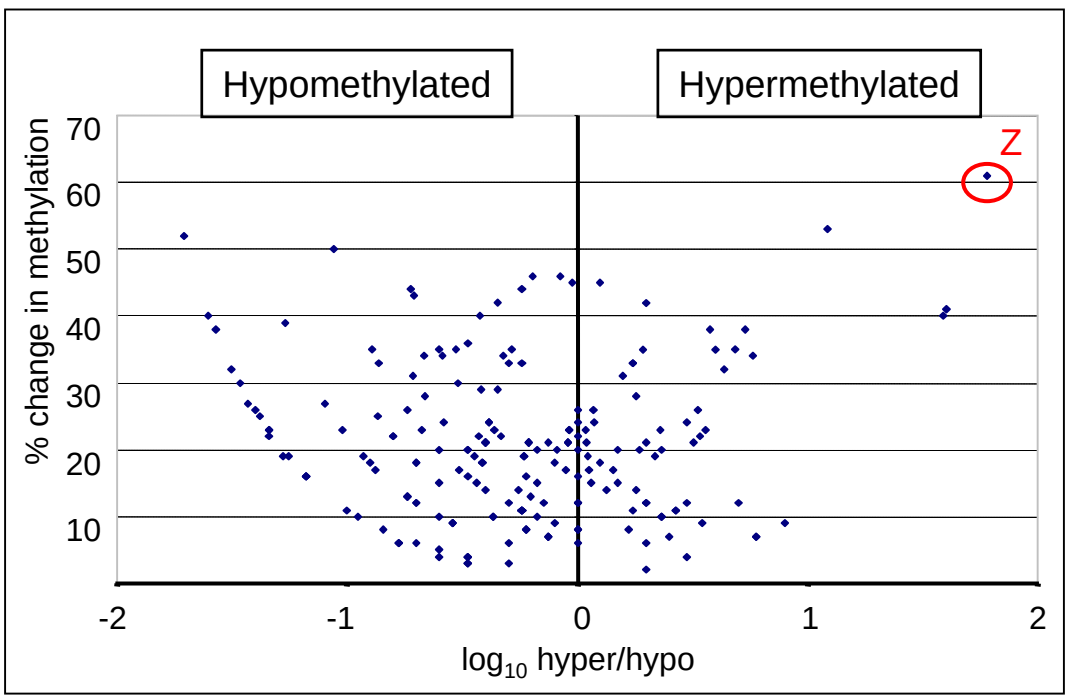
Hypomethylated
Hypermethylated
Z
% change in methylation
70
60
50
40
30
20
10
-2
-1
0
1
2
log10 hyper/hypo

Figure 1

A

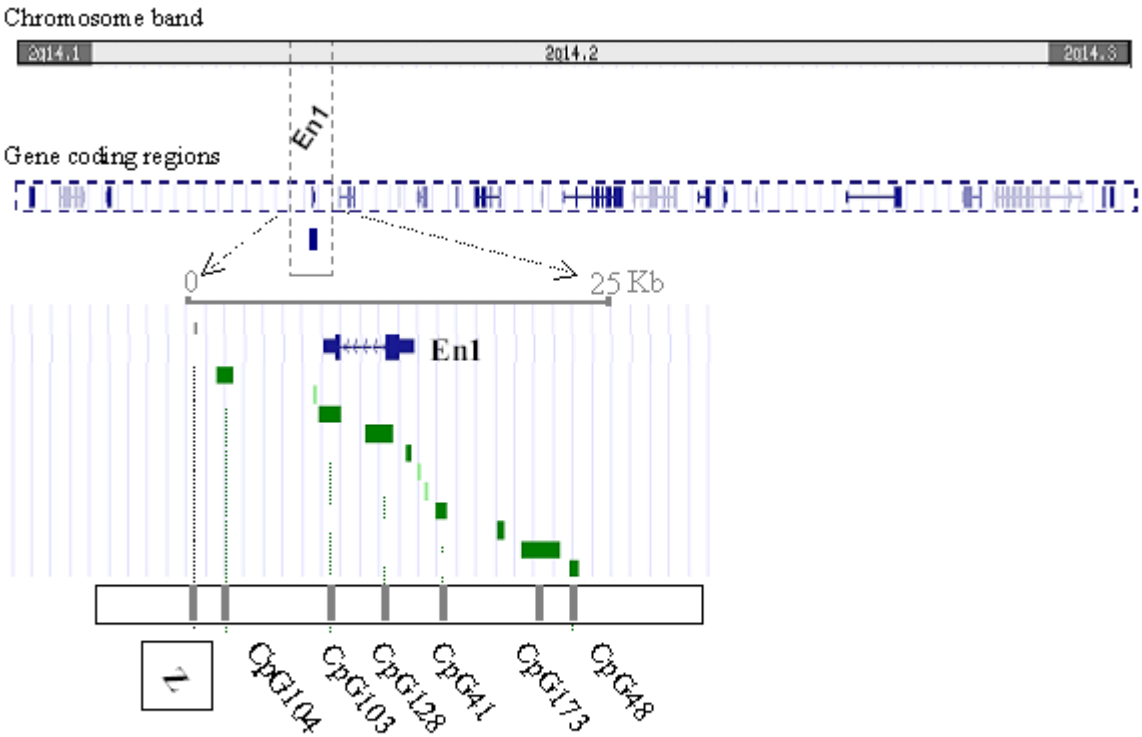
Chromosome band
2q14.1
2q14.2
2q14.3
En1
Gene coding regions
0
25 Kb
En1
Z
CpG104
CpG103
CpG128
CpG41
CpG173
CpG48

B


Z
CpG104
CpG128 (En1)
CpG41
CpG48
HCT116
SW480
9N
9T
165N
165T

Figure 2

A

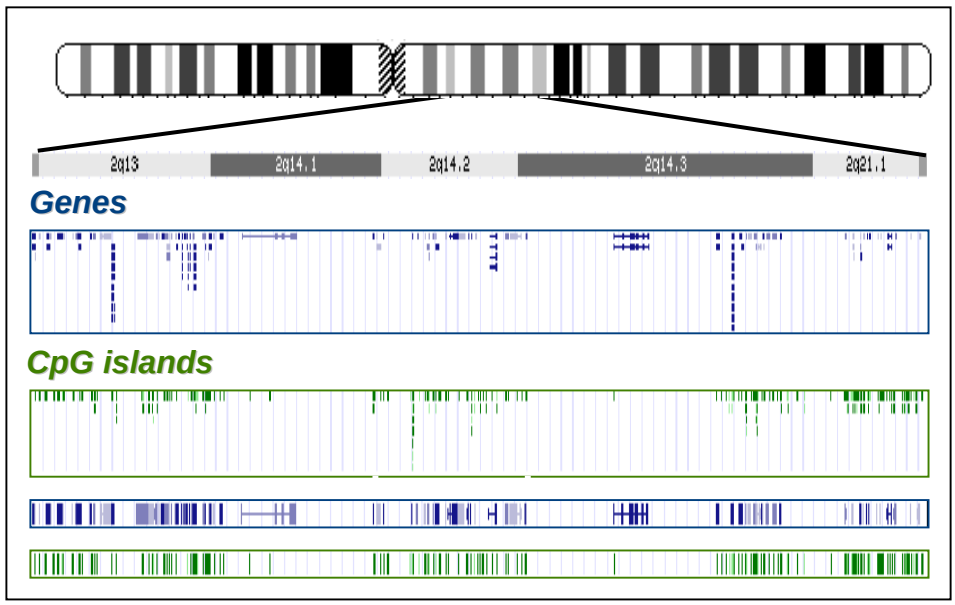

B

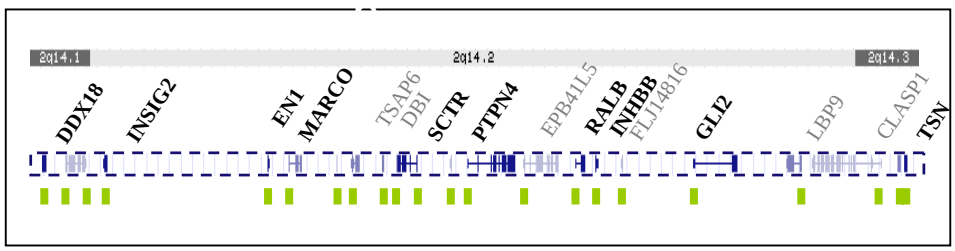

C

NAME	CpGi	Dis.(Kb)	GENE	HCT	SW	9N	9T	165N	165T
CpG48	Yes	-1020	DDX18						
CpG49	Yes	-745	INSIG2						
CpG41.2	Yes	-650	-						
CpG61	Yes	-610	-						
CpG29	Yes	-590	-						
20Kb	No	-25	-						
Z	No	0	-						
CpG104	Yes	2	-						
CpG103	Yes	8	-						
CpG128	Yes	11	EN1						
CpG41	Yes	16							
CpG173	Yes	23	-						
CpG48	Yes	25	-						
5'-MARCO	No	110	MARCO						
CpG229	Yes	320	LOC165257						
CpG85	Yes	390	TSAP6						
CpG85	Yes	540	DBI						
CpG85	Yes	600	-						
CpG67	Yes	690	SCTR						
CpG86	Yes	930	PTPN4						
CpG102	Yes	1180	EPB41L5						
CpG115	Yes	1400	RALB						
CpG285	Yes	1500	INHBB						
CpG26	Yes	1700	-						
CpG206	Yes	1900	-						
CpG22	Yes	2150	3'-GLI2						
CpG112	Yes	2500	LBP9						
CpG51	Yes	2700	-						
CpG104	Yes	2800	CLASP1						
CpG37	Yes	2900	MKI671P						
CpG59	Yes	2920	TSN						

Figure 3

CpG48

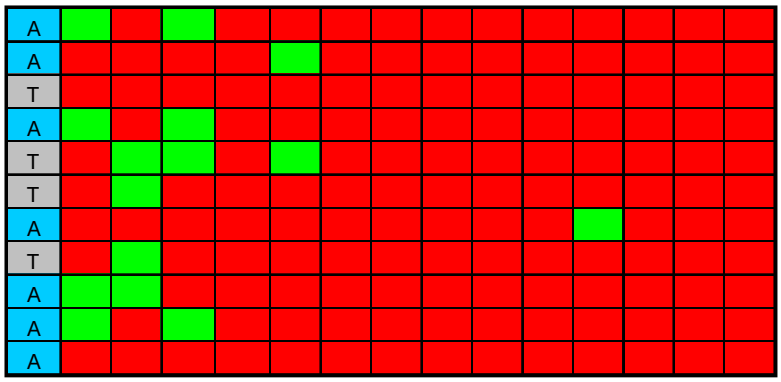

SNP

SCTR

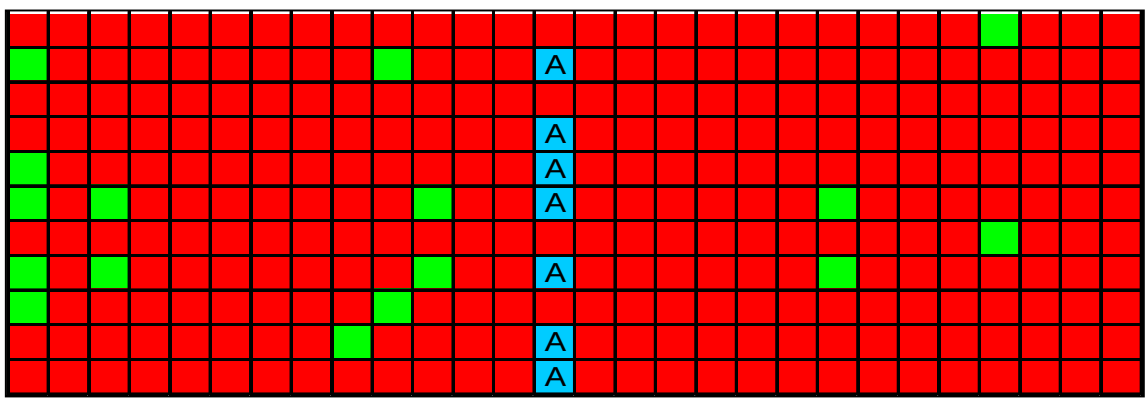

SNP

Figure 4

A

CASE	CpG128	SCTR	INHBB	AGE	SEX	DUKE'S
17				31	W	C2
127				31	W	C2
143				37	W	C1
175				46	W	B2
19				49	W	B1
69				52	M	B2
108				62	M	C2
122				62	M	C1
78				62	M	B2
103				66	M	B2
9				67	M	B2
21				68	W	B2
144				72	W	B2
72				73	M	C2
113				73	W	B2
63				74	W	C2
223				75	M	B2
147				76	W	C2

B

CELL LINE	CpG 128	SCTR	INHBB
HCT			
SW			
LoVo			
KM12sm			
CaCo2			
DLD			
HT29			
KM12c			
LS174			
LS411N			
LISP1			
HCT15			
NC544			

Figure 5

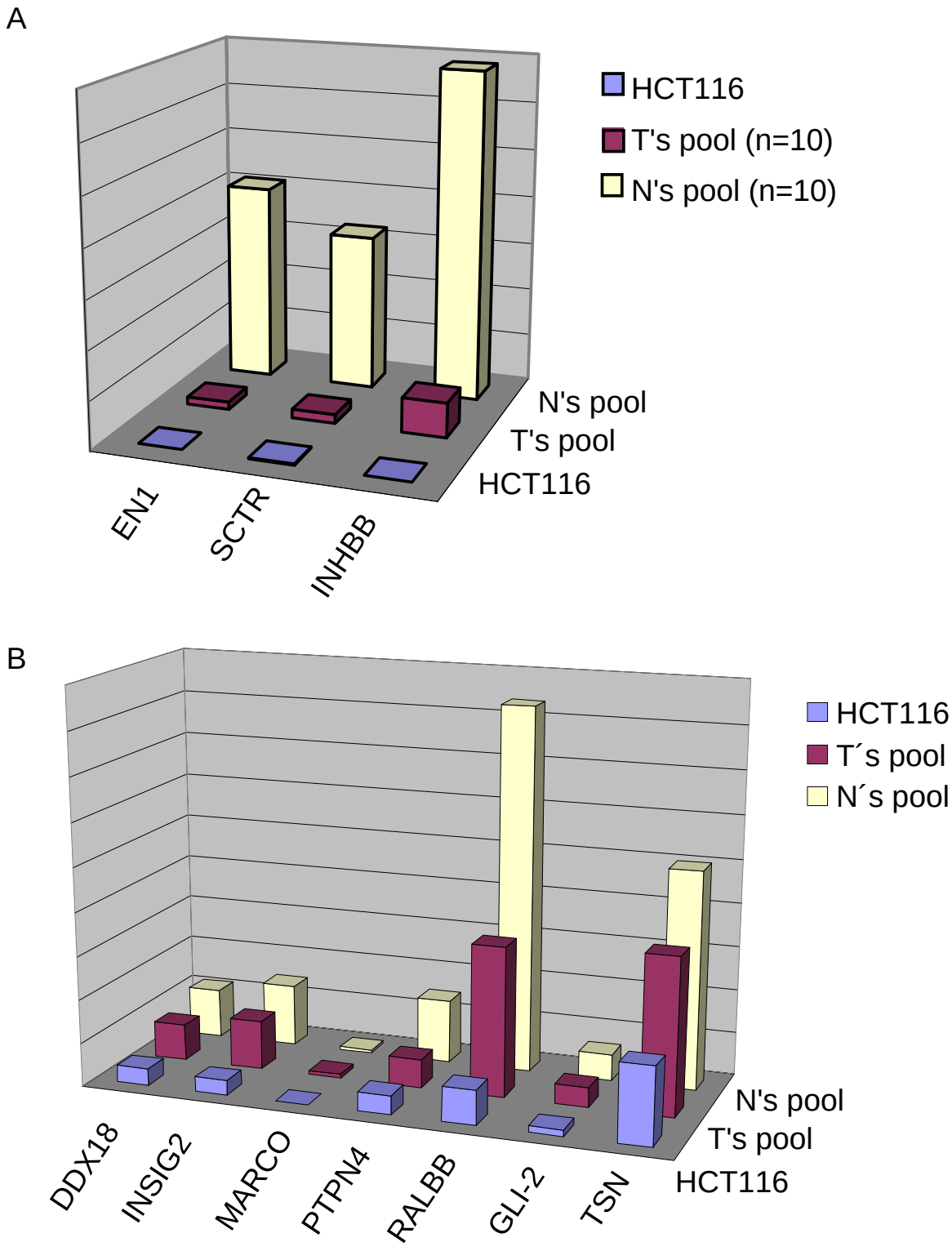
A
HCT116
T's pool (n=10)
N's pool (n=10)
N's pool
T's pool
HCT116
EN1
SCTR
INHBB
B
HCT116
T´s pool
N´s pool
N's pool
T's pool
HCT116
DDX18
INSIG2
MARCO
PTPN4
RALBB
GLI-2
TSN

Figure 6

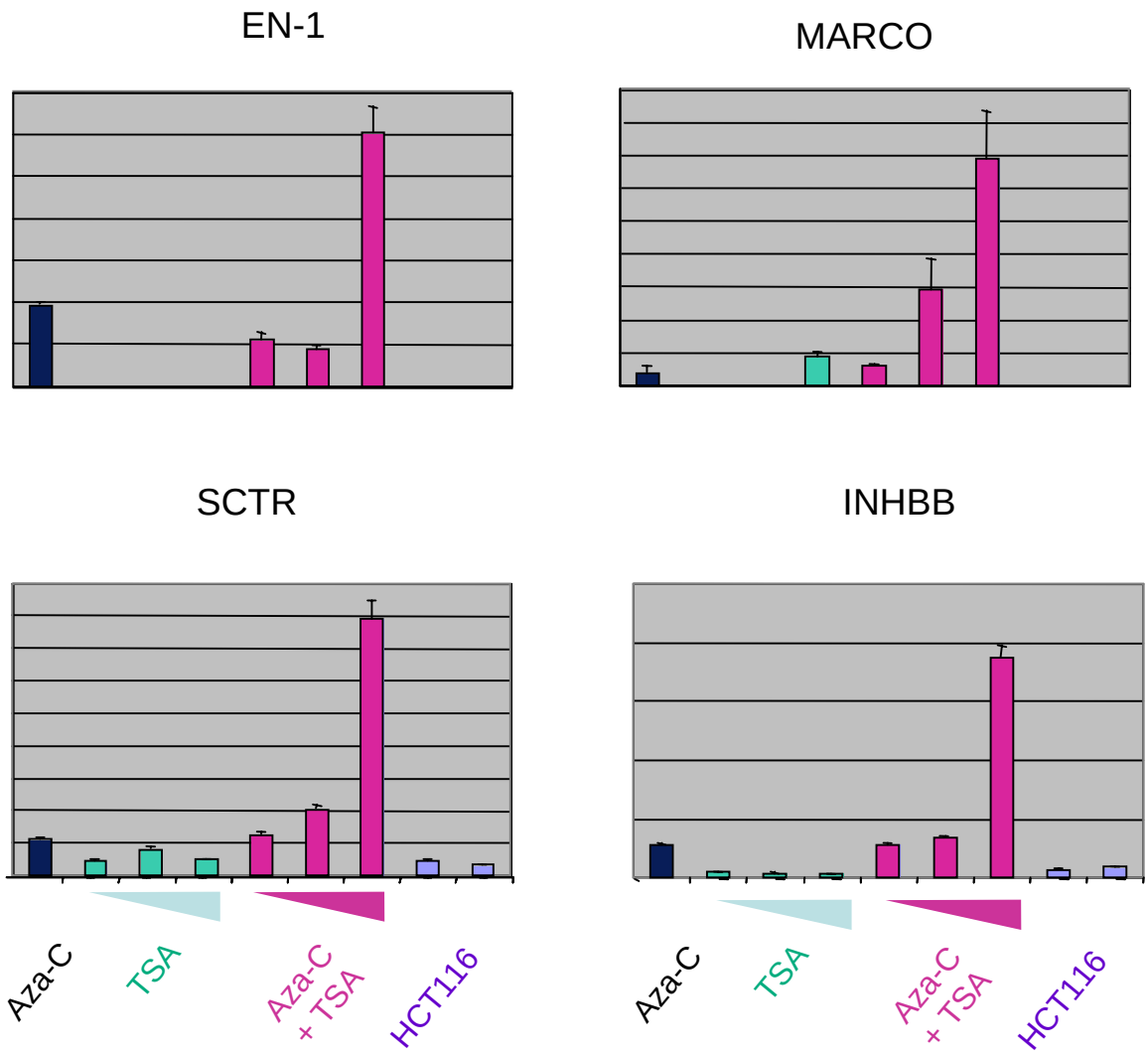
EN-1
MARCO
SCTR
INHBB
Aza-C
TSA
Aza-C + TSA
HCT116
Aza-C
TSA
Aza-C + TSA
HCT116

Figure 7.A

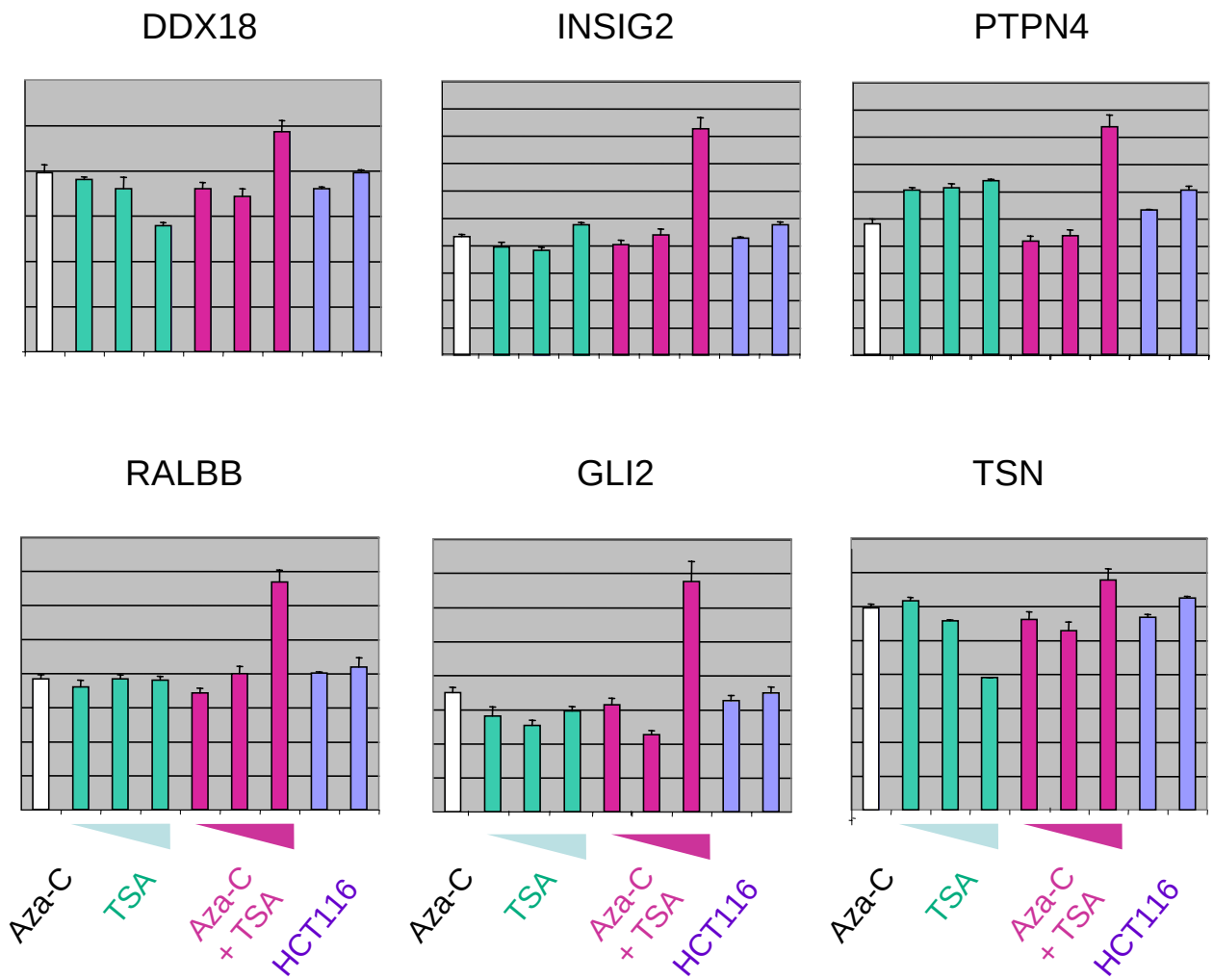

Figure 7.B

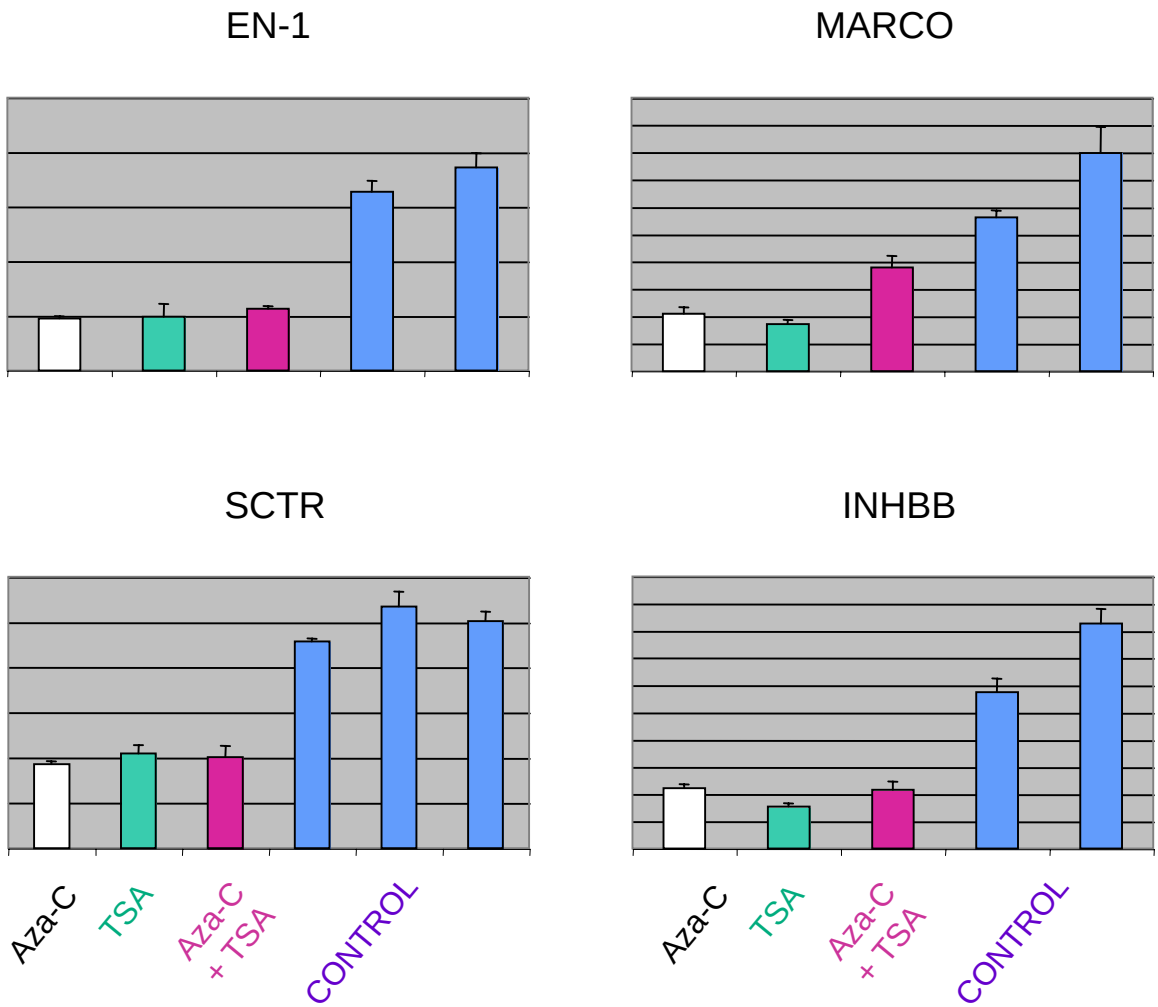
EN-1
MARCO
SCTR
INHBB
Aza-C
TSA
Aza-C + TSA
CONTROL
Aza-C
TSA
Aza-C + TSA
CONTROL

Figure 8.A

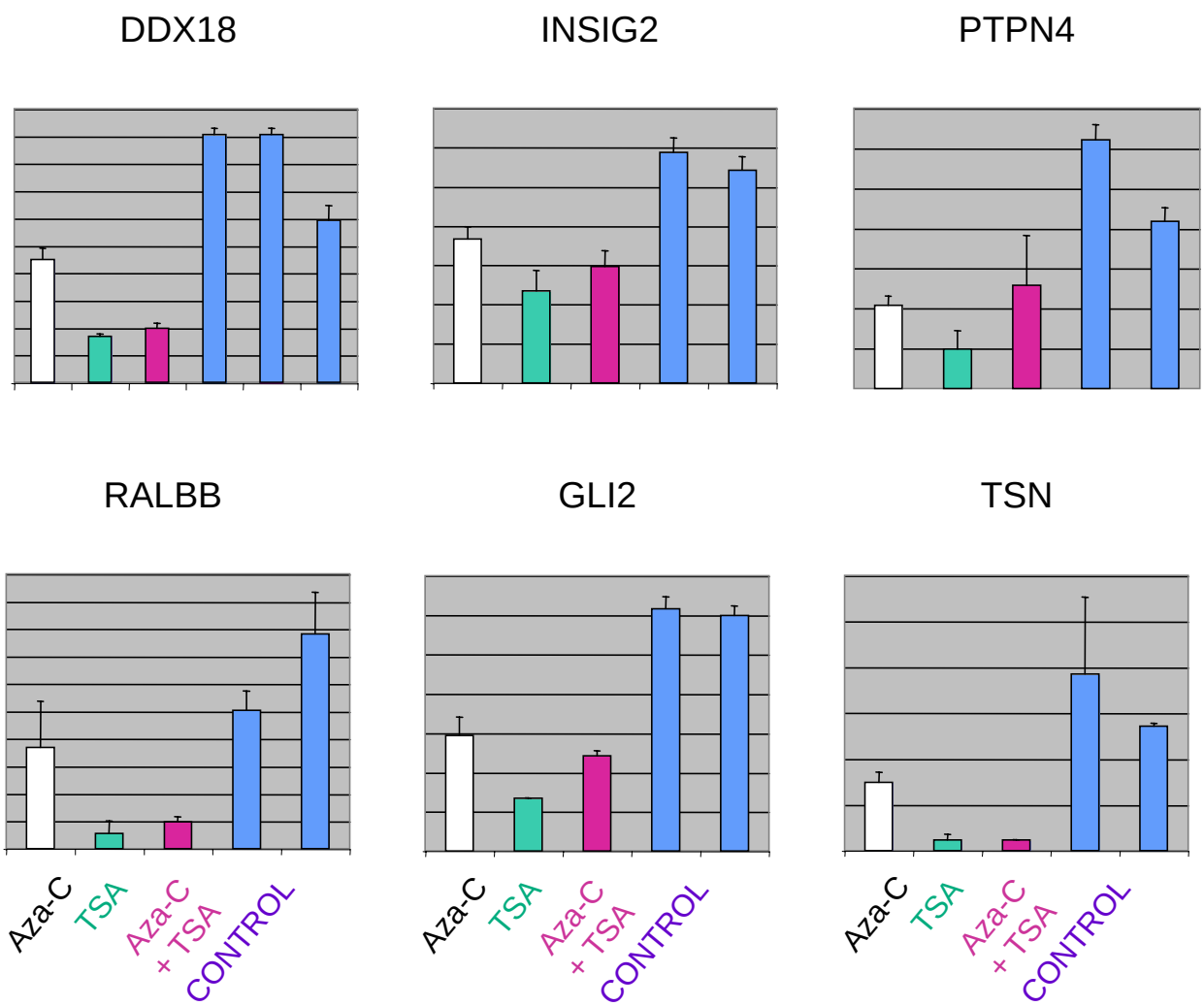

Figure 8.B

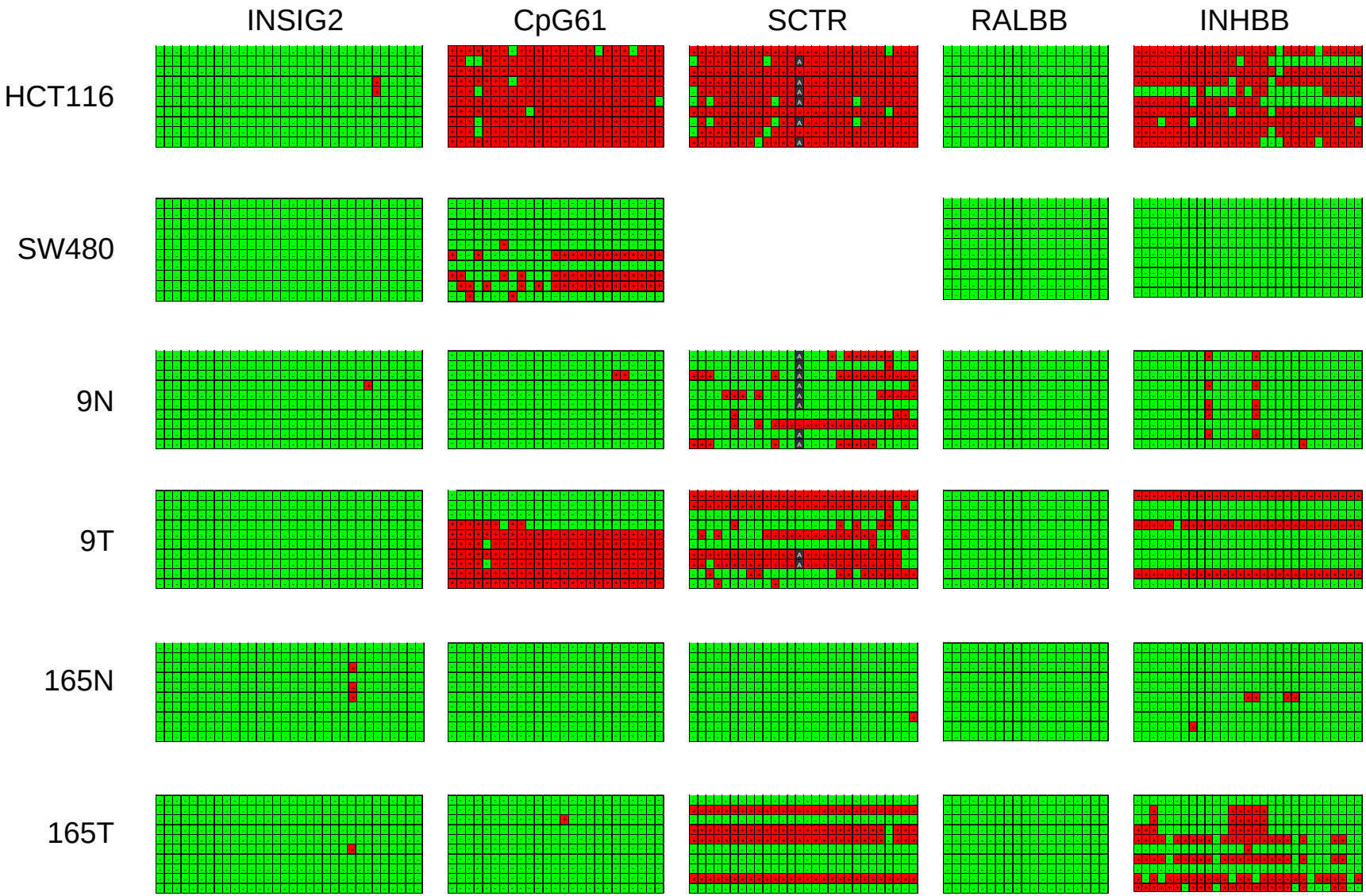

Supplementary S1